ABSTRACT

Title of Document: Functional characterization of Mucin-Associated Surface Protein (MASP) in the human parasite *Trypanosoma cruzi*.

Jung Min Choi, Doctor of Philosophy, 2012

Directed By: Dr. Najib M. El-Sayed, Associate Professor Department of Cell Biology and Molecular Genetics

MASPs are members of a multigenic family recently identified during the sequencing of the *T. cruzi* CL Brener genome. This family contains around 1,400 members, consisting of approximately 6% of the whole coding genes. Highly conserved N- and C-terminal domains, which encode a signal peptide and GPI-anchor addition site respectively, and a hypervariable central region, characterize MASPs. Members of this family are predominantly expressed in the infective trypomastigote form. We hypothesized that members of the *T. cruzi* MASP protein family play a major role in the interaction of the parasite with the host cell. In order to investigate a putative role for *T. cruzi* MASP at the host-pathogen interface, we have used MASP as a bait protein against the human proteome using a high-throughput platform that we have recently established for identifying protein-protein interactions between pathogens and theirs hosts. Yeast two-hybrid screens identified human SNAPIN as one of two

major MASP interacting proteins. SNAPIN is a member of the SNARE protein complex, which may have a role in a calcium-dependent exocytosis. The MASP-SNAPIN interaction was further validated using *in vivo* co-Affinity Purification and *in vitro* pull-down assays. Immunofluorescence assays showed human SNAPIN is recruited to the parasite surface during invasion. Co-localization experiments indicated that SNAPIN is associated with the late endosomes and lysosomes. Supporting our initial hypothesis, SNAPIN depletion using siRNA oligomers in HeLa cells and *snapin*$^{-/-}$ in Mouse Embryonic Fibroblast (MEF) cells significantly inhibited *T. cruzi* invasion, suggesting a role for SNAPIN in this process. Lysosomes in *snapin*$^{-/-}$ MEF cells displayed aberrant morphology and distribution and the parasites did not recruit host lysosomes efficiently when compared to wild-type cells. This was likely due to an impaired calcium-dependent lysosome exocytosis in *snapin*$^{-/-}$ MEF cells. SNAPIN was translocated to the plasma membrane upon calcium influx induced by a calcium ionophore (Ionomycin), resulting in the exposure of the luminal domain of SNAPIN to the extracelluar space. *Leishmania tarentolae* transgenic strains expressing two different MASP proteins were shown to trigger intracellular calcium transients in HeLa cells, presumably by injuring the cell membrane. We propose that *T. cruzi* MASP plays a role in wounding the plasma membrane of the host cell, which in turn elicits a transient intracellular calcium flux and leads to the translocation of lysosome-associated SNAPIN to the plasma membrane. Human SNAPIN, through its exposed luminal domain would then provide an anchor for the entry to the parasite into the cell. The mechanism of *T. cruzi* MASP evoked calcium influx in the host cell membrane remains under investigation.

FUNCTIONAL CHARACTERIZATION OF MUCIN-ASSOCIATED SURFACE PROTEIN (MASP) IN THE HUMAN PARASITE *TRYPANOSOMA CRUZI*.

By

Jung Min Choi

Dissertation submitted to the Faculty of the Graduate School of the
University of Maryland, College Park, in partial fulfillment
of the requirements for the degree of
Doctor of Philosophy
2012

Advisory Committee:
Associate Professor Najib M. El-Sayed, Chair
Professor Stephen M. Wolniak
Professor David M. Mosser
Assistant Professor Volker Briken
Associate Professor Michael P. Cummings, Dean's Representative

Dedication

I dedicate my degree to my parents,

Byungsoon Choi and Jin Bae, for their unconditional love;

and my wife, Inkyoung Cho, for her eternal patience.

Acknowledgements

First and foremost, I would like to thank my mentor, Dr. Najib El-Sayed for his continued support and patient guidance. Not only is he a sharp scientist but also a caring family man who knows the value of life beyond work. I am truly grateful to him for giving me an opportunity to be a part of the El-Sayed lab and motivating me to become an independent researcher.

I would like to thank my committee members, Drs. Steven Wolniak, David Mosser, Volker Briken and Michael Cummings, for their precious time spent meeting with me and insightful comments and assistance throughout the course of my work.

I would like to thank everyone past and present in the El-Sayed lab: Drs. Gustavo Cerqueira, Camila Macedo, Michael Waisberg, Ramzi Temanni, Santuza Teixeira and Beatriz Garat for open and constructive discussions of data, experimental designs and April Hussey, Ginger Houston-Ludlam, Yuan Li, Laura Dillon, Pablo Smircich, Kelly Proimos and MariaSanta Mangione for creating the warm and collegiate atmosphere of the lab and helping my work come along. I give special thanks to Drs. Norma Andrews, Cecilia Fernandes and Mauro Cortez for borrowing muscles and reagents.

I would like to thank my uncle and aunt, Don Bolser and Lynn Bolser, for taking such excellent care of me and making my life more civilized while in graduate school. I would like to thank my younger sister Youmee Choi for being there for Mom and Dad when I am so far away and sharing my responsibilities in the time of need.

I would like to thank my parents, Dr. Byungsoon Choi and Jin Bae, for being number one fans in my path and their everlasting confidence in me. This work could never

have been completed without their immense dedication and support. I would like to thank my parents-in-law Ikyearn Cho and Soondan Kim for their heartfelt encouragement along the way.

And last, but not least, I thank my wife and best friend Inkyoung Cho for listening to me all these years. I look forward to our new exciting journey ahead.

Table of Contents

List of Tables

List of Figures

List of Abbreviations

3AT - 3-Amino-1,2,4-Triazole

6xHis - six histidines

μg - microgram

μM - micromolar

AC6 - adenylyl cyclase VI

AP - affinity purification

ASM - acid sphingomyelinase

BAT3 - HLA-B associated transcript 3

BLAST - the basic local alignment search tool

BLOC-1 - biogenesis of lysosome-related organelles complex-1

CAMLG - calcium modulating ligand

CC - coiled coil

cDNA - complementary deoxyribonucleic acid

CDS - coding sequence

ChIP - chromatin immunoprecipitation

CK1δ - casein kinase 1 delta

CMV - cytomegalovirus

CSN5 - COP9 signalosome subunit 5 variant protein

DALY - disability-adjusted life years

DAPI - 4'-6-diamidino-2-phenylindole

DBD - DNA binding domain

DEAE - diethylaminoethyl cellulose

DEPC - diethylpyrocarbonate

DIRE - degenerate ingi/L1Tc-related elements

DGF-1 - dispersed gene family-1

DMEM - dulbecco’s modified eagle's medium

DNA - deoxyribonucleic acid

DSN - duplex-specific nuclease

DTU - discrete typing units

ds - double-stranded

EBAG9 - estrogen receptor-binding fragment-associated gene 9

E. coli - *Escherichia coli*

EDTA - ethylenediaminetetraacetic acid

ELISA - enzyme-linked immunosorbent assay

ER - endoplasmic reticulum

FBS - fetal bovine serum

GalNAc - N-Acetylgalactosamine

GFP - green fluorescence protein

GlcNAc - N-acetylglucosamine

GP72 - glycoprotein 82

GP82 - glycoprotein 82

GP85 - glycoprotein 85

GPI - glycosylphosphatidylinositol

GST - glutathione S-transferase

GTP - guanosine triphosphate

HEK293T - human embryonic kidney 293 T

HNRNPH3 - heterogeneous nuclear ribocleoprotein H3

HRP - horseradish peroxidase

HS - hydrophobic segment

IBS - Isotonic Buffered Saline

IER3 - immediate early response 3

IFA - immunofluorescence assay

IgG - immunoglobulin G

kD - kilo daltons

KO - knock-out

LAMP1 - lysosomal-associated membrane protein 1

LB - lysogeny broth

LEXSY - *Leishmania tarentolae* expression system

LIT - liver infusion tryptose

Lm, L. major - Leishmania major

LLC-MK_2 - rhesus monkey kidney epithelial

MASP - mucin-associated surface protein

MEF - mouse embryonic fibroblast

mL - millimolar

mM - millimolar

MOI - multiplicity of infection

MT - metacyclic trypomastigote

NCBI - national center for biotechnology information

neo - neocin

NGS - next generation sequencing

Ni-NTA - nickel-nitriloacetic acid

NP-40 - nonidet P-40

NRK - normal rat kidney

NSF - N-ethylmaleimide sensitive fusion protein,

nt - nucleotides

NTC - nourseothricin

ORF - open reading frame

PAGE - polyacrylamide gel electrophoresis

PAHO - Pan American Health Organization

PBS - phosphate-buffered saline

PCR - polymerase chain reaction

Pen-Strep - penicillin-streptomycin

PFA - paraformaldehyde

PI-PLC - phosphatidylinositol-phospholipase C

PKA - protein kinase A

PMSF - phenylmethylsulfonyl fluoride

PPI - protein-protein interaction

PTM - post-translational modification

RBP - RNA binding protein

redox - reduction/oxidation

RFP – red fluorescence protein

RGS7 - regulater of G-protein signaling 7

RHS - retrotransposon hotspot

RNA - ribonucleic acid

RNAi - RNA interference

RNase H - ribonuclease H

RNA-seq - ribonucleic acid-sequencing

RT - reverse transcriptase

RyR - ryanodine receptor

SA - sialic acid

SAP - serine-, alanine-, and proline-rich protein

SAPA - shed acute-phase antigen

SCI - Southern Cone Initiative

SC-LT - synthetic complete minus Leucin and Tryptophan

SC-LTH - synthetic complete minus Leucin, Tryptophan and Histidine

SDS - sodium dodecyl sulfate

SIRE - short interspersed repetitive element

SLO - streptolysin O

SNAP - synaptosomal-associated protein

SNAPIN - SNAP-associated protein

SNARE - soluble NSF attachment protein receptor

SOE - splicing overlap extension

Tb, *T. brucei – Trypanosoma brucei*

TBS - tris-buffered saline

TBST - tris-buffered saline with tween 20

Tc, *T. cruzi – Trypanosoma cruzi*

TcMUCI - *T. cruzi* mucin group I

TcMUCII - *T. cruzi* mucin group II

TcMUCIII - *T. cruzi* mucin group III

TcSMUGL - *T. cruzi* small mucin-like gene family, Large

TcSMUGS - *T. cruzi* small mucin-like gene family, Small

TCT - tissue culture-derived trypomastigote

TRPC6 - transient receptor potential canonical family

TS - trans-sialidase

UT-A1 - urea transporter

UTR - untranslated region

VIPER - vestigial interposed retroelement

VSG - variable surface glycoprotein

WT – wild-type

X-α-Gal - 5-Bromo-4-chloro-3-indoxyl-α-D-galactopyranoside

Y2H – yeast two-hybrid

YFP – yellow fluorescence protein

Zeo - zeocin

Chapter 1: Introduction

1.1 *Trypanosoma cruzi* and Chagas disease

1.1.1 *Trypanosoma cruzi*

Trypanosoma cruzi (T. cruzi) is a monoflagellated intracellular protozoan parasite and the etiological agent of Chagas disease or American trypanosomiasis. It was first identified by Dr. Carlos Chagas, a Brazilian physician, as the causative agent of the disease and named after his mentor, Oswaldo Cruz, in 1909. He characterized the transmission mode, the entire life cycle in vectors and other hosts Chagas discovery was a hallmark in the history of parasitology since he determined almost every aspect of a new neglected tropical disease on his own.

1.1.2 Genetic diversity in *T. cruzi*

T. cruzi strains are classified into six discrete typing units (DTUs) from TcI to TcVI (Zingales, Andrade et al. 2009). It has been widely shown that the major lineages of *T. cruzi* exhibit significant differences in pathogenic potential (Tibayrenc 1995; Souto, Fernandes et al. 1996; Campbell, Westenberger et al. 2004). The reference genome strain, CL Brener (TcVI), is a hybrid of TcII and TcIII. The recently sequenced strain Sylvio X10 belongs to TcI (Franzen, Ochaya et al. 2011). The genomic comparative study revealed that the two strains TcI and TcVI representing different DTUs are virtually identical even though their geographical distribution is quite different. TcI strain predominates North of the Amazon and causes heart disease whereas TcVI strain along with TcII and TcV resides South of the Amazon and gives rise to heart

disease as well as mega syndromes in the colon and esophagus (Vago, Andrade et al. 2000; Coura 2007; Coura and Dias 2009; Rassi, Rassi et al. 2010). It is speculated that the heterogeneity of *T. cruzi* strains could be behind the different clinical manifestations of Chagas disease (Macedo, Machado et al. 2004). Further sequencing of *T. cruzi* strains and a subsequent comparison will allow the discovery of the genetic basis responsible for divergent phenotypes such as cell cycle, host range, vector selection, pathogenic and clinical manifestations.

1.1.3 Transmission

T. cruzi has three distinct morphologies depending on its host environment: the epimastigote, the trypomastigote and the amastigote (Urbina 1999). The epimastigote is a replicative form of *T. cruzi* that resides in the insect vector. The metacyclic trypomastigote (MT) is the infective but non-replicative form of *T. cruzi* found in the hindgut of the insect vector and the trypomastigote is the infective and bloodstream form. Lastly, the amastigote is an intracellular form of *T. cruzi*, replicative and often invasive. Structurally, the three forms of the *T. cruzi* are most easily distinguished by the relative location of nucleus and kinetoplast DNA. The kinetoplast DNA is located anterior to the nucleus in the epimastigote while in the trypomastigote the nucleus is centrally positioned and kinetoplast DNA is located towards the posterior.

T. cruzi has a life cycle alternating between vertebrate hosts and invertebrate hosts. The insect vector, Triatomine bugs (the Reduviidae family, Triatominae sub-family), typically transmits *T. cruzi* through the feces or urine during a bloodmeal. The three main domestic vectors are *Rhodnius prolixus*, *Triatoma dimidiata*, and *Triatoma infestans*. They are popularly referred to as kissing bugs because they often bite the

soft facial skin. These Triatomine bugs can deliver *T. cruzi* to more than 150 species of animal hosts generating an immense animal reservoir of disease. The rate of infection after contact with an infected triatomine bug is estimated to be about one in a thousand people (Rabinovich, Mogilevskii et al. 1990).

Metacyclic trypomastigotes present in excreta can enter the broken skin when the mammalian host rubs or scratches near the bite site and then reach underlying cells. The trypomastigote hijacks the host cellular processes and actively invades nearly any nucleated cells. Once inside the cell they transform into the amastigote form, divide nine times (one trypomastigote produces around 500 amastigote in 5 days), redifferentiate into trypomastigotes and eventually rupture the cell (Carranza, Kowaltowski et al. 2009; Carranza, Valadares et al. 2009; Mazzarotto, Pristipino et al. 2009). Released *T. cruzi* trypomastigotes can infect neighboring cells or circulate in the bloodstream and get transferred back to the insect vector during a blood meal where they transform into epimastigotes, the non-infective and reproductive form of *T. cruzi* (Figure 1-1) (Tyler and Engman 2001).

The insect vector-mediated transmission can occur in the Americas extending from the South of the United States to Argentina where competent vectors reside. *T. cruzi* can be transmitted in non-endemic areas as a result of traveling and migration of infected individuals from endemic countries or organ donation/blood transfusion/vertical transmission (Schofield, Jannin et al. 2006; Tobler, Contestable et al. 2007; Young, Losikoff et al. 2007; Bern and Montgomery 2009). Hence, Chagas disease could be a potential threat that affects global health (Figure 1-2).

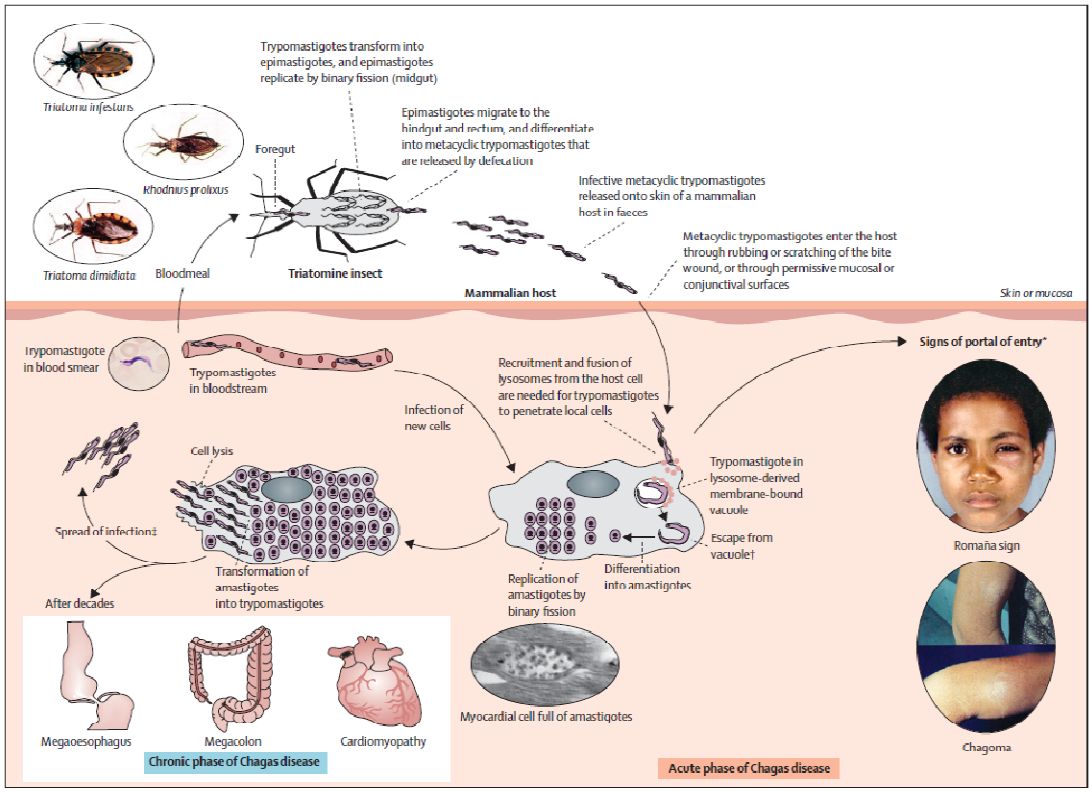

Figure 1-1. Life cycle of *Trypanosoma cruzi.* Cell invasion of the skin by infective trypomastigotes after host scratch near the bite site is followed by transformation into amastigotes and multiple binary divisions in the cell cytoplasm. Upon the rupture of the cell, released trypomastigotes can either invade other cells or get picked up by the insect vector (2010 Rassi *et al*. Lancet).

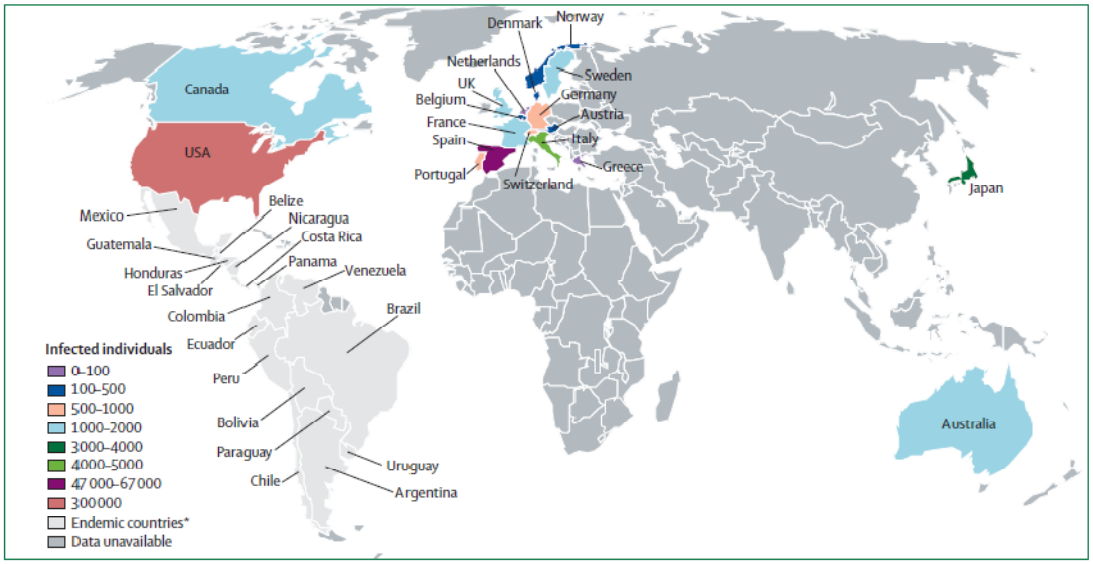

Figure 1-2. Chagas disease distribution and migration route from South America to the non-endemic region (a total number of infected individuals). Infected population in endemic region is indicated in light grey and other infected populations in non-endemic countries are colored individually (2010 Rassi *et al*. Lancet).

1.1.4 Chagas disease

1.1.4.1 Epidemiology and public health concern

Chagas disease is endemic in 21 countries to South America. It is estimated that 10 million people are currently infected worldwide, including 300,000 people in the United States. 25-90 million people are at risk for infection. Every year, 109,000 new infections occur and 11,000 people die from Chagas disease mainly due to heart complication symptoms during the late stage of the disease (WHO 2002; Hotez, Bottazzi et al. 2008; Bern and Montgomery 2009). The economic burden of Chagas disease in South America is immense and this includes unemployment and reduced earning ability estimated at 667,000 disability-adjusted life years (DALY). In Brazil alone, losses of over $1.3 billion were estimated and attributed to the workers with Chagas disease (WHO 2010).

1.1.4.2 Progression

1.1.4.2.1 Acute phase

Chagas disease presents three clinical phases: acute phase, indeterminate phase and chronic phase. The acute phase follows the initial infection by *T. cruzi* and lasts 4-6 weeks. The entry site is often marked by immediate inflammation of the area and the typical swelling in the conjunctiva of the eye, which is referred to as Romaña's sign. During the acute phase, high blood parasitaemia is detected and every nucleated cell in the host is a target for infection. This phase is characterized by mild symptoms such as fever, swelling of lymph nodes and tissues, and malaise. In most cases, it is not specifically diagnosed thus most infected patients are not aware of their infection.

Ironically, this is the only stage where effective treatments are available using the trypanocidal drugs benznidazole and nifurtimox (Villar, Marin-Neto et al. 2002; Wilkinson and Kelly 2009). In fact, even without trypanocidal drug treatment, the acute infection spontaneously resolves in the vast majority of patients. After the host adaptive immunity kicks in, the number of parasites in the blood and tissues significantly declines and it enters the indeterminate phase (Rassi, Rassi et al. 2010). Complications during the acute phase are usually seen in children where 2-8% of symptomatic child patients may die due to cardiac failure (Prata 2001).

1.1.4.2.2 Indeterminate phase

The acute phase is followed by an asymptomatic indeterminate phase. Around 60-70% of patients that progress from the acute phase never develop the chronic symptoms and remain in this phase for life (Macedo 1999). The indeterminate phase is defined by continued positive serology and subpatent parasitaemia but no evidence of organ abnormality (Macedo 1999). One out of three carriers progress to the chronic phase, which can be the first time the individual is diagnosed with Chagas disease even though *T. cruzi* parasites may have persisted for decades (Teixeira, Nitz et al. 2006). It is speculated that host genetic susceptibility may play a role in why a minority of individuals in the indeterminate phase develops chronic Chagas disease while the rest remain in the indeterminate phase.

1.1.4.2.3 Chronic phase

The chronic phase of the *T. cruzi* infection is characterized by cardiac and gastrointestinal complications such as abnormal heart rhythm, heart failure, digestive

malfunction, mega syndrome and sudden cardiac arrest (Rassi, Rassi et al. 2000; Rassi, Rassi et al. 2001). The chagasic cardiomyopathy is the most common cause of death by heart failure during the chronic phase in South America. Both fibrosis and cell apoptosis by parasite persistence as well as amastigotic cyst formation in the area lead to disruption of heart electronic conduction system and eventually myocardial cell loss (Tostes, Bertulucci Rocha-Rodrigues et al. 2005). Enlargement of the heart is common as well. The only option available at this phase is a heart transplant. Another main pathology associated with this chronic phase is often referred to as "megasyndromes", specifically megaoesophagus and megacolon. Those are less common than the cardiac symptoms of Chagas disease but more dramatic. Amastigotic cysts in digestive organs, the colon or the esophagus, damage nerves thus decreasing the ability of smooth muscle to dilate and contract. The loss of this activity causes a loss of rigidity and an enlargement of organs. This involvement of the nervous system is another hallmark of the chronic phase of Chagas disease. Megaesophagus and megacolon can result in death due to malnutrition.

1.1.4.3 Chagas disease pathogenesis

The pathogenesis of Chagas disease is controversial. Two generally accepted hypotheses are autoimmunity (Leon and Engman 2001) and parasite-persistence (Tarleton 2001). The autoimmunity model is based on the observation of inflammatory cells and *T. cruzi*-induced disease symptoms in tissues even in the absence of the apparent intracellular parasites. The traditional diagnostic methods such as the inspection of blood samples under microscopy and examination of feces

from blood-fed triatomine bugs often fails to detect *T. cruzi* in the blood of chronic Chagas patients. This led people to propose a model of autoimmunity that was originally initiated by the parasite but eventually the host immune system begins to attack its own tissues even after parasite clearance (Cunha-Neto, Duranti et al. 1995; Cunha-Neto and Kalil 1995). However, the emergence of more sensitive immunohistochemical and polymerase chain reaction (PCR)-based diagnostic tests questions the autoimmunity model by demonstrating the parasites' persistence deep inside the tissues including myocardium. The parasite persistence is notably supported by the successful treatment of infected patients with trypanocidal drugs. The recent advances in clinical trials have put significant weight to the parasite-persistence model (Zhang and Tarleton 1999; Gutierrez, Guedes et al. 2009) although the autoimmunity model cannot be ruled out completely.

1.1.4.4 Prevention and treatment

Chagas disease control attempts in South America have focused mainly on vector control along with public campaigns to raise awareness (Petherick 2010). Vector eradication programs were organized by the Pan American Health Organization (PAHO) as well as multinational initiatives such as the Southern Cone Initiative (SCI), which included a number of countries such as Argentina, Belize, Bolivia, Brazil, Chile, Colombia, Costa Rica, Ecuador, El Salvador, Guatemala, Honduras, Nicaragua, Panama, Peru, Uruguay and Venezuela. These programs have been very successful and the efforts of SCI ceased transmission in Uruguay, Chile and large parts of Brazil thus reducing the number of Chagas disease cases (Gurtler, Kitron et al. 2007;

Vazquez-Prokopec, Spillmann et al. 2009). However, the disease is still prevalent in some areas in South America such as the Gran Chaco, a sparsely populated region covering mainly Bolivia, Paraguay and Argentina where one out of sixteen people is infected (Hotez, Bottazzi et al. 2008).

Despite the intensive effort to identify the potential vaccine candidates, no vaccines are currently available for Chagas disease (Garg and Bhatia 2005; Dumonteil 2007). The only existing options have been the two drugs, nifurtimox and benznidazole, since the 1960s (Castro and Diaz de Toranzo 1988). However, they are effective in the early acute phase when administered for 60 days at the correct dose but not in the chronic phase (Urbina 1999). These drugs also display severe side effects (Croft 1999; Tarleton, Reithinger et al. 2007). Furthermore, parasite resistance to the drugs was reported (Wilkinson, Taylor et al. 2008), prompting needs to identify additional drugs. Nifurtimox works on the nitroreductase in *T. cruzi* and can be used to treat *T. brucei* as well. It generates a nitroanion, which is a radical anion leading to the formation of reactive species that *T. cruzi* fails to remove (Wilkinson, Taylor et al. 2008; Cerecetto and Gonzalez 2011). Benznidazole creates a covalent bond with various parasite components and eventually inhibits the parasitic redox (reduction/oxidation) processes. It is very urgent to develop vaccines and drugs to prevent and cure the Chagas disease and a fundamental understanding of pathological mechanism of Chagas disease by *T. cruzi* at the cellular and molecular level will help this long process.

1.2 The cell and molecular biology of host cell invasion

1.2.1 Host cell invasion by trypomastigotes

T. cruzi is the only parasite among the Tritryps, three related trypanosomes, which can actively invade any nucleated host cells (Burleigh and Andrews 1995; Alves and Colli 2007; Yoshida and Cortez 2008), whereas *T. brucei* resides in the bloodstream extracellularly and *L. major* is passively phagocytosed by macrophages. *T. cruzi* mammalian host cell invasion has been extensively studied *in vitro* using non-professional phagocytic cells since chronic Chagas disease is characterized by the persistence of parasites in muscle tissues. In 1992, a very unique mechanism for *T. cruzi* invasion was described and generally accepted as a major cell entry pathway (Tardieux, Webster et al. 1992). This invasion mechanism exploits the host lysosome in a manner that is quite different from those previously described for other intracellular microbes. *T. cruzi* trypomastigote invasion does not seem to involve phagocytosis since no evidence of actin polymerization or the formation of a phagocytic cup surrounding the invading trypomastigote were found (Schenkman, Robbins et al. 1991; Tardieux, Webster et al. 1992). Cytochalasin D, an actin polymerization and phagocytosis inhibitor, promotes the *T. cruzi* invasion process supporting the fact that parasites gain entry to host cells in a non-phagocytic mechanism (Schenkman, Robbins et al. 1991; Tardieux, Webster et al. 1992). This is very intriguing considering the size of the trypomastigotes (~15 µm long), the driving force promoting the fairly big parasite internalization was elusive if it is not host cell actin polymerization. It was later shown that host lysosomes were recruited to the parasite invasion site using lysosomal membrane glycoprotein (Lamp1) antibodies

A

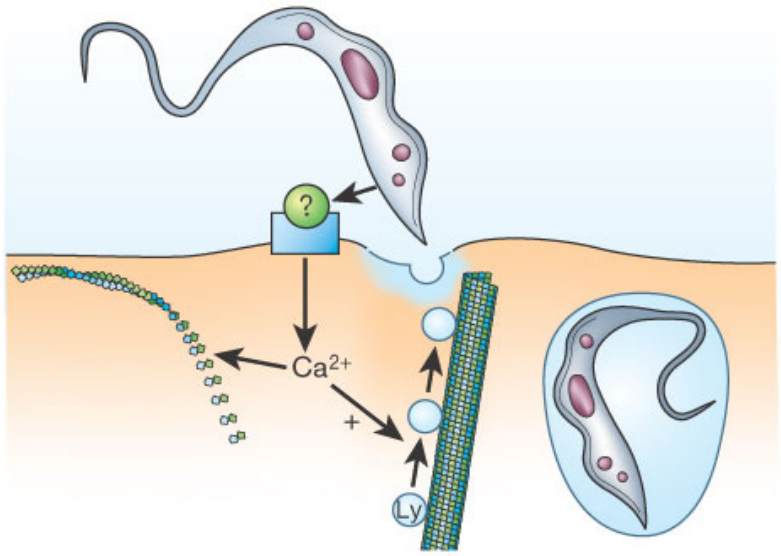
?
Ca2+
+
Ly

B

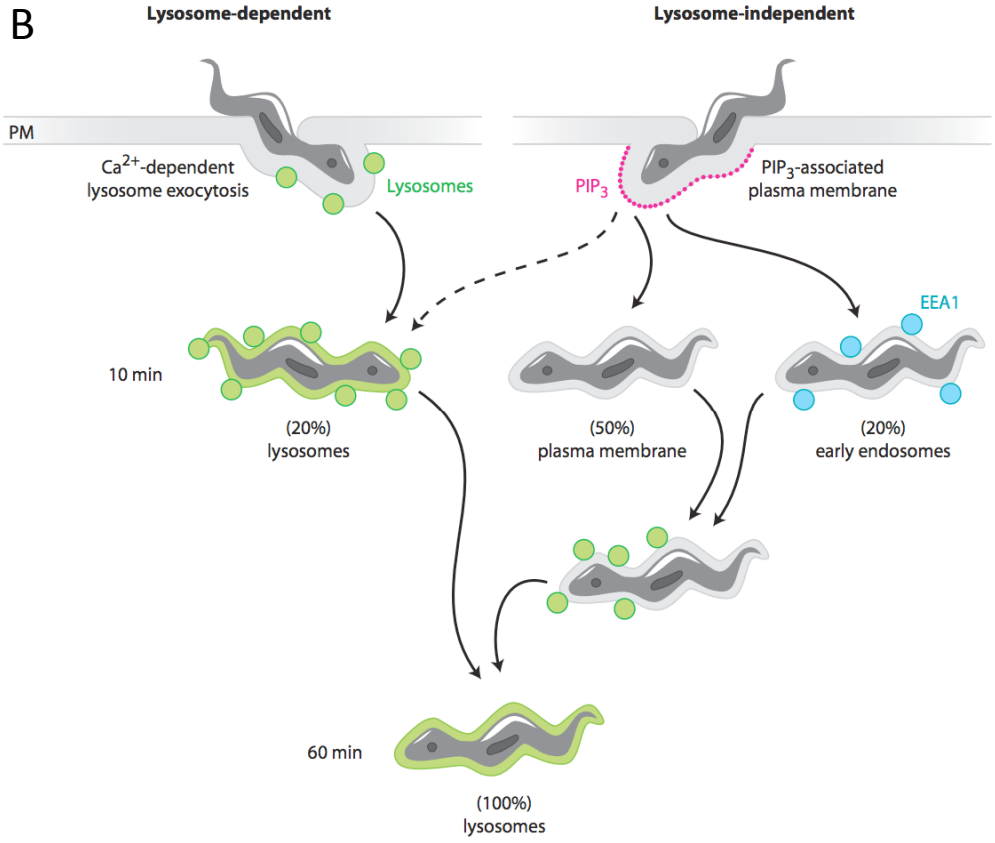
Lysosome-dependent
Lysosome-independent
PM
Ca2+-dependent
lysosome exocytosis
Lysosomes
PIP3
PIP3-associated
plasma membrane
EEA1
10 min
(20%)
lysosomes
(50%)
plasma membrane
(20%)
early endosomes
60 min
(100%)
lysosomes

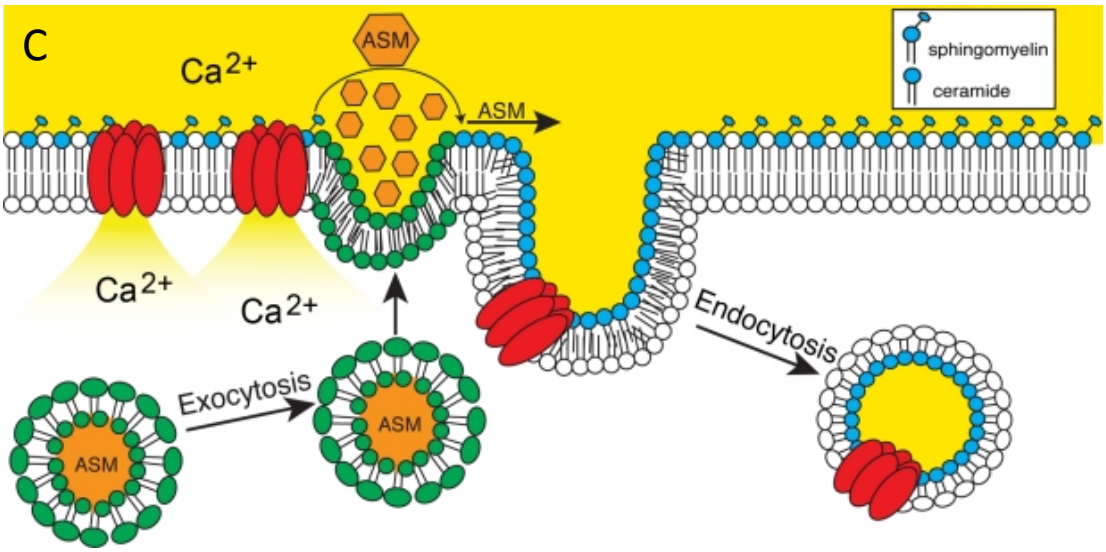

Figure 1-3. *T. cruzi* host cell invasion. (A) *T. cruzi* invades the host cell exploiting a calcium-dependent lysosome recruitment along the micrutubule and fusion to the plasma membrane and depolymerization of actin filaments. (2003 Gruenheid *et al.* Nature) (B) *T. cruzi* enters the cell in two ways. The major entry mechanism is mediated by lysosome recruitment and but *T. cruzi* can get internalizaed by plasma membrane invagination followed by lysosome fusion. (2005 Burleigh *et al.* Sci STKE) (C) Plasma membrane repair mediated by a calcium-regulated lysosomal exocytosis followed by complement endocytosis caused by the enzyme ASM is a housekeeping mechanism in mammalian cells (2010 Tam *et al.* JCB)..

(Tardieux, Webster et al. 1992). *T. cruzi* invasion was also significantly reduced upon treatment with the drugs, colchicine and vinblastine that disrupts microtubule formation (Rodriguez, Samoff et al. 1996), presumably by inhibiting the recruitment of host lysosomes to the plasma membrane where the trypomastigote penetrates (Figure 1-3 A) (Tyler, Luxton et al. 2005). A recent study also suggests that host autophagosomes may be able to replace the role of lysosomes in *T. cruzi* invasion (Romano, Arboit et al. 2009). After host cell entry, the *T. cruzi* trypomastigote stays in a host lysosome-derived parasitophorous vacuole, which is a required event for the successful cell invasion (Andrade and Andrews 2004), and eventually escapes from the parasitophorous vacuole into the cytosol where it starts differentiation into the amastigote form and then replicates. It is well established that cells ingest small molecules through clathrin-mediated endocytosis whereas large particles are phagocytosed driven by an actin polymerization (Kaplan 1977). The lysosome-dependent invasion mechanism for *T. cruzi* trypomastigote was a novel discovery (Tardieux, Webster et al. 1992). Subsequently, lysosome recruitment was found not to be the only way *T. cruzi* trypomastigote could enter the cell. *T. cruzi* can also invade the host cells by being engulfed by invaginated plasma membrane and subsequently fusing with lysosomes. This pathway appears to be host cell actin-independent, another characteristic that differentiates it from traditional phagocytosis (Figure 1-3 B) (Woolsey, Sunwoo et al. 2003). The amastigote, the intracellular form of *T. cruzi*, was also shown to be infective as it was observed that amastigotes were taken up by monocytes almost readily and even by non-professional phagocytic cells occasionally (Ley, Andrews et al. 1988; Mortara, Andreoli et al. 2008). This invasion

mechanism is presumed to be traditional phagocytosis. Once inside the host cell, the amastigote behaves the same as trypomastigote but readily starts binary division after being release into cytosol.

1.2.2 The role of host lysosomes in *T. cruzi* invasion

Experiments using the fluorescent calcium sensor Fluo-3 revealed that *T. cruzi* trypomastigotes trigger transient intracellular calcium increase thus leading to subsequent calcium-dependent lysosomal exocytosis (Tardieux, Nathanson et al. 1994). It was shown that calcium transients were required for *T. cruzi* trypomastigote invasion since depletion of calcium reduced the host lysosome recruitment to the plasma membrane and thus *T. cruzi* invasion rate (Tardieux, Nathanson et al. 1994). As stated earlier, it was proposed that *T. cruzi* trypomastigote can gain entry into the host cell either by lysosome-mediated pathway or plasma membrane-mediated pathway. *T. cruzi* trypomastigotes were able to successfully invade host cells treated with Wortmannin, an inhibitor of phosphoinositide 3-kinases (PI3Ks), where lysosome-dependent pathway was blocked, demonstrating that another invasion mechanism exists (Woolsey, Sunwoo et al. 2003). Interestingly, the subsequent work has shown *T. cruzi* inside the host cell should reside in the lysosome-derived parasitophorous vacuole regardless of the host cell invasion mechanisms (Andrade and Andrews 2004). The failure to reside within a parasitophorous vacuole after invasion results in the escape of *T. cruzi* to the extracellular space, indicating the importance of the microtubular network within the cell for *T. cruzi* cellular retention. This observation suggests that host lysosome fusion is required for the viable infection of *T. cruzi* trypomastigotes. Trypomastigotes reside within the acidic pH

parasitophorous vacuole, which seems to initiate the differentiation program from the trypomastigote to amastigote. Trypomastigotes in the parasitophorus vacuole facilitate their own escape by secreting TcTox, a hemolysin forming a pore active at low pH, on the vacuolar membrane and by removing sialic acids from lysosomal glycoproteins on the vacuolar membrane with trans-sialdase (Andrews 1990; Andrews, Abrams et al. 1990). Upon disruption of the parasitophorous vacuole, intracellular amastigotes asexually divide nine times until they redifferentiate to trypomastigotes (Figure 1-4).

1.2.3 The role of glycoprotein 82 in calcium transients.

Calcium-regulated lysosomal exocytosis seems to be the major mechanism that *T. cruzi* trypomastigotes exploit for cell entry (Burleigh 2005) and it was shown that *T. cruzi* trypomastigotes trigger calcium transients in the host cells (Tardieux, Nathanson et al. 1994). Further studies demonstrated that similar calcium transients also occur within the invading trypomastigote and these calcium transients in both host cells and the trypomastigote are required for invasion (Moreno, Silva et al. 1994; Yakubu, Majumder et al. 1994). Glycoprotein 82 (GP82) was found to be responsible for these calcium transients (Manque, Neira et al. 2003). Endogenous GP82 is expressed in the metacyclic trypomastigote stage, the infective form of *T. cruzi*, and when GP82 is overexpressed in epimastigotes, the non-infective insect forms of *T. cruzi*, transgenic parasites were able to induce calcium transients in the host cells. However, the receptor for GP82 on the host cell is not identified. Calcium transients within the invading trypomastigote were proposed to occur via GP82-mediated

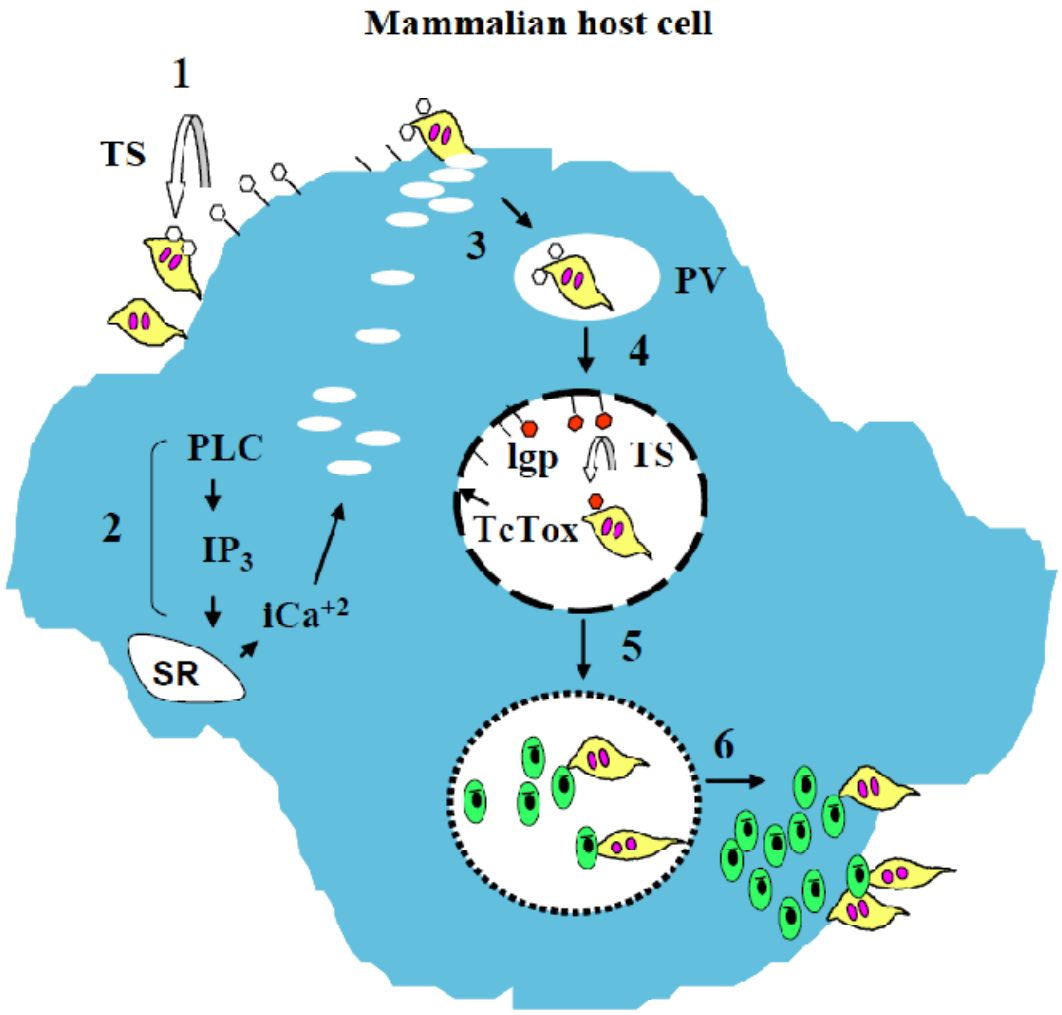

Figure 1-4. *T. cruzi* host cell invasion process. 1) Trypomastigotes catalyze host sialic acid to mucins on the parasite surface by trans-sialidase for efficient entry. 2) Phospholipase C-mediated intracellular calcium increase in the host cytoplasm due to the release from the internal stores occurs by parasite surface protein GP82. 3) Calcium transients lead to host lysosomal exocytosis and the trypomastigotes are internalized. 4) Trans-sialidase on the parasite transfers sialic acids from host lysosomal glycoproteins and the secreted TcTox forms a pore on the vascuolar membrane. Altogether, the parasitophorous vacuole becomes susceptible and

eventually lysed. 5) Trypomastigotes start differentiation into amastigotes, which replicate multiple times in the cytoplasm. 6) After redifferentiation into trypomastigotes, trypomastigotes and few immature amasitigote gets released the bloodstream **(**2007 Zacks *et al.* from the dissertation).

phosphorylation although the exact mechanism remains largely unclear. Other trypomastigote glycoprotein molecules that could possibly trigger calcium transient in the host cells include GP35/50 and GP90 but the induction by both glycoproteins are negligible compared to GP82 (Ruiz, Favoreto et al. 1998).

1.2.4 Membrane repair and *T. cruzi* invasion

Other studies suggest that this unusual calcium-dependent lysosome-mediated exocytosis being exploited by *T. cruzi* may be a housekeeping mechanism in mammalian cells (McNeil and Steinhardt 1997; Reddy, Caler et al. 2001; Idone, Tam et al. 2008). It was shown that plasma membrane repair requires calcium-dependent exocytosis of lysosomes followed by endocytosis to get rid of membrane lesions (Idone, Tam et al. 2008). Further analysis revealed that lysosomal enzyme acid sphingomyelinase (ASM) is secreted as a result of calcium-dependent lysosomal exocytosis when cells are injured and converts plasma membrane sphingomyelin into ceramide (Schissel, Jiang et al. 1998; Tam, Idone et al. 2010). Ceramides on the plama membrane associate themselves into microdomains that generate endosomes and promote the complement endocytosis for plasma membrane lesion internalization (Holopainen, Medina et al. 2000; Gulbins and Kolesnick 2003). ASM-deficient cells were unable to repair the wounding caused by bacterial pore forming toxin, SLO, but the restoration of plasma membrane repair was observed when the recombinant ASM proteins were added exogenously indicating this lysosomal enzyme reseals the plasma membrane and maintain the plasma membrane integrity by removing membrane lesion (Tam, Idone et al. 2010).

More recently a study revealed that *T. cruzi* host cell entry mimics the same process (Fernandes, Cortez et al. 2011). *T. cruzi* trypomastigotes, but not epimastigotes, can directly wound the plasma membrane by unknown mechanism and trigger cytosolic calcium transients. Elevation of the intracellular calcium concentration induces the exocytosis of lysosomes and the release of host lysosomal enzyme ASM to the outer leaflet of the plasma membrane. Again, a rapid complement endocytosis reseals the injury site by internalization and *T. cruzi* gain entry into the cell taking advantage of the endocytosis near the wounding site. The depletion of ASM representing the plasma membrane non-repair condition in the host cell significantly reduces the *T. cruzi* invasion rate whereas the addition of recombinant ASM restores the host endocytosis as well as the *T. cruzi* invasion rate in ASM-deficient cells. This also demonstrated that tissue tropism with the preference of cardiomyocytes and smooth muscle cells may be related to the fact that these tissues are susceptible to injury, and thus is easier to invade. However, the exact molecule(s) responsible for the injury on the membrane triggering the calcium transients remain unclear (Figure 1-3 C).

1.3 Genome sequencing of *T. cruzi* CL Brener reference strain

The sequencing of the *T. cruzi* genome was completed and published in 2005 along with the sequenced genome of two other trypanosomatids human parasites: *Typanosoma brucei* and *Leishmania major* (Berriman, Ghedin et al. 2005; El-Sayed, Myler et al. 2005; Ivens, Peacock et al. 2005). The genomes of these three model trypanosomatids (also referred to as TriTryps) were sequenced, assembled, and then genes were predicted, annotated and compared to each other by reciprocal blast (Figure 1-5 A). A comparative analysis of gene content of the three parasites showed

surprisingly conserved gene synteny between the three species, despite the ancient divergence (200-500 millions of years ago) indicating very strong selective pressure the gene order and orientation. The set of gene clusters shared by the TriTryp species, also known as the TriTryp core, has 6,157 gene members and represents a valuable opportunity in terms of possible drug targets that can affect the three organisms at the same time (El-Sayed, Myler et al. 2005). The fact that roughly 2,000 out of those 6,157 core genes are not present in the human host makes the potential chemotherapeutic approach more viable. In addition, the genome analysis revealed that many species-specific genes clusters encode for proteins responsible for the distinct nature of the disease: different strategies of survival and immune evasion used in each organism (Figure 1-5 B).

The genome size of *T. cruzi* is around 100 Mb with 12,000 genes in the haploid genome of the CL-Brener strain. One of the unique features of the *T. cruzi* genome over *T. brucei* and *L. major* is the massive expansion of *T. cruzi*-specific surface protein gene families such as Mucins, trans-sialidase (TS) / GP85 and DGF-1 which may play a role in cell adherence and the active host cell invasion.

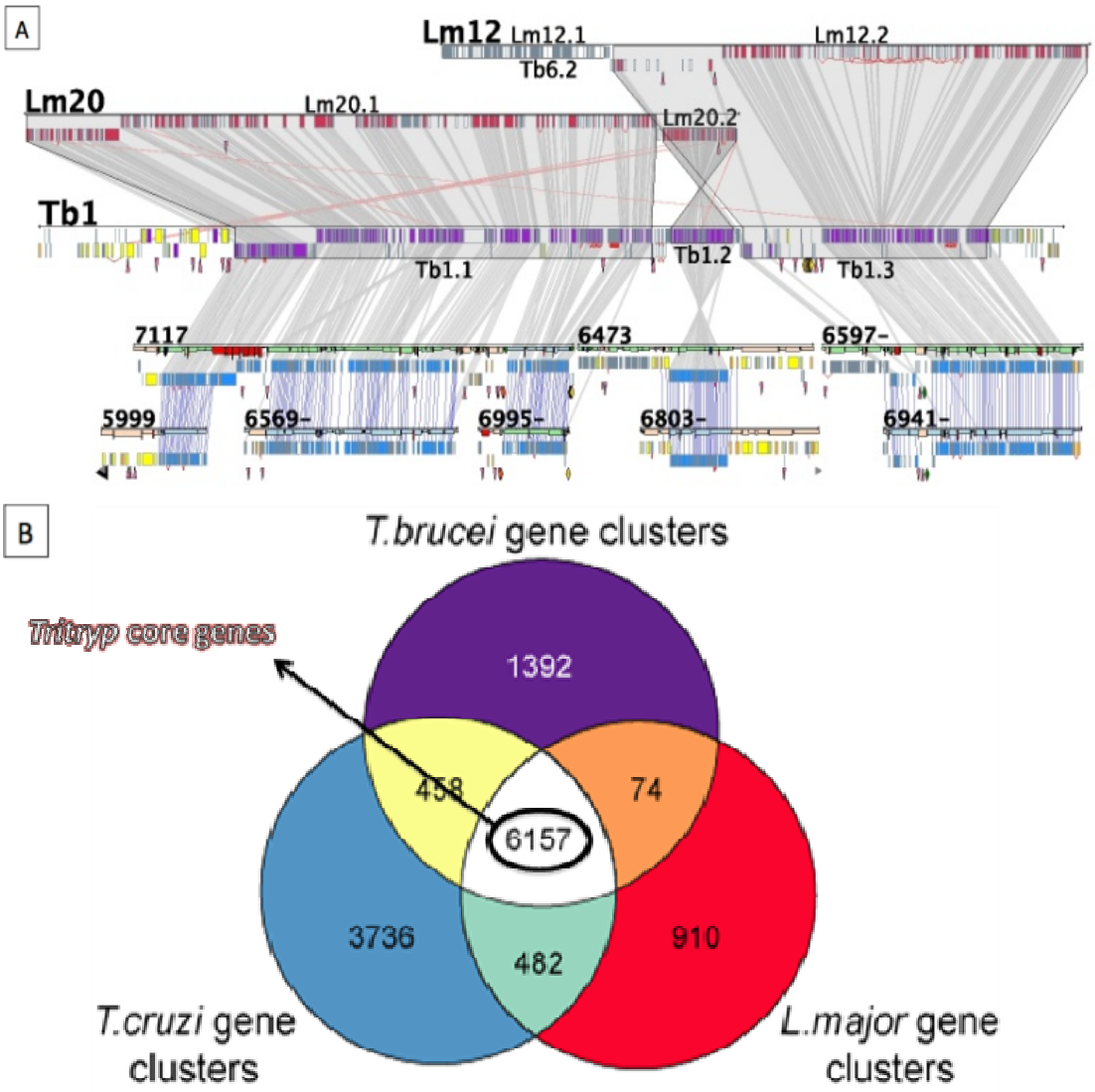

Figure 1-5. Tritryp comparative genomics. (A) A physical arrangement of the Tritryps genomes revealing a conserved synteny as well as synteny breaks mainly in subtelomeric regions (Red : *Leishmania major*, Purple : *Trypanosome brucei*, Blue : *Trypanosome cruzi*) (B) A Venn diagram comparing the gene contents of the Tritryps and depicting a core proteome of the Tritryps and species-specific proteins (2005 El-Sayed *et al.* Science).

1.4 Multigenic families in *T. cruzi*

1.4.1 Trans-sialidases and GP85

Trans-sialidases (TS) are members of the largest multigenic family in *T. cruzi* consisting of 1430 members including 693 pseudogenes. Similar to *T. brucei*, *T. cruzi* lacks the sialic acid biosynthesis pathway components in the genome (El-Sayed, Myler et al. 2005). *T. cruzi* expresses trans-sialidase, a protein that transfers sialic acid residues from host glycoconjugate to *T. cruzi* mucins (Schenkman, Jiang et al. 1991; Ferrero-Garcia, Trombetta et al. 1993) (reviewed below). Unlike a conventional sialidase located at the Golgi apparatus, it is located on the surface of *T. cruzi*, thus making it much more efficient in terminal sialic acid transfer (Buscaglia, Campo et al. 2006; Agusti, Giorgi et al. 2007). TS expression is coordinated with *T. cruzi* mucin due to its associated genomic location indicating the possible interplay between TS and mucin (Buscaglia, Campo et al. 2006). TS is also GPI-anchored to the plasma membrane of *T. cruzi* and can be shed into the bloodstream by endogenous phosphatidylinositol-phospholipase C (PI-PLC) inducing different biological effects by altering the sialylation profile on the host cell surface. Among more than 1400 members, only around 70 members are enzymatically active and most of active TSs contain SAPA (shed acute-phase antigen) (Cazzulo and Frasch 1992). Another set of 70 members share more than 95% identity with active TS but they are enzymatically inactive due to a point mutation in a key residue, Tyrosine 342 (Buschiazzo, Amaya et al. 2002). These inactive TS members can still bind to sialic acids, however, indicating that they may play a role in cell adhesion despite the loss of their sialylation activity (Magdesian, Giordano et al. 2001). The remaining TS

genes sharing a sialidase motif (VTVxNVxLYNR) have more or less 30% identity to active TS thus are inactive (El-Sayed, Myler et al. 2005; Tonelli, Giordano et al. 2010). This suggests that there is a strong selective pressure on the TS superfamily to achieve this diversity. Furthermore, TS seems to play a role in the escape of *T. cruzi* from the parasitophorous vacuole and it is speculated that the sialylation during this process protects *T. cruzi* from a rapid acidification of the parasitophorous vacuole by lysosome fusion events (Frasch 2000). Also the removal of sialic acids from lysosomal glycoproteins on the parasitophorous vacuole may make the parasitophorous vacuole membrane more susceptible to TcTox and eventually lead to loss of membrane integrity (Andrews 1990). TS-mediated sialylation in trypomastigotes mucin also protects *T. cruzi* from the complement pathway in the host by binding to complement factors C3b and C4b and triggering their inactivation by protease activity although this protease is not fully characterized (Figure 1-6) (Tomlinson, Pontes de Carvalho et al. 1992; Mucci, Risso et al. 2006). GP85 is a non-catalytic member of the TS superfamily, known to bind to laminin and cytokeratin 18 (Giordano, Chammas et al. 1994), indicating it is involved in the *T. cruzi* adhesion to the host cell surface and thus very important for *T. cruzi* invasion process.

1.4.2 Mucins

The surface of *T. cruzi* contains other major surface glycoproteins including mucins, which are heavily O-glycosylated molecules important in cell-cell interactions. The *T. cruzi* mucin gene family comprises 863 members corresponding to around 1% of the diploid genome and 6% of all coding genes (El-Sayed, Myler et al. 2005).

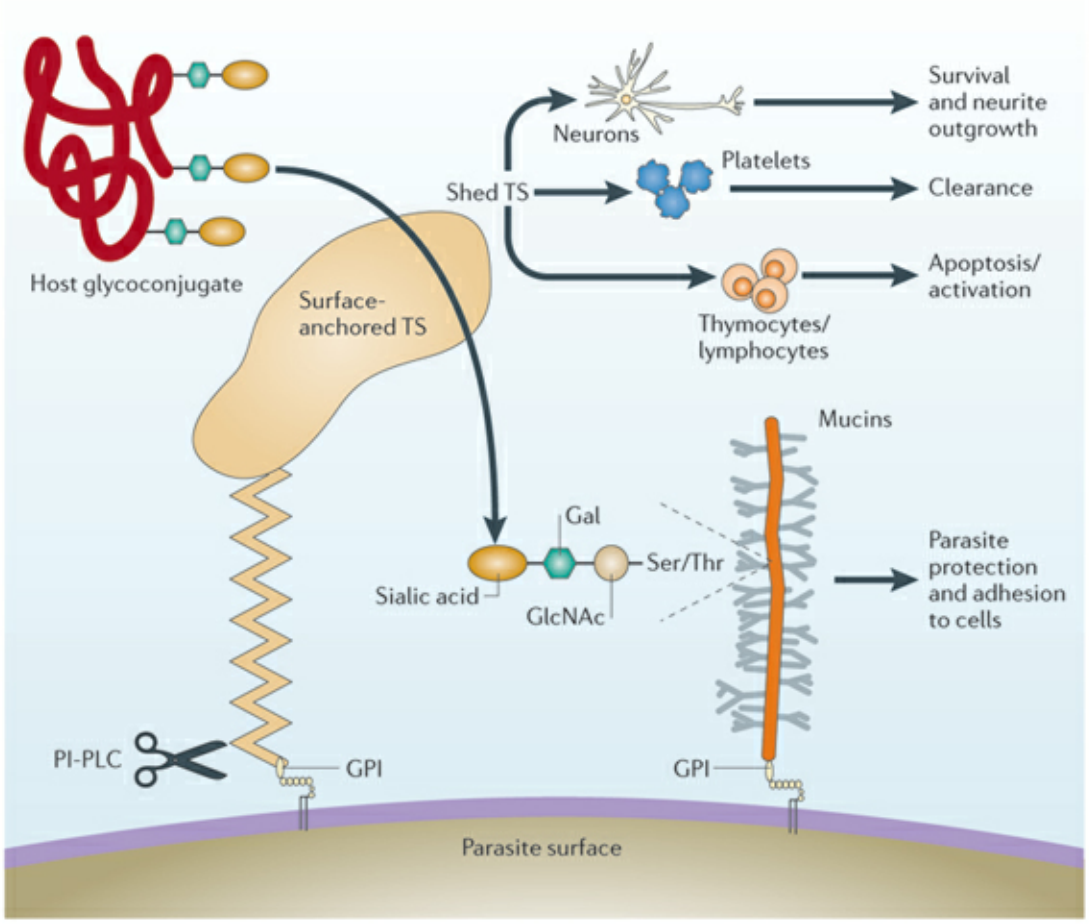

Figure 1-6. Trans-sialidase in *Trypanosoma cruzi.* Trans-sialidase is GPI-anchored on the parasite surface and transfer sialic acid residues from host glycoconjugates to the β-galactose on the parasite TcMUC group II thus, infers the parasite protection and cell adhesion. Shed trans-sialidase is enzymatically active and can trigger various biological outcomes in different cell types (2006 Buscaglia *et al.* Nature Reviews Microbiology).

The mucin gene repertoire shows greater genetic diversity than that of the trans-sialidases (TS) in terms of its complexity (Frasch 2000; Eugenia Giorgi and de Lederkremer 2011). *T. cruzi* mucins were named after mammalian mucins, due to their sequence similarity (Eugenia Giorgi and de Lederkremer 2011). The mucins on the surface of the *T. cruzi* are anchored to the outer leaflet of the plasma membrane through a glycosylphosphatidylinositol (GPI) anchor. The extensive O-glycosylation on mucin accounts for almost 60% of the molecular mass (Almeida, Ferguson et al. 1994; Previato, Jones et al. 1994; Buscaglia, Campo et al. 2006). Mucins are expressed throughout the *T. cruzi* life cycle (Buscaglia, Campo et al. 2006). Depending on the host environment, different mucins are expressed such as TcSMUG and TcMUC families. The TcSMUG family is relatively small in number (19 members) and size (35-50 kDa), homogenous and expressed in the epimastigote, the insect form of *T. cruzi*. However, TcMUC group I and II are much larger in number (844 members) and size (60-200 kDa) and expressed in the vertebrate stage. TcMUC group I and II were classified by repetitive and non-repetitive central regions (Di Noia, Buscaglia et al. 2002). The unique feature of TcMUC group II is its genomic location in subtelomeric region along with TS genes. Considering the polycistronic transcription in *T. cruzi*, there may be an important interplay between TS and Mucins (Campo, Buscaglia et al. 2006). Within the same large cluster of TS and TcMUC group II, a novel large *T. cruzi*-specific gene family was identified and they were frequently found downstream of TcMUC group II so the family was named mucin-associated surface protein (MASP) (El-Sayed, Myler et al. 2005).

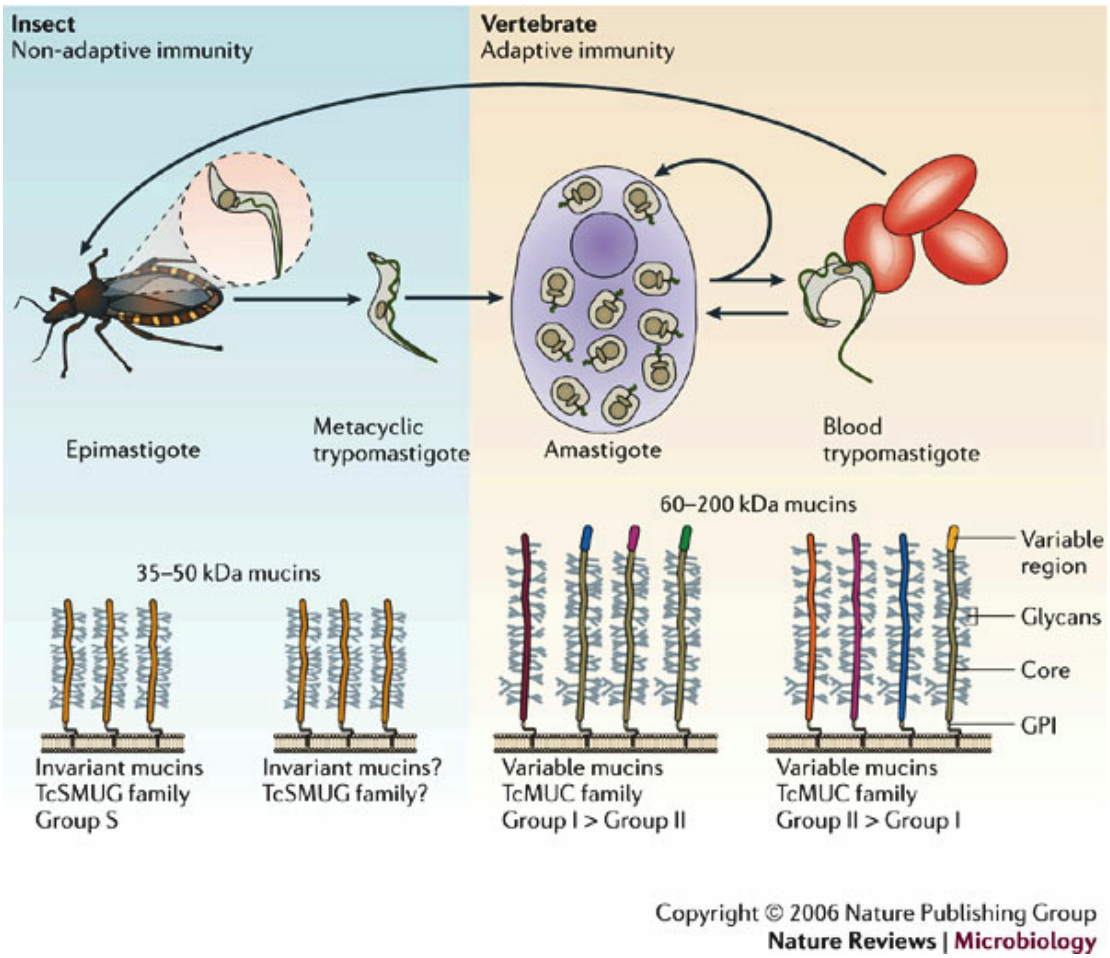

Figure 1-7. *T. cruzi* mucins during life cycle. Invertebrate-dwelling *T. cruzi* parasites display invariant mucins on the surface whereas vertebrate-dwelling *T. cruzi* parasites present bigger and variable mucins (2006 Buscaglia *et al.* Nature Reviews Microbiology).

One of the key functions of mucin, especially TcMUC group II, is the role as the acceptors of sialic acid (SA) from the host cell glycoconjugate (Buscaglia, Campo et al. 2006). Even though *T. cruzi* have several glycosyltransferases, it is unable to biosynthesize sialic acid. Instead they can utilize GPI-anchored TS and transfer sialic acid from the host sialoglycoconjugates to the terminal β–galactose on the highly O-glycosylated TcMUC group II. This ability is important for *T. cruzi* to invade the host cells and to escape from the parasitophorous vacuole. Also a thick layer of mucin on the surface is speculated to contribute to the parasite protection from complement-mediated lysis and improve the adhesion of *T. cruzi* to the host extracellular matrix. *T. cruzi* mucin does not have orthologs in other trypanosomes, *Trypanosoma brucei* and *Leishmania major.* It is noteworthy that the O-linked chains are connected to the protein by α–GlcNAc instead of α–GalNAc found in the majority of mammals (Eugenia Giorgi and de Lederkremer 2011). This unusual feature can help design drugs and target *T. cruzi* mucin specifically (Figure 1-7).

1.4.3 DGF-1

Dispersed Gene Family-1 (DGF-1) members constitute the fifth largest gene family in *T. cruzi* genome, consisting of 565 genes (El-Sayed, Myler et al. 2005). It is the third largest among *T. cruzi*-specific large gene families after MASP and mucin. The vast majority of this gene family is found in subtelomeric regions along with retrotransposon hotspot (RHS) proteins, transsialidases and many retroelements such as VIPER/SIRE and DIRE (El-Sayed, Myler et al. 2005). DGF-1 proteins harbor conserved adhesion motifs and they are localized on the surface of *T. cruzi* (Kawashita, da Silva et al. 2009), suggesting a possible role in binding to host

extracellular matrix protein such as fibronectin and laminin. In contrast, one of these proteins (DGF-1.2) was reported to localize intracellularly in different life cycles of *T. cruzi* and to be more abundant in amastigotes than epimastigotes or trypomastigotes (Lander, Bernal et al. 2010). DGF-1.2 was also detected in the culture medium indicating some level of secretion. The high copy number of this gene family in *T. cruzi* genome strongly implicates the importance of its role in *T. cruzi* biology but the putative function of DGF-1 gene family remain largely unknown.

1.4.4 MASP (mucin-associated surface protein)

The comparative analysis also includes a major discovery of a 1,377-gene family encoding the novel mucin-associated surface proteins (MASP). Despite its large size (the largest *T. cruzi*-specific multigenic family representing 1% of the whole diploid genome and 6% of the coding genes), the *masp* family has not been characterized to date. Many large gene families that encode surface antigens including MASP are clustered mainly in large, nonsyntenic subtelomeric regions that include trans-sialidase (TS) superfamily, RHS and DGF-1. Within these large clusters, *masp* genes are preferentially located downstream of mucins, especially TcMUC group II genes and so were named mucin-associated surface proteins although MASP and TcMUC group II only resemble each other in structure not in sequence (Figure 1-10) (El-Sayed, Myler et al. 2005; Bartholomeu, Cerqueira et al. 2009). MASP members contain N- and C-terminal conserved domains that encode a putative signal peptide and a GPI-anchor addition site respectively. The central region is variable both in its length and contents, and contains a large repertoire of repetitive motifs (Figure 1-9 A). In contrast to the highly heterogeneous coding region, *masp* mRNAs show highly

conserved 5' and 3' untranslated regions (UTRs) (Figure 1-8 A). Western blots of phosphatidylinositol specific phospholipase C (PI-PLC)-treated parasites suggest that MASP is GPI-anchored and can be cleaved upon PI-PLC treatment. The presence of MASP in the culture medium even without PI-PLC treatment indicates that MASP can be shed or secreted into the bloodstream. MASP transcripts were preferentially expressed during the trypomastigote (bloodstream form) stage (Figure 1-8 B). Interestingly, despite the large number of genes, an examination of the expression profile of *masp* using trypomastigote cDNA library reveals that a subset of *masp* members is preferentially expressed in a parasite population at a specific time point, demonstrating that multiple *masp* members can be expressed in a population unlike VSG proteins in *T. brucei* and that the expression is biased toward a subset of members that might depend on the host cells. MASP protein was also predominantly expressed in the trypomastigotes, confirming its differential expression and the regulation of the MASP family during the life cycle (Figure 1-9 B). Immunofluorescence assay revealed the subcellular location of MASP to surface of the *T. cruzi* as expected presumably by GPI-anchor (Figure 1-9 C). MASP proteins were predicted to have multiple N- and O-glycosylation sites based on *in silico* analysis. Extensive posttranslational modifications of MASP, including possible heavy glycosylation, may explain why MASPs were not previously discovered using proteomic approaches (Atwood, Minning et al. 2006; Parodi-Talice, Monteiro-Goes et al. 2007; Nakayasu, Yashunsky et al. 2009).

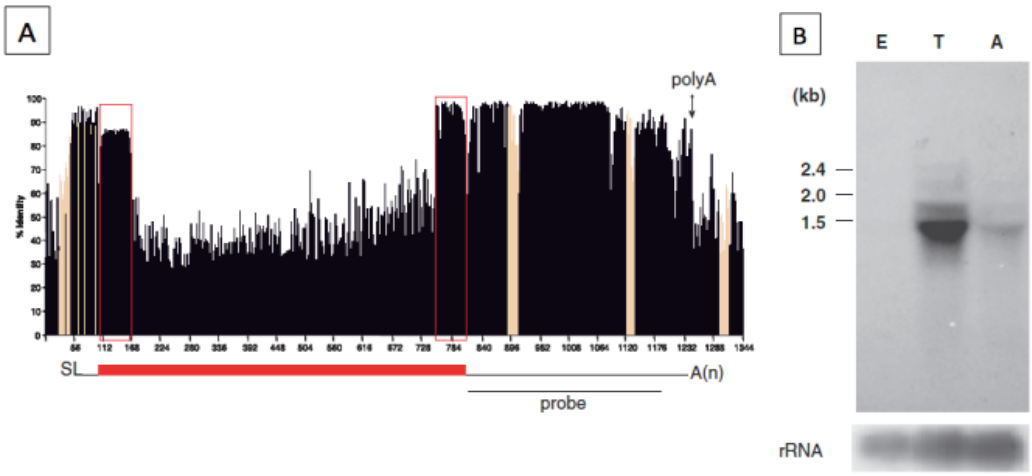

Figure 1-8. MASP mRNA transcript features. (A) Alignment of all 771 MASP full-length transcripts. The coding region is represented by a red box and the UTRs by black lines (B) Northern blot analysis with total RNA isolated from epimastigotes, E, trypomastigotes, T and amastigotes, A probed with the conserved 3' UTR region (indicated in Figure 1-9 A) (Bartholomeu *et al.* NAR 2009).

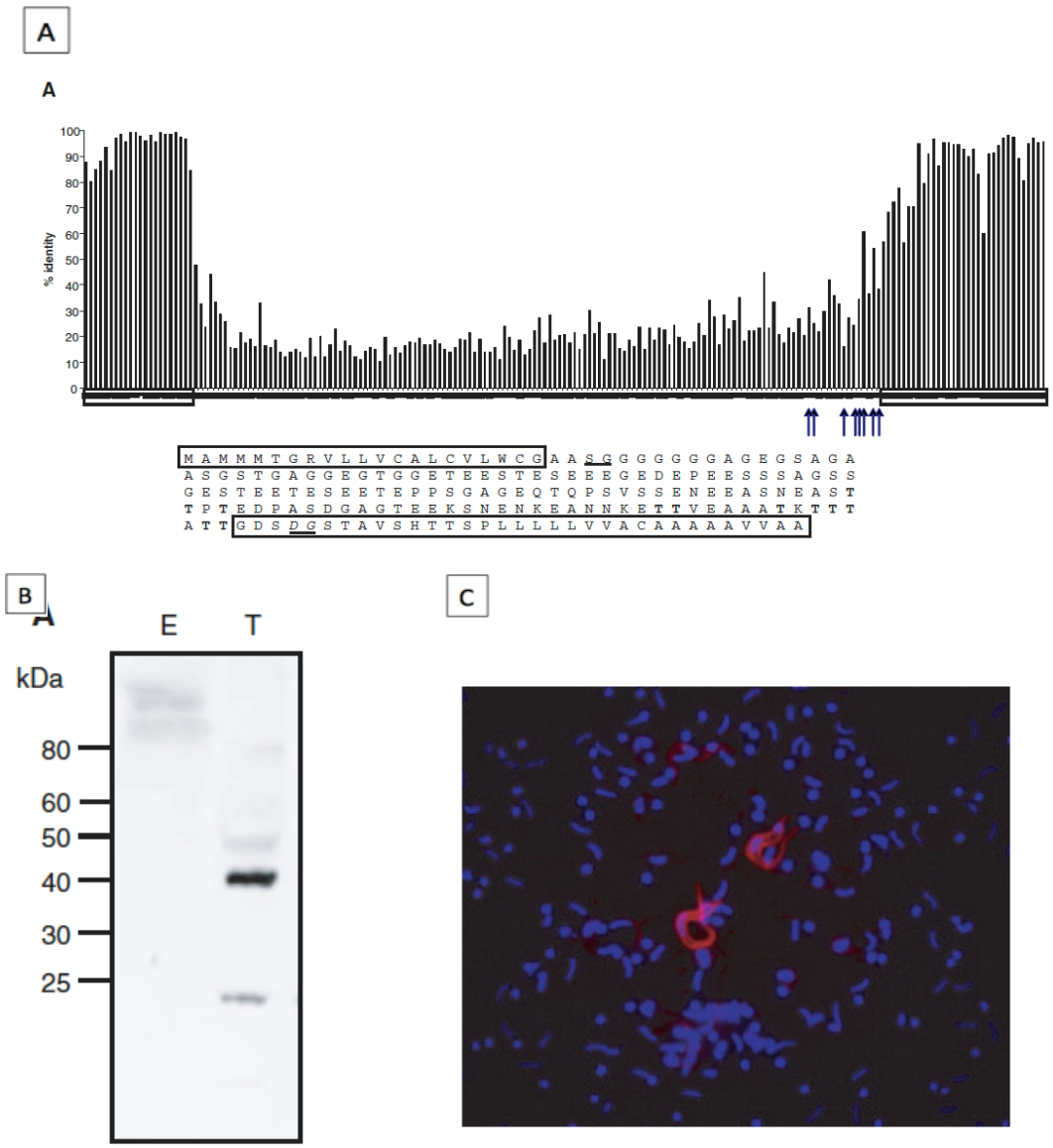

Figure 1-9. MASP protein features. (A) All 771 MASP protein sequence alignment using ClustalW algorithm. (B) Western blot analysis of total protein extracts from the epimastigote, E, and trypomastigote, T, forms using anti-MASP peptide 7 antibodies (C) IFA assay of trypomastigotes incubated with anti-MASP peptide 7 antibodies (Red), nucleus and kinetoplastid DNA were stained with DAPI (Blue) (Bartholomeu *et al.* NAR 2009).

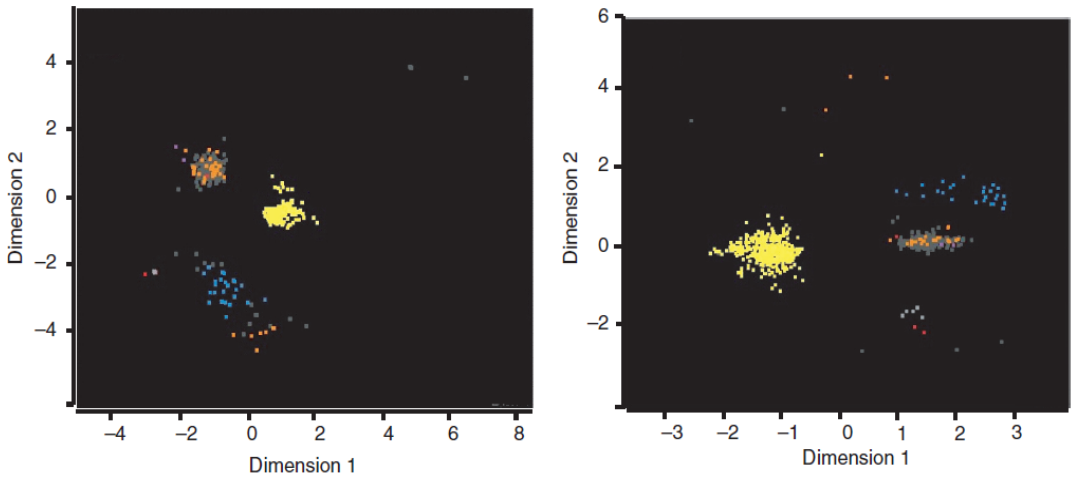

Figure 1-10. Sequence similarity between multigenic families in *T. cruzi*. Multidimensional scaling plot representing the matrix of distance among the sequences derived from the N- (right panel) and C-terminal (left panel) conserved domains from MASP (yellow), TcMUCI (dark gray), TcMUCII (orange), TcMUCIII (pink), TcSMUGS (light gray), TcSMUGL (red) and SAP genes (turquoise) (Bartholomeu *et al.* NAR 2009).

Recently, MASP52, a 52-kDa protein secreted from the trypomastigote form of *T. cruzi*, was identified and characterized that it is involved in *T. cruzi* infectivity as IgG antibodies against the catalytic region of MASP52 protein decreased the *T. cruzi* invasion rate and the MASP52-coated bentonite particles were phagocytosed by the host cells (De Pablos, Gonzalez et al. 2011). Using the antibodies against the signal peptide of this *masp* family, a differential expression of MASP during the *T. cruzi* life cycle was confirmed as previously described (Bartholomeu, Cerqueira et al. 2009). Interestingly MASP52 was found in the culture medium only when *T. cruzi* were incubated with the host cells indicating the shedding or secretion of MASP is promoted by the interaction with the host cells.

1.4 SNAPIN

SNAPIN was originally identified in 1999 as a neuronal SNAP-25-binding protein by a yeast two-hybrid screen of a human brain cDNA library using SNAP-25 as bait (Ilardi, Mochida et al. 1999). Later it turned out SNAPIN not only binds to SNAP-25 but so does its ubiquitously expressed homolog SNAP-23 indicating that SNAPIN might be a general component of the SNARE (Soluble NSF Attachment Protein Receptor) machinery not necessarily in limited to neuronal cells (Buxton, Zhang et al. 2003). SNAPIN is a 136 amino acid protein that is characterized by an amino-terminal hydrophobic domain, a potential transmembrane domain and a carboxyl-terminal coiled-coil domain (Gowthaman, Silvester et al. 2006). SNAPIN mediates the activation of synaptotagmin, the calcium sensor in the regulation of neurotransmitter release and enhances the association of synaptotagmin to the SNARE complex thus stabilizing the binding of the Synaptotagmin-SNARE protein

complex (Chheda, Mochida et al. 1999). The interacting domain of SNAPIN to SNAP-25 and SNAP-23 proteins was determined to be the coiled-coil domain in the carboxyl-terminus. The peptide of this domain blocks the binding of full-length SNAPIN to SNAP-25 and SNAP-23 and thus reduces synaptic transmission. SNAPIN activity is regulated by phosphorylation specifically at serine 50 by Protein Kinase A (PKA) (Thakur, Stevens et al. 2004). When this serine was mutated to an aspartic acid (S50D), a constitutive mutant, the association with SNAP-25 was increased whereas serine to alanine (S50A), a dominant negative mutant, showed reduced vesicle-mediated neurotransmitter release event. The study using SNAPIN knockout mice demonstrated that calcium-dependent exocytosis in chromaffin cells was significantly decreased (Tian, Wu et al. 2005) possibly due to the critical function of SNAPIN in priming large dense-core vesicles for fusion to neuronal plasma membrane and in facilitating synchronized fusion of synaptic vesicles in neurons (Pan, Tian et al. 2009). More recently, it was suggested that SNAPIN is involved in the late endosome transport and lysosome maturation by interacting with dynein motor complex and the maintenance of autophagic-lysosomal function in neurons (Lu, Cai et al. 2009; Cai, Lu et al. 2010).

It is very interesting that at least 20 proteins were reported to be SNAPIN interacting partner proteins demonstrating that SNAPIN might be an important scaffold protein participating in a number of cellular processes in various cell types. Other than SNARE proteins such as SNAP-25, SNAP-23 and synaptotagmin, SNAPIN was shown to be associated with the biogenesis of lysosome-related organelles complex-1 (BLOC-1) regulating the normal biogenesis of specialized organelles such as

melanosomes and platelet dense granules (Starcevic and Dell'Angelica 2004). The ryanodine receptor (RyR), a calcium channel located in the ER and one of the players in calcium-induced calcium influx and/or calcium release from internal stores, interacts with SNAPIN (Zissimopoulos, West et al. 2006). Cypin, a dendrite patterning protein, also interacts with SNAPIN and competes with tubulin for binding (Chen, Lucas et al. 2005). RGS7 (regulater of G-protein signaling 7) is a GTPase and binds to SNAPIN indicating a possible role of SNAPIN in G-protein signaling modulator (Hunt, Edris et al. 2003). SNAPIN can associate with the Exo70 subunit of the exocyst in regulating the trafficking and fusion of GLUT4 vesicles in adipocytes (Bao, Lopez et al. 2008). Other SNAPIN interactors include UT-A1 urea transporter (Mistry, Mallick et al. 2007), the transient receptor potential canonical family (TRPC6) (Suzuki, Morishima et al. 2007), dysbindin-1 and adenylyl cyclase VI (AC6) (Wang, Lin et al. 2009).

Additional layers of SNAPIN regulation were discovered other than PKA phosphorylation. Casein kinase 1 delta (CK1δ) can phosphorylate SNAPIN and estrogen receptor-binding fragment-associated gene 9 (EBAG9) can bind to the domain of SNAPIN containing the phosphorylation site and regulate the function (Ruder, Reimer et al. 2005).

1.5 Summary of dissertation work

The long-range goal of this project was to better understand the biology of the human parasite *Trypanosoma cruzi*, particularly focusing on the role of surface proteins in invasion and survival inside human host cells. *T. cruzi* is a kinetoplastid protozoan and presents a remarkable capacity to invade almost every nucleated cell. This

unusual ability gives *T. cruzi* access to the cytoplasm, which is critical for its survival and replication. One of the primary surface proteins in the infective form of *T. cruzi*, known as the Mucin-Associated Surface Protein (MASP), is encoded by a *T. cruzi*-specific large multigenic family recently identified during the genome sequencing of *T. cruzi* CL Brener strain, the etiological agent of Chagas disease or American trypanosomiasis. This family consists of approximately 1,377 members that make up 6% of all coding genes in the genome, suggesting that it has an important role in *T. cruzi* biology (El-Sayed, Myler et al. 2005; El-Sayed, Myler et al. 2005). The structure of MASPs is characterized by highly conserved amino- and carboxyl-terminal domains encoding a signal peptide and GPI-anchor addition site respectively, and a hypervariable central region. Northern and Western blot analyses reveal that this family is predominantly expressed in the trypomastigote, the infective form of *T. cruzi*. Genome-scale microarray analysis indicates that steady-state MASP transcripts are highly expressed in the tissue-culture derived trypomastigote (TCT) form. In addition, *in silico* predictions suggest that MASP proteins are heavily glycosylated (7 sites per sequence in average) and GPI anchored (Bartholomeu, Cerqueira et al. 2009). The role of the *T. cruzi* surface protein family MASP remained largely unknown. Based on previously reported results by our lab (El-Sayed), I hypothesized that members of the *T. cruzi* MASP protein family play a major role in the interaction of the parasite with the host cell. To test my hypothesis, I utilized molecular, genetic and cell biological approaches to investigate the role of the MASP family in host cell invasion.

The MASP family is predominantly expressed in *T. cruzi* trypomastigotes, the infective form of the parasite. In addition, members of this family are localized on the surface of the parasite by GPI-anchor (Bartholomeu, Cerqueira et al. 2009). Taken together, this evidence suggests that MASP could be involved in a host cell invasion process by interacting with human partner proteins. The experiments documented in Chapter 2 identified interacting partner proteins of MASP proteins in the human proteome using yeast two-hybrid (Y2H) screen and confirm interactions by *in vivo* co-affinity purification (co-AP) and *in vitro* pull-down assays.

Preferential MASP expression in the infective stage (trypomastigote), as well as its cellular localization (Bartholomeu, Cerqueira et al. 2009), suggests a possible role of MASP in host cell invasion. Depleting endogenous MASP and overexpressing MASP in *T. cruzi* will help evaluate the role of MASP family and determine its biological relevance in the process of host cell invasion. Depletion or deletion of its human interacting partner protein would also allow us to investigate the function of putative MASP human interactors during *T. cruzi* invasion process. Therefore, my experiments documented in Chapter 3 were aimed at the investigation of a putative role of MASP human interacting partner proteins in the host cell invasion process using RNA interference (RNAi) technology, gene knockout primary cell lines, parasite invasion assay, co-localization studies and biochemical enzymatic tools. In addition, my experiments described in Chapter 4 were aimed at examining the putative function of MASP in the host cell invasion using MASP overexpression, protein purification, *in vitro* pull-down assays, live cell imaging and gene knockdowns.

Although more than a thousand genes in the *T. cruzi* genome encode MASP, we (The El-Sayed lab) have previously shown that only a small subset of this family is expressed in the trypomastigote cell population at a certain time point. Also the immunofluorescence data strongly suggests that MASP expressed is biased towards a subset of members (Bartholomeu, Cerqueira et al. 2009). To enter a wide variety of non-professional phagocytic cells, trypomastigotes seem to exploit heterogeneous glycoproteins such as mucin, trans-sialidase and GP85 (Buscaglia, Campo et al. 2006). However, the MASP expression pattern is still not clear. Our experiment documented in Chapter 5 studied the expression profile of *masp* genes and determined a subset of MASPs that correlates with host cell selection using the trypomastigote cDNA library and RNA-seq technology.

1.6 Significance

The *masp* family contains around 1,377 members and 771 intact genes, which consist of 6% of all coding genes in the *T. cruzi* genome implying its important role in *T. cruzi* biology. MASP is expressed preferentially in the trypomastigote form (infective stage) of *T. cruzi* on the plasma membrane by GPI-anchor, thus suggesting an important role in host cell invasion. Elucidation of the role of MASP in *T. cruzi* as well as its human interacting partner protein will help us better understand the biology of *T. cruzi* and its interactions with the mammalian host, knowledge which can eventually improve the public health in the developing countries where research funds for the development of drugs and vaccines are limited .

Chapter 2: Identification of interacting partner proteins of MASP proteins in the human proteome

2.1 Objective of Study

The MASP family is predominantly expressed in *T. cruzi* trypomastigotes, the infective forms of the parasite. In addition, at least some members of this family are localized on the surface of the parasite and attached through GPI-anchors. Taken together, this evidence suggests that MASP could be involved in a host cell invasion process by interacting with human partner proteins. We aimed to identify human interacting partner protein(s) of *T. cruzi* MASP proteins via yeast two-hybrid screens and other biochemical protein-protein interaction assays.

2.2 Materials and Methods

2.2.1 Materials

Materials	Catalogue numbers	Sources
Pretransformed normalized Matchmaker Human Universal cDNA Library	638874	Clontech
Glutathione-Uniflow Resin	635610	
Drop Out Supplement –Ade/–His/–Leu/–Trp	630428	
Drop-out Mix Synthetic Minus Leucine (SC-L)	D9526	United States Biological
Drop-out Mix Synthetic Minus Tryptophan (SC-T)	D9530	
Drop-out Mix Synthetic Minus Leucine, Tryptophan (SC-LT)	D9537	
Drop-out Mix Synthetic Minus Leucine, Tryptophan, Histidine (SC-LTH)	D9539	
X-α-Gal	B2175-05	
Human Embryonic Kidney 293 T (HEK293T)		Dr. Iqbal Hamza (University of Maryland, College

		Park)
pGBKT7g and pGADT7g vectors		Dr. Peter Uetz (Virginia Commonwealth University)
pGEX-5 vector		Dr. Vincent Lee (University of Maryland, College Park)
Heat-inactivated BenchMark™ Fetal Bovine Serum (FBS)	100-106	Gemini Bio-Products
Gateway® pDEST™27	11812-013	Invitrogen
Gateway® pDEST™26	11809-019	
Gateway® pDEST™15	11802-014	
Gateway® pDEST™17	11803-012	
Gateway® pDONR™/Zeo	12535035	
Gateway® BP Clonase® II Enzyme mix	11789100	
Gateway® LR Clonase® II Enzyme mix	11791100	
E. coli BL21-AI strain	C607003	
Pfx50™ DNA polymerase	12355012	
Ni-NTA Agarose resin	R90101	
Lipofectamine™ 2000	11668-019	
mouse anti-GST monoclonal antibodies	136700	
CCSB Human ORFeome (hORFeome) Collection (Releases 1+2)	OHS4297	Open Biosystems
Zymoprep™ Yeast Plasmid Miniprep II	D2004	Zymo Research
Biomek® FXP Laboratory Automation Workstation	A31842	Beckman Coulter
3-Amino-1,2,4-triazole (3AT)	A8056	Sigma-Aldrich
mouse anti-c-Myc antibody	M4439	
DNase I	M0303	New England BioLabs
Lysozyme	4403	Calbiochem®
Dulbecco's Modification of Eagle's Medium (DMEM)	15-013	Cellgro
Protease Inhibitor Cocktail Set I	539131	Qiagen.
Mouse anti-His monoclonal antibody	34660	

2.2.2 Methods

Host cells and Yeast cells: HEK293T (Human Embryonic Kidney 293 T) cells were maintained in Dulbecco's Modification of Eagle's Medium (DMEM) supplemented with 10% heat inactivated Fetal Bovine Serum (FBS) at 37ºC with 5% CO_2. *Saccharomyces cerevisiae* strains AH109 and Y187 were cultured on YPAD agar plate at 30ºC in a humid incubator.

Protein-protein interaction screens, generating bait and prey plasmids: Primers (See Appendix B.1 for sequence) were designed to anneal to the first and last 20 nt of the coding sequence (CDS) in *T. cruzi* MASP1 (Tc00.1047053504587.30/6336.m00003) and MASP4 (Tc00.1047053509979.350/8263.t00035) Open Reading Frames (ORFs). Stop codons were excluded from reverse primer sequences to allow downstream cloning into vectors with C-terminal fusion tags. Primers also included *att*B overhang sequences providing the recombination sites for Gateway® universal cloning (Invitrogen). *T. cruzi* MASP genes were amplified by the polymerase chain reaction using the *Pfx50*™ DNA polymerase according to the manufacturer's instructions. Thermal amplification consisted of an initial denaturation step at 94ºC for 2 minutes, followed by 25 cycles of denaturation at 94ºC for 20 seconds, annealing at 60ºC for 45 seconds (decreased by 0.2ºC per cycle), and extension at 68ºC for 90 seconds (increased by 3 seconds per cycle), followed by another 10 cycles of denaturation at 94ºC for 15 seconds, annealing at 55ºC for 45 seconds and extension at 68ºC for 150 seconds, with a final extension step of 68ºC for 10 minutes. Amplicons were cloned into the pDONR™/Zeo vector and plasmids were submitted for sequencing of both ends using M13 Forward

and M13 Reverse primers. Inserts were also shuttled in parallel to the GAL4 DNA Binding Domain (GAL4 DBD) bait vector, pGBKT7g.

Two human libraries served as prey in independent screens: 1) Pretransformed normalized Matchmaker Human Universal cDNA Library and 2) hORFeome 3.1 (a 12,000 human ORF collection cloned into a Gateway recombinational entry vector).

Yeast transfection, mating and screening: *Saccharomyces cerevisiae* strains AH109 (*MATa, trp1-901, leu2-3, 112, ura3-52, his3-200, gal4*Δ*, gal80*Δ*, LYS2::GAL1*$_{UAS}$*-GAL1*$_{TATA}$*-HIS3, GAL2*$_{UAS}$*-GAL2*$_{TATA}$*-ADE2, URA3::MEL1*$_{UAS}$*-MEL1*$_{TATA}$*-lacZ, MEL1*) and Y187 (*MAT*α*, ura3-52, his3-200, ade2-101, trp1-901, leu2-3, 112, gal4*Δ*, met–, gal80*Δ*, MEL1, URA3*::*GAL1*$_{UAS}$ *-GAL1*$_{TATA}$*-lacZ*) were used and transfected with bait and prey vectors, respectively, according to the ProQuest™ Two-Hybrid System transfection protocol (Invitrogen).

Two MASP test baits, pGBKT7g-MASP1 & pGBKT7g-MASP4, and control bait, pGBKT7-p53, were screened against the pretransformed normalized Matchmaker Human Universal cDNA Library according to the manufacturer's instructions. Briefly, bait plasmids were transfected into AH109 (MATa strain) and the transfectants were selected on SC-Trp (SC-T) plates. One fresh and large bait colony was inoculated into 50 mL of SC-T liquid medium and incubated at 30ºC with shaking (250 rpm) until OD_{600} reached 0.8. The cells were harvested at 1,000x *g* for 5 minutes and resuspended in 5 mL SC-T. The 5 mL bait cells were combined with 1 mL of Y187 (MATα strain) pretransformed cDNA library and added to 45 mL of 2X YPAD liquid medium. Combined bait and prey cells were incubated at 30ºC for 20~24 hours with shaking (30 rpm). Mated diploid cells were pelleted at 1,000x *g* for 10 minutes and

resuspended in 10 mL 0.5X YPAD. The resuspended diploid cultures were spread onto 150 mm SC/-Ade/-His/-Leu/-Trp/X-α-Gal (Quadruple Drop-Out [QDO]+X-α-Gal) agar plates and incubated for a week at 30ºC. Positive blue colonies were picked and further cultured in SC/-Leu/-Trp (SC-LT). Positive bait and prey plasmids were isolated by Zymoprep™ Yeast Plasmid Miniprep II and isolated prey plasmids were identified by sequencing the insert using T7 primer (5'-TAATACGACTCACTATAGGG-3'). Preys identified as TP53 positive interactors were confirmed against known TP53 interactors in the IntAct database (http://www.ebi.ac.uk/intact/).

For screens against the human ORFeome, pools of 128 AD fusion proteins were shuttled from hORFeome 3.1 into the GAL4 AD prey vector pGADT7g, transfected into the Y187 yeast strains, selected on SC-Leu (SC-L) media and re-arrayed into a 96-well format. Mating of the yeast strains was carried out in Nunc™ OmniTrays containing solid media and performed on a Biomek® FXp laboratory automation workstation equipped with a 96-pin tool. Baits (AH109 yeast strain harboring pGBKT7g-MASP1 or pGBKT7g-MASP4), and preys were transferred onto selective media (SC-T and SC-L, respectively) and grown for 2 days at 30ºC. Mating was carried out by transferring bait and prey cells onto the same spot on the OmniTray containing complete media (YPAD), followed by a 16-hour incubation at 30ºC. Following mating, colonies were transferred to SC-Leu-Trp (SC-LT) media to select for diploid cells containing both bait and prey plasmids. Positive and negative controls for protein interaction were added to those plates. Diploid cells transfected with each bait vector and a control prey vector (containing no insert) were used to test

for auto-activation of the HIS3 reporter gene. Colonies were cultured on multiple plates containing SC-Leu-Trp-His (SC-LTH) and distinct concentrations of 3-Amino-1,2,4-Triazole (3AT) in order to determine 3AT sensitivity and the optimal 3AT concentration for efficient HIS3 inhibition. For each of the baits, the concentration of 3AT, which provided minimal growth, comparable to a negative control, was later used to suppress auto-activation. Bait/prey coding genes clones in the pGBKT7g/pGADT7g vector system were evaluated with 3AT concentrations of in 0, 2.5, 5.0, 7.5, 10.0, 12.5, 15.0 and 25.0 mM. Diploid cells containing bait and prey vectors were transferred to SC-LTH media lacking adenine and complemented with 40 µg/ml of X-α-Gal and appropriate 3AT concentration, enabling the evaluation of 3 different gene reporters at once. Cells were incubated at 30°C and inspected over a period of one week. Diploid cells that exhibited the phenotype associated with the expression of three gene reporters were assigned as positives.

In vivo co-affinity purification (co-AP) assays: Commercially available full-length human Snapin ORFwas shuttled from pDONR™/Zeo into the mammalian expression vector pDEST™27 containing an N-terminal glutathione *S* transferase (GST) tag. MASP1 and MASP4 fragments lacking the signal peptide and GPI anchor addition site (described in Figure 2-8) were cloned into pDONR™/Zeo and recombined into pDEST™26 containing an N-terminal 6xHis tag. Empty pDEST™27 served as a negative control. The interacting protein pairs of GST-bait (GST alone, GST-sMASP1 and GST-sMASP4) and 6xHIS-prey (6xHIS-Snapin) were co-transfected into HEK293T using Lipofectamine™ 2000 according to the manufacturer's instructions. Cells were harvested 48 hours after transfection and incubated on ice for

30 minutes with lysis buffer containing 1% NP-40, 50 mM Tris-HCl pH 7.5, 150 mM NaCl, 1 mM EDTA, 1 mM Phenylmethylsulfonyl fluoride (PMSF) and a cocktail of additional protease inhibitors. Cell lysates were cleared by centrifugation at 15,000x g for 15 minutes at 4°C, and soluble protein complexes were purified using Glutathione-Uniflow Resin. Resin-protein complexes were washed extensively with cell lysis buffer and analyzed by SDS-PAGE. GST- and 6xHis-tagged proteins were detected by standard immunoblotting techniques using mouse anti-GST and anti-His monoclonal antibodies.

In vitro Pull-down assays: Full-length *T. cruzi* MASP1 and MASP4 ORFs and *snapin* ORF were cloned into bacterial expression vectors pDEST™15 harboring an N-terminal GST tag and pDEST™17 harboring a C-terminal 6xHis tag, respectively. pGEX-5 vector was used to express the GST protein as a negative control. The expression vectors were transformed into *E. coli* BL21-AI strain according to the manufacturer's instructions. Transformants were cultured for 3 hours at 37ºC and 225 rpm until the logarithmic phase and the recombinant protein expression was induced by addition of L-arabinose to the final of 0.2%. Cells were harvested by centrifugation 4 hours after induction and lysed in lysis buffer (50 mM Potassium Phosphate, pH 7.8, 400 mM NaCl, 100 mM KCl, 10% glycerol, 0.5% Triton X-100, 10 mM Imidazol) supplemented with DNase I and lysozyme. Cell lysates were cleared by centrifugation and each supernatant fraction was combined with another interaction pair. After 1-hour incubation at 4ºC, interacting protein complexes were purified by Ni-NTA agarose resin and analyzed by SDS-PAGE followed by standard immunoblotting techniques.

2.3 Results and Discussion

2.3.1 Yeast two-hybrid screening identified human SNAPIN as a putative MASP interacting protein

To identify the putative human interacting partner proteins of *T. cruzi* MASP protein family, two distinct yeast two-hybrid prey libraries were employed: the normalized human cDNA library and the full-length open reading frame (ORF) collection (human ORFeome corresponding to ~12,000 protein coding genes) (Rual, Venkatesan et al. 2005; Lamesch, Li et al. 2007). To reduce the abundant transcripts, normalization of a mixture of poly-A RNAs from a collection of male and female tissues was performed using kamchatka crab duplex-specific nuclease (DSN) and the normalized human cDNA library was available as pretransformed in yeast Y187 (MATα) strain. MASP1 was initially chosen as bait among 771 MASP family members because the high expression of this member was reported in our previous *T. cruzi* trypomastigote cDNA library screening study (Bartholomeu, Cerqueira et al. 2009) (Figure 2-2). MASP4 was selected as an additional representative of the family due to its different size (estimated molecular weight of MASP1 is 16 kDa and MASP4 is 32kDa) and a different central domain composition from MASP1 (Figure 2-4) although it still retains the conserved N-terminal (amino acids 1-28 in both MASPs) and C-terminal domains (amino acids 126-177 in MASP1 and 270-321 in MASP4) that are one of the characteristics of MASP multigenic family (Figure 2-3). The two MASP ORFs were amplified directly from the *T. cruzi* CL Brener genome with a pairs of gene-specific primers containing *attB* sequence overhangs for the following BP reaction to yield the entry clones (pENTR™/Zeo-*masp*).

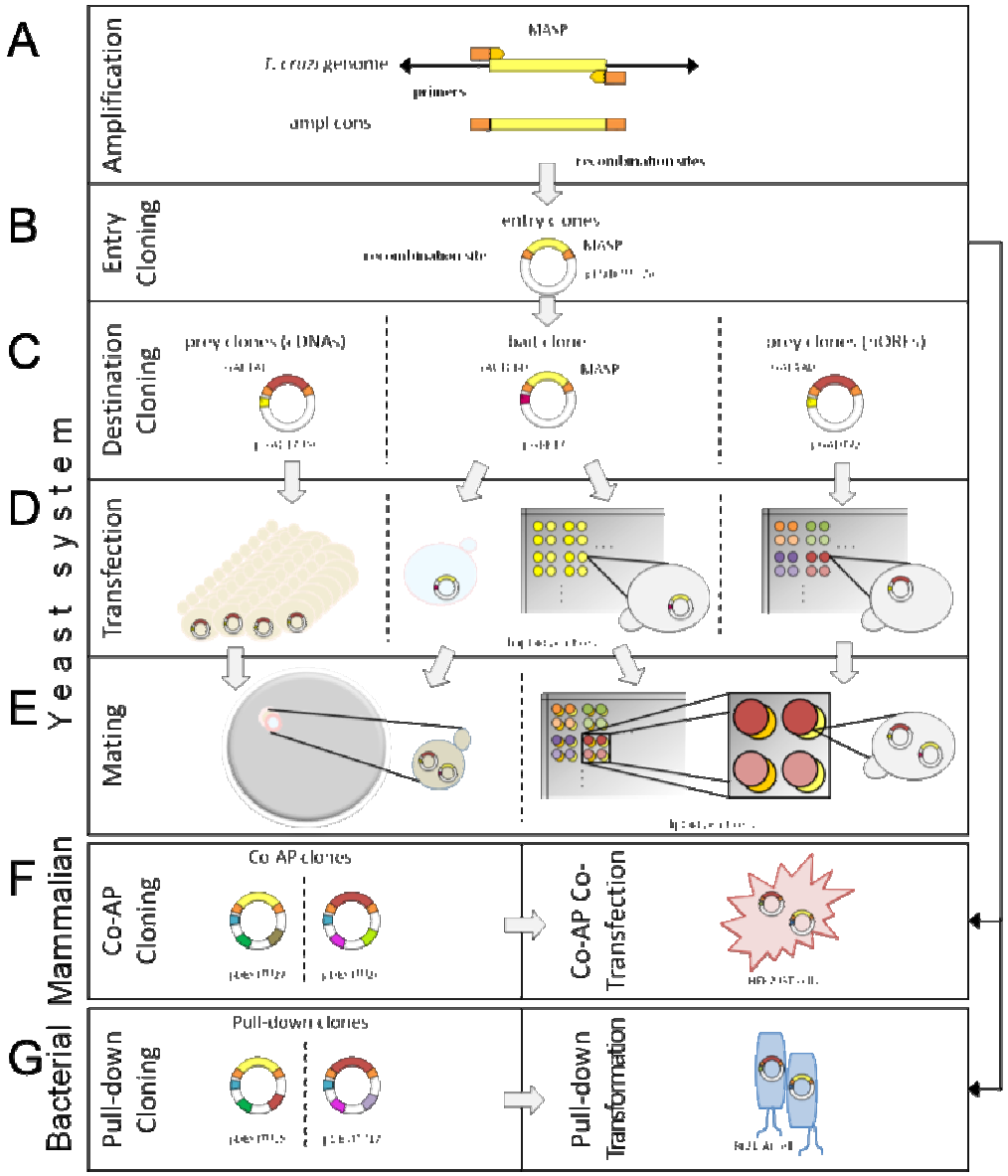

Figure 2-1. Y2H screen pipeline and validation of PPIs in two heterologous systems. (A) Amplification: *masp* genes, *masp1* (Tc00.1047053504587.30/6336.m00003) and *masp4* (Tc00.1047053509979.350/8263.t00035), were amplified from *T. cruzi* genomic DNA using gene-specific primers preceded by *att*B recombination site for the Gateway® cloning system. (B) Entry cloning: *masp* amplicons were recombined into the Gateway® pDONR™/Zeo vector, which contains *att*P recombination sites by BP

reaction. (C) Destination cloning: *masp1* and *masp4* were then shuttled to the pGBKT7g vector (bait) by LR reaction. Human ORFs in the entry vectors were pooled and recombined into pGADT7g (prey) as a batch. (D) Transfection: Bait and prey clones were transfected into yeast cells, AH105 (MATa) and Y187 (MATα), respectively and plated on media lacking Tryptophan or Leucine for the selection. Prey clones containing normalized human universal cDNAs were provided as a pre-transformed library (Clontech) (left) and pools of 128 ORFs from hORFeome 3.1 were transfected into Y187 (MATα) yeast strain and selected on media lacking Leucine in a 96-well format (right). (E) Mating: Transfected yeast haploid cells were mated for 24 hrs and plated on the selective media lacking Tryptophan, Leucine, Adenine, and Histidine but supplemented with X-α-gal for the screen (left). For hORFeome library, mating of the yeast strains were perfomed on a robot using a 96-pin. Bait and Prey were spotted onto selective media lacking Tryptophan and Leucine and grown for two days and subsequently transferred to the selective media lacking Tryptophan, Leucine, Adenine, and Histidine but supplemented with X-α-gal for the screen (right) (F) co-AP: Interactions identified from the previous Y2H screen were validated by a co-Affinity Purification (co-AP) method in HEK293T cells using pDEST™27 (bait) and pDEST™26 (prey) vectors. (G) Pull-down: Parallel evaluation of the interaction was conducted in *E. coli BL21-AI* strain using pDEST™15 (bait) and pDEST™17 (prey) vectors.

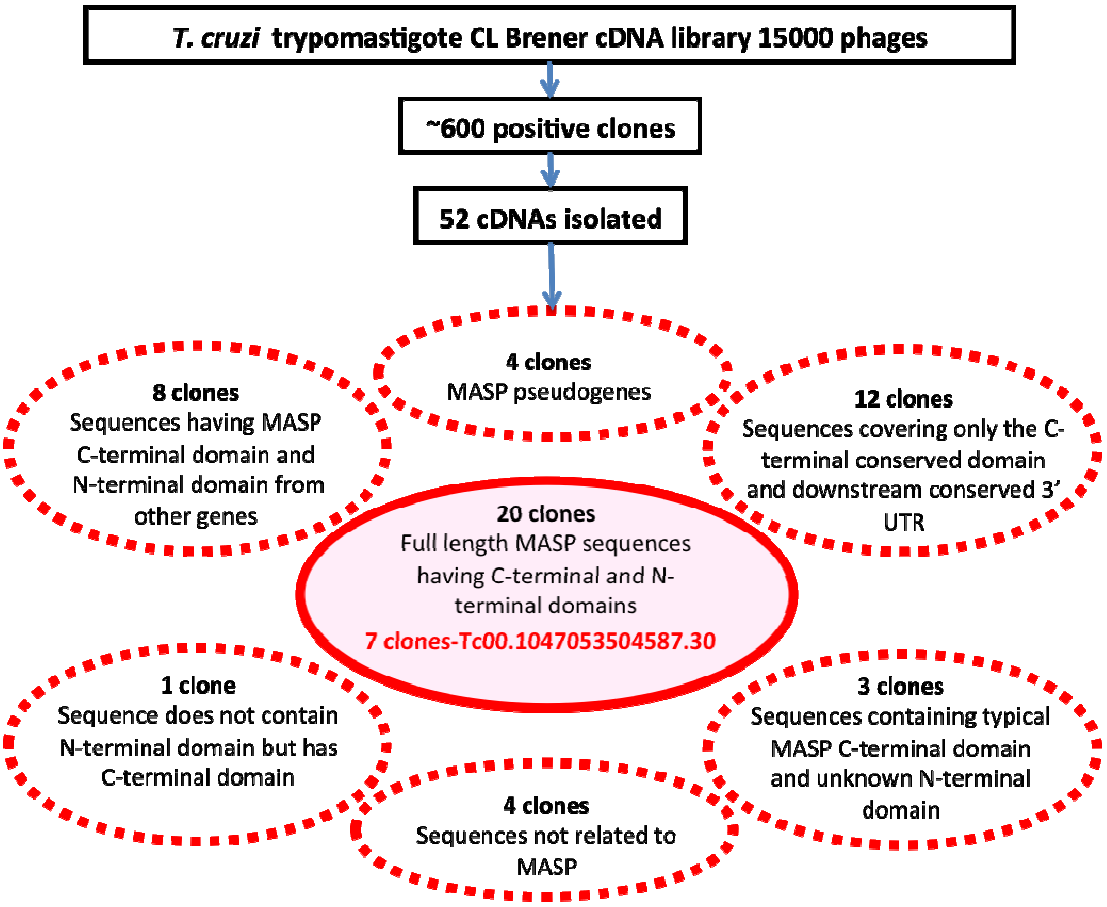

Figure 2-2. *masp* expression profiling in trypomastigote population. A *T. cruzi* CL Brener strain trypomastigote cDNA library was probed with 3' UTR conserved region and 15,000 phages were screened generating around 600 positive clones (~ 4%). 52 cDNA clones were sequenced and BLASTed against *T. cruzi* genome. This analysis revealed 20 clones of full-length MASP sequences where one copy (*masp1*, Tc00.1047053504587.30) was enriched (modified from 2009 Bartholomeu *et al.* NAR).

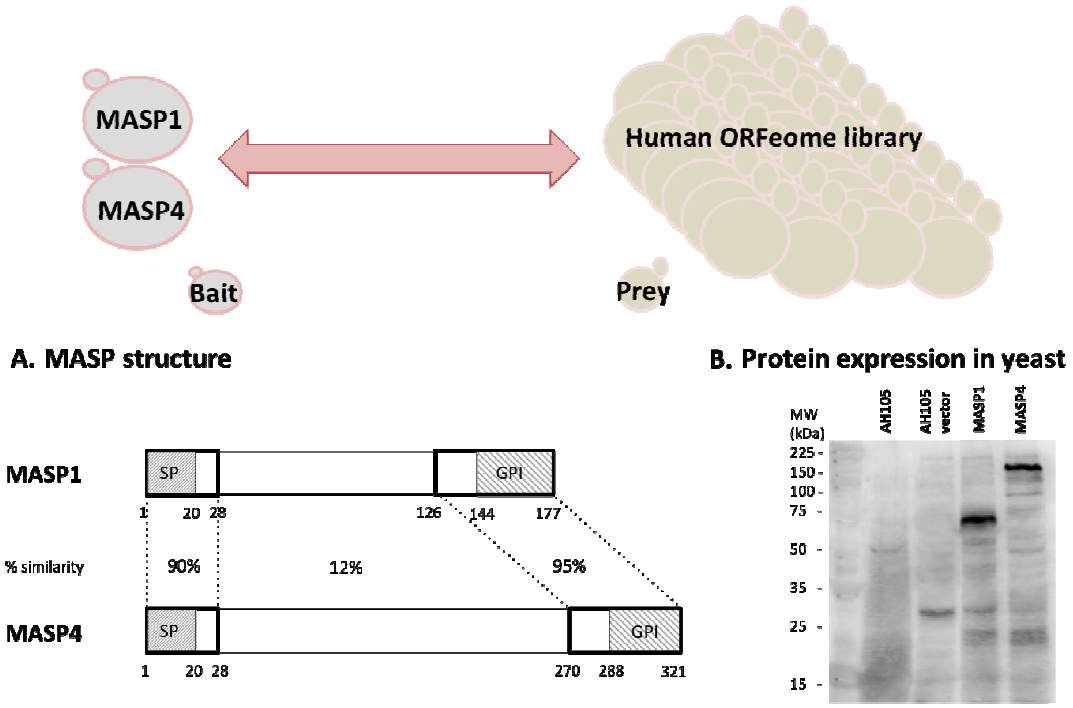

Figure 2-3. The two MASP baits used in Y2H screen (A) A schematic map of MASP proteins. Boxes with bold line represent N- and C- terminal conserved sequences with 96.4% and 90.4% similarity respectively. SP: signal peptide, GPI: GPI-anchor addition site. (B) Immunoblot analysis demonstrates the expression of c-Myc-tagged MASP1 and MASP4 recombinant proteins in yeast AH109 cells. Untransfected AH109 cell lysates (lane 1), pGBKT7g-transfected AH109 cell lysates (lane 2), pGBKT7g-MASP1-transfected AH109 cell lysates (lane 3), and pGBKT7g-MASP4-transfected AH109 cell lysates (lane 4) were probed with anti-c-Myc antibodies. (* Lower mobility (i.e. higher molecular weights) for MASP1 and MASP4 suggest possible glycosylation events as expected from *in silico* analysis)

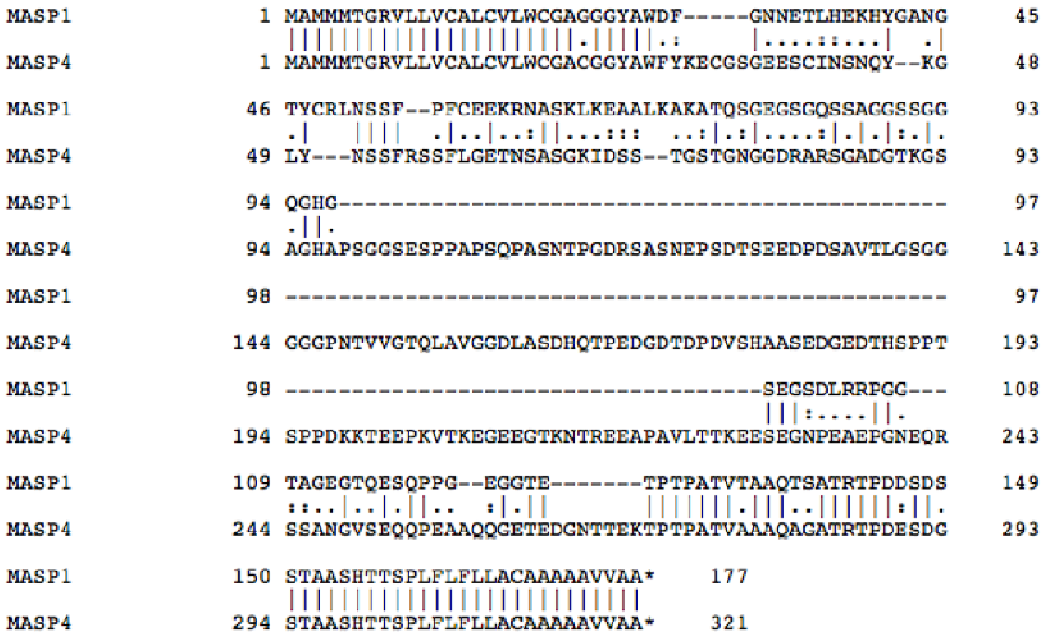

Figure 2-4. Protein sequence comparison between MASP1 and MASP4. MASP1 and MASP4 amino acid sequences were analyzed by EMBOSS Needle program to find the optimal global sequence alignment. Highly conserved N- terminal and C-terminal regions are indicated by | (identical), : (very similar) and . (somewhat similar).

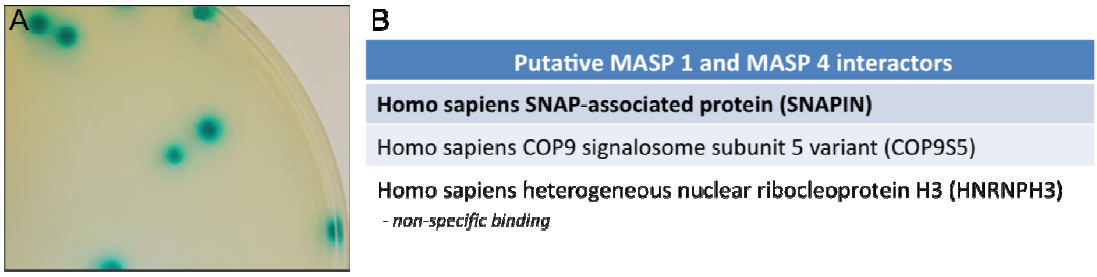

Figure 2-5. Putative human interacting partner proteins that bind to both MASP1 and MASP4. (A) Blue yeast colony growth on the selective media representing positive protein-protein interactions. (B) Yeast 2-hybrid (Y2H) screening analysis revealed several interactors of MASP including human SNAP-associated protein (SNAPIN) and COP9 signalosome subunit 5 variant (CSN5). Heterogeneous nuclear ribocleoprotein H3 (HNRNPH3) turned out to be non-specific binding by the following pairwise Y2H confirmation.

Subsequently, they were gateway-cloned into pGBKT7g yeast two-hybrid (Y2H) expression vector that was engineered by Dr. Peter Uetz to generate pGBKT7-*masp* plasmids (bait) (Rajagopala, Casjens et al. 2011). Following the transfection of AH109 (MATa) yeast strain with each bait plasmid, the expression of yeast recombinant proteins (DBD-MASP-c-Myc) in fusion to Gal-4 DNA binding domain (DBD) was validated by the standard immunoblotting analysis using anti-c-Myc antibodies (Figure 2-3 B). Detection of bigger recombinant MASP1 and MASP4 proteins expression than the expected sizes (26 kDa and 42kDa theoretically) may represent a different post-translational modification (PTM) in the heterologous system especially a heavy glycosylation decoration event in yeast is well-documented elsewhere (Figure 2-3 B) (Conde, Cueva et al. 2004). The suppression of transcription auto-activation of baits was evaluated with the various concentration (0 ~ 100mM) of 3-Amino-1,2,4-triazole (3-AT) in the selective media and achieved by applying 2.5 mM 3-AT for both MASP baits. Thereafter the selective media plates were supplemented with 2.5 mM 3-AT to prevent the leaky expression of bait unless noted otherwise. The initial screening against the pretransformed normalized Matchmaker Human Universal cDNA Library, Y187 (MATα) yeast strain containing normalized human cDNAs in fusion to Gal-4 activation domain (AD) in pGADT7-rec Y2H expression vector, yielded 62 and 86 putative protein-protein interactions (PPIs) for baits, MASP1 and MASP4, respectively (Table 2-1). The plasmids from each yeast colony were extracted using Zymoprep yeast plasmid miniprep kit and the prey plasmid harboring an Ampicillin resistant gene was separated from the bait plasmid after *E.coli* transformation.

A

Putative human interacting partner proteins of MASP1	# of interactors
Homo sapiens SNAP-associated protein (SNAPIN), mRNA	23
Homo sapiens heterogeneous nuclear ribonucleoprotein H3 (2H9) (HNRNPH3), transcript variant 2H9, mRNA	12
Homo sapiens mRNA for COP9 signalosome subunit 5 variant protein	8
Homo sapiens contactin associated protein-like 2 (CNTNAP2) on chromosome 7	3
Homo sapiens calcium modulating ligand (CAMLG), mRNA	3
Homo sapiens ring finger protein 2 (RNF2), mRNA	4
Homo sapiens HLA-B associated transcript 3 (BAT3), transcript variant 4, mRNA	1
Homo sapiens heat shock 70kDa protein 2 (HSPA2), mRNA	1
Homo sapiens Brk1-like protein mRNA	1
Homo sapiens layilin (LAYN), mRNA	1
Homo sapiens proteasome (prosome, macropain) subunit, alpha type, 7 (PSMA7), mRNA	1
Homo sapiens carbohydrate kinase domain containing (CARKD), mRNA	1
Homo sapiens chromosome 2 open reading frame 42 (C2orf42), mRNA	1
Homo sapiens killer cell lectin-like receptor subfamily B, member 1 (KLRB1), mRNA	1
N/A	1
total	62

B

Putative human interacting partner proteins of MASP4	# of interactors
Homo sapiens SNAP-associated protein (SNAPIN), mRNA	42
Homo sapiens mRNA for COP9 signalosome subunit 5 variant protein	22
Homo sapiens ring finger protein 2 (RNF2), mRNA	8
Homo sapiens quaking homolog, KH domain RNA binding (mouse) (QKI), transcript variant 1, mRNA	2
Homo sapiens HLA-B associated transcript 3 (BAT3), transcript variant 2, mRNA	1
Homo sapiens ER degradation enhancer, mannosidase alpha-like 3 (EDEM3), mRNA	1
Homo sapiens suppression of tumorigenicity 13 (colon carcinoma) (Hsp70 interacting protein) (ST13), mRNA	1
Homo sapiens BAC clone RP11-507C18 from 2, complete sequence	1
Homo sapiens BAC clone RP11-568N6 from 2, complete sequence	1
N/A	7
Total	86

Table 2-1. The list of putative human interactors of MASP. The inserts of individual cDNA plasmids retrieved from the yeast 2-hybrid screening using (A) MASP1 or (B) MASP4 as bait were sequenced and searched against the NCBI non-redundant (nr) database. The BLAST searches showed several interesting putative interactors of MASP including human SNAP-associated protein (SNAPIN) and COP9 signalosome subunit 5 variant (CSN5).

The insert of the isolated prey plasmids was subsequently sequenced and 37% (24/62) and 49% (42/86) of the sequenced cDNA inserts from each screening were identified as SNAP-associated protein (SNAPIN), the protein implicated to function in a calcium-dependent exocytosis in neurons by binding to SNAP25 (Ilardi, Mochida et al. 1999; Buxton, Zhang et al. 2003; Tian, Wu et al. 2005). COP9 signalosome subunit 5 variant protein (CSN5), a protein shown to regulate multiple signalling pathways (Kim, Lee et al. 2004; Yoshida, Yoneda-Kato et al. 2010), was also found to be a putative interactor with both MASP proteins (Figure 2-5). Several nuclear proteins including heterogeneous nuclear ribonucleoprotein H3 and ring finger protein 2 turned out to be non-specific binding based on a pairwise Y2H assay. Presumably they directly interact with the DNA binding domain (DBD) sequence even in the absence of protein-protein interaction. We identified a few additional putative interactors. Although they looked interesting, we did not pursue them in this study because they were only detected in one of two Y2H screens thus it is likely to represent a non-specific binding. For instance, killer cell lectin-like receptor and layilin containing a lectin domain were identified as MASP1 interactors in our Y2H screens, showing the MASP recombinant protein expressed in yeast is very likely glycosylated. Another interactor, contactin-associated protein is one of cell adhesion molecules and located on the membrane and this suggests a biologically relevant interaction and the putative function of MASP protein in cell attachment but contactin-associated protein was only found in Y2H screening when MASP1 protein was used as bait. Also the interaction with calcium modulating ligand (CAMLG) revealed a possible function in calcium signaling.

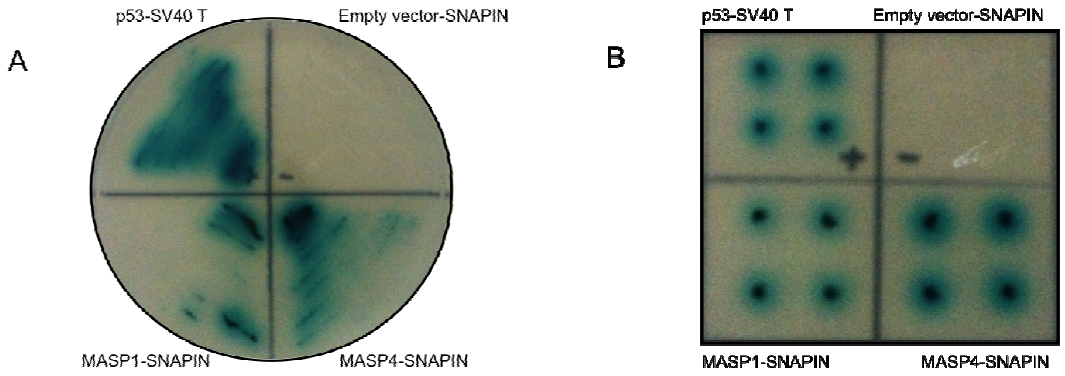

Figure 2-6. Protein-protein interaction from Y2H screens was confirmed in pairwise assays. Mated bait and prey yeast strains were either streaked manually or pinned in quadruplicate using a 96-pin tool on a Biomek® FXp onto the quadruple dropout media lacking Tryptophan, Leucine, Adenine, and Histidine but supplemented with X-α-gal.. MASP1 and SNAPIN (bottom left, A and B) and MASP4 and SNAPIN (bottom right, A and B) are indicating positive protein-protein interactions. Human TP53 protein (pGBKT7-p53: bait) and SV40 large T-antigen (pGADT7-SV40 large T-antigen: prey) were used as a positive control for Y2H interaction (upper left, A and B) and an empty pGBKT7g vector and pGADT7g-*snapin* were used as a negative control (upper right, A and B).

MASP also pulled out the protein complex that consists of HLA-B associated transcript 3 (BAT3), CAMLG and immediate early response 3 (IER3) that are implicated in the regulation of apoptosis (Table 2-1). These putative interactors were excluded primarily because they were not detected from both screenings and a couple of them were nuclear such as BAT3 and IER3 so these interactions do not likely occur *in vivo*. Between SNAPIN and CSN5, we decided to focus on SNAPIN for the downstream analyses rather than CSN5 since CSN5 is nuclear/cytosolic (Tomoda, Kubota et al. 2002) whereas SNAPIN is membrane-bound (Buxton, Zhang et al. 2003), thus more biologically relevant for our work. Bait and prey plasmids rescued from the positive yeast colony were again used for a Y2H assay in a pair-wise manner to confirm the direct interaction between MASP and SNAPIN. This excludes the possibility of indirect interaction, i.e. the interaction within the same complex or false positive due to yeast diploid cells harboring multiple prey plasmids. Human TP53 and SV40 large T-antigen were used to validate the Y2H system and the empty Y2H expression vector (pGBKT7g) and SNAPIN were used as a negative control and demonstrated that SNAPIN does not bind non-specifically to DBD sequence (Figure 2-6 A and B top). Both MASP1 and MASP4 showed strong interactions with SNAPIN as indicated by blue yeast diploid cell growth on the selective media when they were streaked manually (Figure 2-6 A bottom) or they were pinned in quadruplicate by Biomek® FXp.

Next, we performed the screening against the human ORFeome (hORFeome 3.1) in an array format. The prey library was prepared by transfecting the Y187 (MATα) yeast strain with 94 mini-libraries each containing a pool of 128 human ORFs from

the hORFeome collection fused to Gal-4 AD in the pGADT7g Y2H expression vector, and spotting the 94 mini-libraries on Nunc™ OmniTrays in a 96-well format. The mating of bait and prey and the transfer of the mated diploid cells onto the selective media were conducted on a Biomek® FXp laboratory automation workstation equipped with a 96-pin tool. As expected, we could detect the PPI signal from a colony from a pool containing SNAPIN. This consistency in screen result using two different Y2H platforms adds confidence and reliability to the interaction between both MASP proteins and SNAPIN as well as the sensitivity of Y2H screening. The development of a high-throughput Y2H system will facilitate the emergence of the host-pathogen interactome (infectome) field by taking advantage of our automated workflow.

2.3.2 MASP and human SNAPIN protein interaction was confirmed using other heterologous systems

In order to rule out that the interaction is not the result of the yeast two-hybrid system, we validated the physical interaction between MASP and SNAPIN using additional approaches. We conducted two additional PPI assays in heterologous biological systems. 6xHis-SNAPIN (bait) and the GST alone and GST-MASPs (prey) were independently transformed and expressed in *E. coli* overexpression strain, BL21-AI. An equimolar amount of total cell lysates was combined in a pair of bait and prey and incubated for 1 hour at 4ºC followed by the purification of protein complexes using Ni-NTA agarose beads. Recovered protein complexes were subjected to standard immunoblotting analysis. The results clearly demonstrated 6xHis-tagged recombinant SNAPIN protein was expressed and present in soluble fraction of total cell lysates

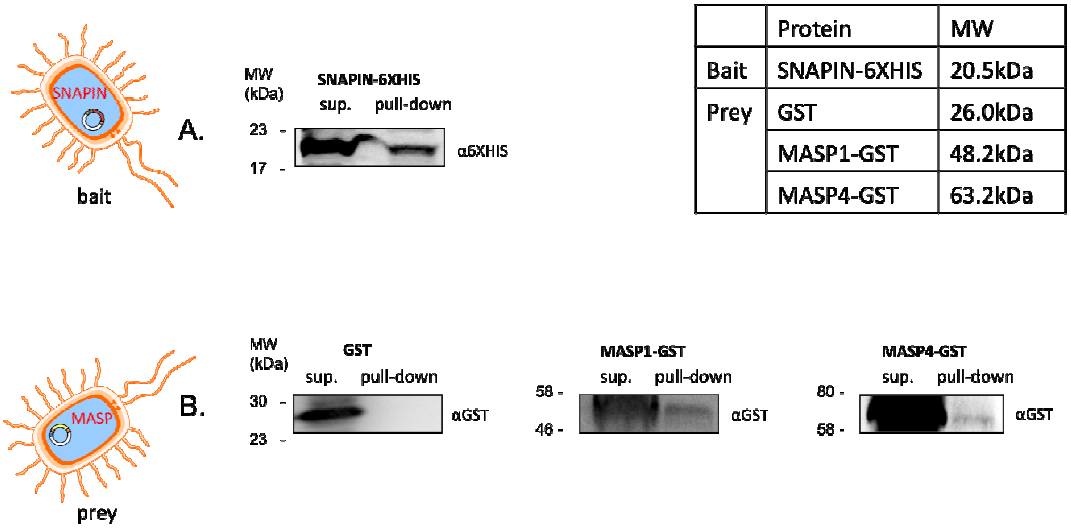

	Protein	MW
Bait	SNAPIN-6XHIS	20.5kDa
Prey	GST	26.0kDa
	MASP1-GST	48.2kDa
	MASP4-GST	63.2kDa

Figure 2-7. *in vitro* pull-down assay confirms MASP-SNAPIN interaction. Each construct was transformed and expressed in *E. coli BL21-AI* strain. Bacterial cultures were lysed and each bait and prey pair was combined for the incubation for 1 hour at 4ºC. Protein complexes were purified by Ni-NTA agarose resin. The eluates were subjected to the standard immunoblotting analysis using anti-GST antibodies and anti-6XHIS antibodies. (A) Soluble 6xHis-tagged SNAPIN was expressed in *E. coli* (sup.) and present in the pull-down protein complexes (pull down). (B) GST protein alone was expressed (sup.) but absent in a protein complex with 6xHis-tagged SNAPIN. GST-tagged MASP1 and MASP4 were expressed in supernatant (sup.) and detected in pull-down (pull down).

and captured by Ni-NTA resin as expected (Figure 2-7 A). Also GST and GST-tagged MASP proteins were expressed and present in soluble fraction but only GST-tagged MASP proteins were purified along with SNAPIN in a complex by Ni-NTA resin (Figure 2-7 B). This data indicates that both MASP1 and MASP4, but not GST protein alone, are interacting with SNAPIN in a bacterial system (Figure 2-7) even in the absence of post-translational modification such as N-linked or O-linked glycosylations previously predicted on MASP proteins *in silico* (Bartholomeu, Cerqueira et al. 2009). This rules out the possibility of non-specific binding due to the putative sticky nature of the MASP glycoprotein.

We next performed *in vivo* co-affinity purification (co-AP) assay to test the interaction between MASP and SNAPIN in a mammalian system, representing another heterologous system in order to add confidence on our PPI data. HEK293T cells were transiently co-transfected with a pair of GST-bait (GST alone and GST-sMASPs) and 6xHis-prey (6xHis-SNAPIN) constructs. Fusion proteins were overexpressed for 48 hours and the interacting protein complexes in the cell lysates were purified using glutathione sepharose (GSH) resin. MASP proteins, despite their soluble GST tag, were mostly insoluble when overexpressed in a mammalian system. This is likely due to the hydrophobic signal peptide and GPI-anchor regions at their N- and C-terminal domains, respectively (Figure 2-8) (Bartholomeu, Cerqueira et al. 2009; De Pablos, Gonzalez et al. 2011). We removed these hydrophobic sequences from the full-length MASP ORFs in order to improve the solubility of the recombinant proteins expressed in the mammalian cells in this experiment with the assumption that this will not interfere with the function of MASP because the signal

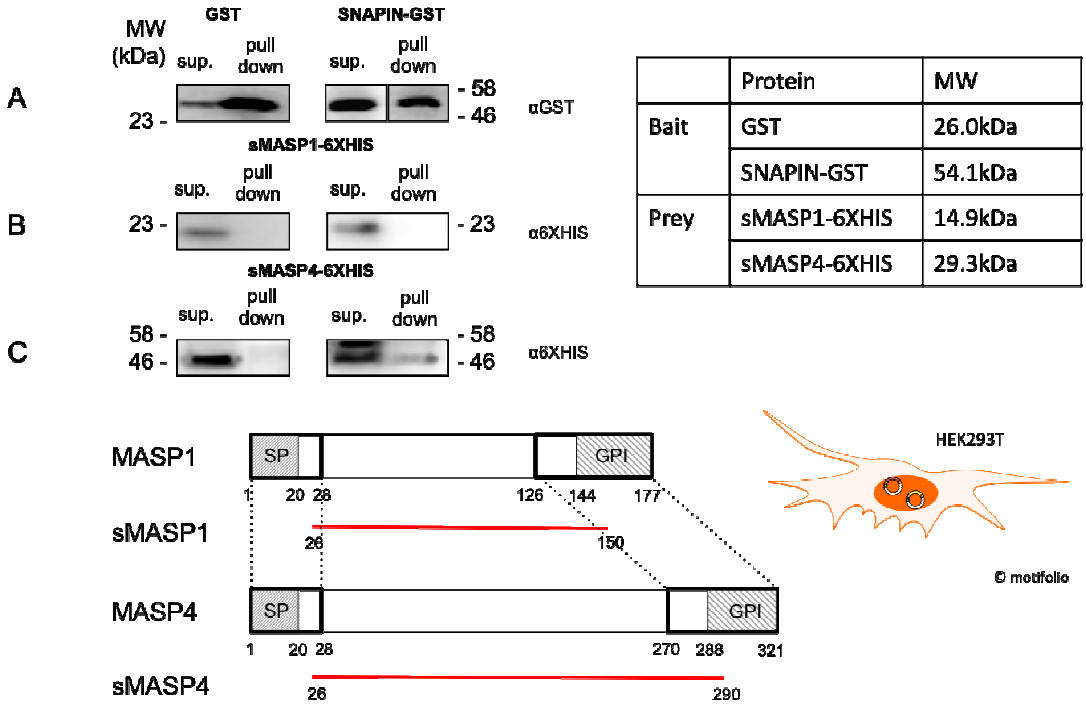

	Protein	MW
Bait	GST	26.0kDa
	SNAPIN-GST	54.1kDa
Prey	sMASP1-6XHIS	14.9kDa
	sMASP4-6XHIS	29.3kDa

Figure 2-8. Validation of MASP-SNAPIN interaction by *in vivo* co-Affinity Purification. GST protein alone and GST-tagged SNAPIN served as bait. MASP fragments (sMASP1: 25~146 a.a. and sMASP4: 25~290 a.a.) were constructed and used in this assay to increase the solubility of 6xHis-tagged MASP proteins as prey. Each bait and prey pair was co-transfected into HEK293T cells, which were then grown at 37ºC for the next 48hrs. Cells were lysed and the protein complexes were purified using Glutathione-conjugated sepharose resin and subjected to the standard immunoblotting analysis using mouse monoclonal anti-GST antibodies and anti-6xHis antibodies. (A) GST protein and GST-tagged SNAPIN protein were expressed in HEK293T supernatant (sup.) and pulled down by Glutathione-conjugated sepharose resin (pull down). (B) 6xHis-tagged MASP1 fragment protein was expressed and but not present in the pull-down protein complex when GST proteins alone or GST-tagged SNAPIN were used as bait. (C) 6xHis-tagged MASP4 fragment

protein was expressed and not pulled down by GST protein alone but only by GST-tagged SNAPIN indicating the interaction between 6XHis-tagged MASP4 and GST-tagged SNAPIN.

peptide and GPI addition site domains predicted by *in silico* analysis are eventually cleaved out during the post transcriptional processing in *T. cruzi*. GST alone was used as a negative control and showed that GST protein alone does not interact with either MASP1 fragment or MASP4 fragment (Figure 2-8 A-C, left panel). GST-tagged SNAPIN was expressed in soluble and purified by GSH resin (Figure 2-8 A, right panel). The expression of soluble 6xHis-tagged MASP1 fragment was still poor in spite of our attempt to cleave the hydrophobic region and absent in the protein complex when purified with GSH resin (Figure 2-8 B, right panel). Soluble 6xHis-tagged MASP4 fragment expression in HEK293T cells was better than MASP1 fragment and detected faintly in the protein complex along with GST-tagged SNAPIN (Figure 2-8 C, right panel). Our results show SNAPIN is interacting albeit weakly with the MASP4 fragment (sMASP4) but not with the MASP1 fragment (sMASP1) in the mammalian system (Figure 2-8). It is possible that the interaction with MASP1 was not detectable due to low expression level or persistent insolubility of the MASP1 fragment.

2.4 Conclusions and significance

In this section of the work, we have established a robust high-throughput platform for screening protein-protein interactions between trypanosomatid and human proteins.and used the system to identify for the first time the human interacting partner protein of *T. cruzi* MASP proteins. Although we have tested only two out of 771 members, human SNAPIN turned out to be physically interacting with both MASP1 and MASP4 despite the striking differences in hypervariable domains. It is possible the conserved domain at its N-terminus or C-terminus (Figure 2-3) is

responsible for this interaction. It will be interesting to study the 3D structures of MASP family and determine if they could share any common structure overcoming the sequence variation like variant surface glycoprotein (VSG) family in *T. brucei*. VSG family consists of 806 members in *T. brucei* genome and antigenic variation is achieved by switching a member of glycoprotein in the bloodstream of the host (Berriman, Ghedin et al. 2005). Even though the primary sequence of VSG N-terminal domain show low similarity, the crystallized 3D structure revealed strikingly high similarity in N-terminal domain demonstrating VSG family may have a common N-terminal structure (de Carvalho, da Silva et al. 2002). Hence, it cannot be ruled out that the central hypervariable region of MASP may have a common structure playing a major role in the protein-protein interaction with SNAPIN. Yeast two-hybrid offers a great advantage as a high throughput screen method for the rapid identification of protein-protein interaction between host and pathogens. Potentially yeast two-hybrid screening method, combined with next generation sequencing technology will allow massive PPI identification that will be beneficial in speed and quantity to unexplored host-pathogen interactome or infectome. Also the confirmation by other heterologous systems will provide confidence in the PPI identified from Y2H screen.

The MASP and SNAPIN interaction identified from Y2H screens and confirmed in two different heterologous systems was very interesting since *T. cruzi* was known to exploit the host calcium-regulated lysosome pathway for cell invasion (Schenkman, Robbins et al. 1991; Tardieux, Webster et al. 1992). *T. cruzi* causes a transient intracellular calcium increase in the host cell that initiates the recruitment and fusion of host lysosomes to the plasma membrane. This process involves many SNARE

complex protein actions and SNAPIN was one of them (Ilardi, Mochida et al. 1999). Also SNAPIN was implicated in calcium-dependent exocytosis in neurons (Tian, Wu et al. 2005). In Chapter 3, we tested if the interaction between MASP and SNAPIN has a biological relevance in the parasite invasion process using several functional assays.

Chapter 3: The putative role of SNAPIN in host cell invasion

3.1 Objective of Study

Preferential MASP expression in the infective stage of *T. cruzi* as well as its cellular localization, suggest a possible role of MASP in the host cell invasion process. As our attempt to raise antibodies against MASP has been difficult (Bartholomeu, Cerqueira et al. 2009) and the range of genetic tools for the functional analysis of *T. cruzi* genes, multigenic gene family in particular, was limited, we aimed to characterize the putative function of MASP by elucidating the role of SNAPIN, a human interacting partner protein of MASP, via several genetic, molecular, biochemical approaches available for human and mouse cell lines.

3.2 Materials and Methods

3.2.1 Materials

Materials	Catalogue numbers	Sources
HeLa (CCL-2.1)		Dr. Norma Andrews (University of Maryland, College Park)
Rhesus Monkey Kidney Epithelial (LLC-MK_2)		
Normal Rat Kidney (NRK)		
adenovirus encoding LAMP1-RFP		
mouse anti-LAMP1 (H4A3 clone) antibodies		
SNAPIN Wild-Type (WT) Mouse Embryonic Fibroblast (MEF)		Dr. Zu-Hang Sheng (National Institute of Neurological Disorders and Stroke, National Institutes of Health)
SNAPIN Knock-Out (KO) Mouse Embryonic Fibroblast (MEF)		
Glass coverslips	12-545-82	Fisher

		Scientific
Ionomycin	I9657	Sigma-Aldrich
p-nitrophenyl-N-acetyl-β-D-glucosaminide	N9376	Invitrogen
4-methylumbelliferyl-β-D-galactoside	M1633	
DEAE cellulose	D3764	
SNAPIN siRNA oligomers	HSS118960, HSS118961, HSS118962	
Control siRNA oligomers	12935300	
Lipofectamine™ 2000 Transfection Reagent	11668-019	
FuGENE® HD Transfection Reagent	04 709 691 00	Roche
Rabbit anti-SNAPIN polyclonal antibodies	148 002	Synaptic Systems
Mouse anti-SNAPIN monoclonal antibodies	75-045	NeuroMab
6-well tissue culture plates	12-566-80	Thermo Scientific
Dulbecco's Modification of Eagle's Medium (DMEM)	15-013-CV	Cellgro
Heat-inactivated Fetal Bovine Serum (FBS)	100-106	Gemini Bio-Products
Lgp120-YFP vector		Dr. Iqbal Hamza (University of Maryland, College Park)
Rab5-YFP vector		
Rab9-YFP vector		
Rab11-YFP vector		

3.2.2 Methods

Host cells and Parasites: HeLa cells (CCL-2.1), LLC-MK_2 (Rhesus Monkey Kidney Epithelial) cells and NRK (Normal Rat Kidney) cells were maintained in DMEM supplemented with 10% heat-inactivated FBS at 37ºC with 5% CO_2. SNAPIN Wild-Type (WT) and Knock-Out (KO) Mouse Embryonic Fibroblast (MEF) cells at passage 8 were cultured in DMEM supplemented with 10% FBS at 37ºC and 5% CO_2. *Trypanosoma cruzi* epimastigotes (CL Brener and Y strains) were maintained in Liver Infusion Tryptose (LIT) medium (Villar, Jimenez-Yuste et al. 2002) with 10% heat-inactivated FBS at 28ºC. Metacyclic trypomastigotes (MTs) of *T. cruzi* were

purified from 10-day old LIT culture by ion-exchange chromatography (DEAE cellulose) and Tissue-Culture derived Trypomastigotes (TCTs) were obtained from infected LLC-MK_2 cells.

Mouse SNAPIN RNAi assays: HeLa cells ($2x10^5$) in DMEM with 10% heat-inactivated FBS were plated on glass coverslips in a 6-well plate 24 hours prior to transfection. HeLa cells were transfected with 180 pmoles of a pool of three SNAPIN siRNA oligomers or control siRNA oligomer using Lipofectamine™ 2000 according to the manufacturer's instruction. Forty-eight hours following transfection, the efficiency of SNAPIN depletion was assessed using standard immunoblotting techniques using mouse anti-SNAPIN monoclonal antibodies and Immunofluorescence assay (IFA) using mouse anti-SNAPIN monoclonal antibodies and Alexa Fluor 488–labeled secondary antibodies. Images were acquired by Zeiss epifluorescence microscope (Observer Z1).

Parasite invasion assays: Y strain *T. cruzi* TCTs ($4x10^7$) were incubated with transfected HeLa cells (MOI=200) for 20 minutes and washed extensively with PBS. Infected HeLa cells were immediately fixed with Bouin's solution (71.4% saturated picric acid, 23.8% formaldehyde, and 4.8% acetic acid) for 20 minutes, followed by Giemsa staining overnight at room temperature. A series of dehydrations in a gradient solution of acetone, 9:1, 7:3, 3:7 acetone/xylene, and xylene enabled the differentiation of intracellular and extracellular parasites (Fernandes, Cortez et al. 2011). Intracellular TCTs show a halo surrounding the parasite due to the parasitophorous vacuole whereas TCTs outside the cell do not. The number of intracellular parasites in 200 HeLa cells was counted twice under the microscope and

averaged. For MEF cells, $4x10^5$ cells were plated in a 6-well plate 24 hours prior to infection and then exposed to $4x10^7$ TCTs of *T. cruzi* Y strain (MOI=100) for 20 minutes and further processed as described above.

SNAPIN subcellular localization: HeLa cells ($2x10^5$) were plated on glass coverslips in a 6-well plate 24 hours before experiments and transfected with the Rab9-YFP plasmid using FuGENE® HD. HeLa cells were infected 48 hours after transfection with $1x10^7$ *T. cruzi* Y strain metacyclic trypomastigotes (MOI=50) for 1 hour and subjected to IFA as described below. For adenovirus transduction, HeLa cells were transduced 24 hours prior to the experiment by adding adenovirus encoding LAMP1-RFP at a 1:10 MOI to the culture media.

Immunofluorescence: Cells were fixed with fresh 4% paraformaldehyde (PFA) diluted in PBS for 10 minutes at room temperature, washed with PBS 3 times, and quenched with 15 mM NH_4Cl. The samples were then blocked with 2% BSA-containing PBS for 1 hour at room temperature. Cells on the glass coverslip were permeabilized with 0.1% Saponin for 10 minutes if necessary. The samples were incubated with mouse anti-SNAPIN monoclonal antibodies for 1 hour followed by anti-mouse Alexa Fluor 594 secondary antibody incubation. Images were acquired using the confocal microscope (Leica SP5 X) in the imaging core facility (University of Maryland, College Park). For MEF cell IFAs, both SNAPIN WT and KO MEF cells were stained with mouse anti-LAMP1 (H4A3 clone) antibodies for 1 hour followed by anti-mouse Alexa Fluor 594 secondary antibodies.

Host lysosome recruitment quantification: MEF cells ($6x10^5$) were seeded onto glass coverslips in a 6-well plate 24 hours prior to infection. Cells were incubated

with $6x10^7$ *T. cruzi* Y strain TCTs expressing GFP (MOI=100) for 20 minutes and washed extensively with PBS in order to synchronize the entry of the parasite. Washed MEF cells were fixed either immediately, or following a 20 minute- or 40 minute- additional incubation and processed with for IFA. Acquired images from each time point were analyzed with Leica LAS AF Lite software (version 2.4.1) for the host lysosome pixel intensity quantification surrounding the invading parasite.

Lysosomal enzyme release assay: The release of two different lysosomal enzymes, β-hexosaminidase and β-galactosidase, was measured using a fluorometric method. MEF ($6x10^5$) cells were plated 24 hours prior to the experiment and treated with or without 10 μM ionomycin. Secreted β-hexosaminidase and β-galactosidase present in the supernatant and total cell lysates were incubated in sodium citrate-phosphate buffer, pH 4.5 containing 6 mM **p**-nitrophenyl-**N**-acetyl-β-D-glucosaminide and in acetate buffer pH 5.0 containing 5 mM 4-methylumbelliferyl-β-D-galactoside respectively for 20 minutes at 37°C. The reaction was terminated by the addition of stop buffer (2M Na_2CO_3, 1.1M glycine). Absorbance at 405 nm was read in an enzyme-linked immunosorbent assay (ELISA) reader and the results were normalized as the percentage of enzyme activities released into the supernatant over the total cell lysates.

Calcium-dependent SNAPIN exposure assay: NRK ($4x10^5$) cells were plated on glass coverslips in a 6-well plate 24 hours before experiments. The cells were incubated for 10 minutes in the presence or absence of 10 μM ionomycin in the buffer with or without 20 mM calcium and fixed with 4% fresh PFA for 10 minutes. The fixed cells were blocked with 2% BSA containing PBS but not allowed to be

permeabilized for the detection of exposed SNAPIN. The glass coverslips were incubated further with rabbit anti-SNAPIN polyclonal antibodies followed by anti-rabbit Alexa Fluor 594 secondary antibodies and examined by the confocal microscope (Leica SP5 X) in the imaging core facility (University of Maryland, College Park)..

3.3 Results and Discussion

3.3.1 Depletion or deletion of SNAPIN reduces cells invasion of *T. cruzi*

Since the deletion of 1,377 copies of a MASP family in *T. cruzi* is not feasible and the RNA interference (RNAi) pathway is absent in *T. cruzi* (DaRocha, Otsu et al. 2004; El-Sayed, Myler et al. 2005; El-Sayed, Myler et al. 2005), we decided to deplete SNAPIN in the HeLa cells with three human SNAPIN small interfering RNA (siRNA) oligomers and perform a *T. cruzi* invasion assay to investigate the possible role of human SNAPIN protein in the parasite invasion process. Recently RNAi has been used extensively as a great reverse genetic tool to identify host proteins that might be crucial for the *T. cruzi* invasion and intracellular survival from a single gene (Nde, Simmons et al. 2006; Simmons, Nde et al. 2006; Claser, Curcio et al. 2008) to the genome-wide level (Genovesio, Giardini et al. 2011). Unlike *T. brucei* where the full RNAi machinery is present in the genome, genome sequencing of *T. cruzi* revealed that *T. cruzi* lacks two components, AGO1 and dicer, therefore RNAi is inactive. The majority of *Leishmania spp.* are also RNAi-incompatible but *Leishmania brazilnensis* was shown to retain the RNAi machinery recently (Lopez-Molinero, Villareal et al. 2002). Three siRNA oligemers were pre-designed with

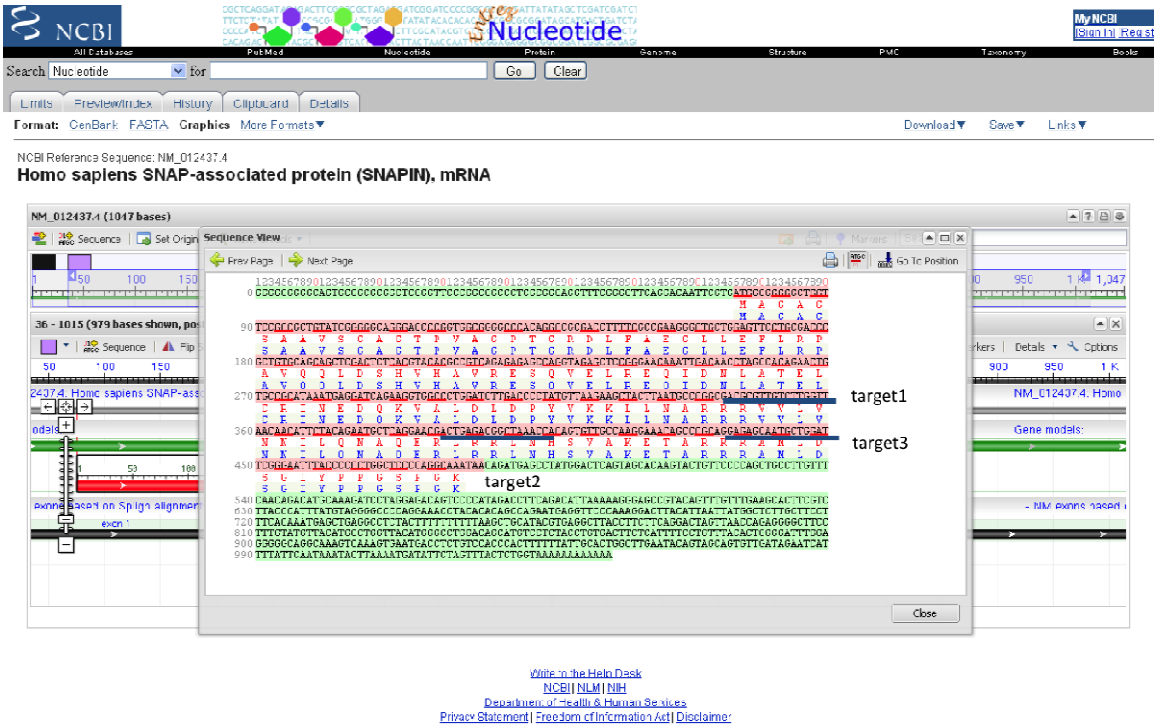

Figure 3-1. Three targets of snapin siRNA oligmers. Untranslated regions (in green) and coding sequence (in red) of *snapin* transcript is indicated. Three siRNA oligomers (target1, target2 and target3) were synthesized (underlined) based on the most up-to-date bioinformatics.

targets towards C-terminal region of *snapin* based on the most up-to-date bioinformatics and known information about miRNA seed region (Figure 3-1). The efficiency of gene silencing was validated with standard immunoblotting and immunofluorescence analyses (Figure 3-2 B-D). A pool of three SNAPIN siRNA oligomers was used for the following experiment. The three siRNAs combined proved to be the most effective in gene expression down-regulation according to the immunoblotting analysis result (Figure 3-2 B). HeLa cells transfected with either a pool of SNAPIN siRNA oligomers or the scrambled control siRNA oligomers designed to not target any genes in the human genome 24 hours prior to the invasion assay were exposed to *T. cruzi* Y strain trypomastigotes (MOI=250) for 20 minutes to evaluate the initial infection of *T. cruzi.* Following exposure, infected HeLa cells were fixed with Bouin's fixative and stained with Giemsa solution. The cells were dehydrated by a gradient of acetone/xylene solution that enabled us to distinguish the intracellular parasites and the extracellular parasites due to the presence of the halo. Once *T. cruzi* invades the cell, it resides within the parasitophorous vacuole. During the dehydration process, the parasite inside the parasitophorous vacuole displays the halo caused by the luminal space between the parasite surface and the vacuole membrane (Figure 3-2 E). The number of intracellular parasites per 200 HeLa cells were counted and compared to each other. SNAPIN siRNA-transfected HeLa cells displayed a significant reduction in the parasite invasion rate by 66% compared to the cells transfected with the scrambled control siRNA oligomer (Figure 3-2 A). This data suggests that SNAPIN plays an important role in the invasion process although the interaction with MASP or the role of MASP in this process cannot be depicted in

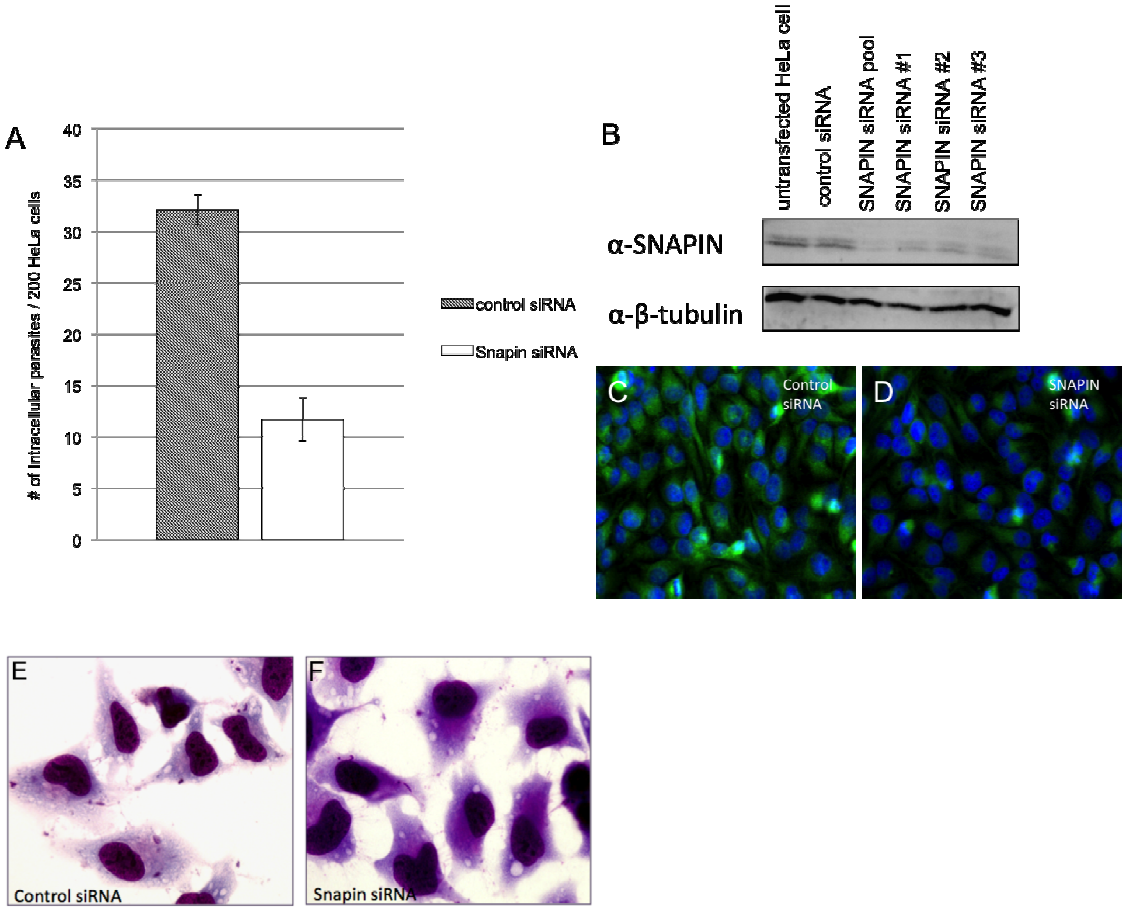

Figure 3-2. Depletion of SNAPIN shows a significant reduction in invasion rates. (A) HeLa cells were transfected by either a control siRNA or a pool of snapin siRNA oligomers for 48 hours and infected by Y strain tissue-culture derived trypomastigotes for 20 minutes. The infected HeLa cells were extensively washed and stained with Giemsa. The number of intracellular parasites in 200 HeLa cells was counted twice under the microscope and averaged. Parasite invasion rate was reduced (66%) by SNAPIN depletion in HeLa cells as compared to the control. Control siRNA in a hashed column, snapin siRNA in a white column. (B) HeLa cells were prepared after being transfected with a control siRNA, a pool of snapin siRNA oligomers and each

of three snapin siRNA oligomers respectively. Cells were lysed with NP40-containing lysis buffer and total cell extracts were analyzed in SDS-PAGE gel followed by the standard immunoblotting with rabbit polyclonal anti-SNAPIN antibodies (upper panel) or rabbit polyclonal anti-β-tubulin antibodies (bottom panel) and anti-mouse HRP conjugated antibodies. The result confirms the efficiency of depletion in SNAPIN especially when HeLa cells were treated with a snapin siRNA pool. (C, D) Endogenous SNAPIN in HeLa cells was stained with mouse monoclonal anti-SNAPIN and anti-mouse Alexa488 antibodies after transfecting HeLa cells with the control siRNA and a pool of snapin siRNA oligomers respectively. This Immunofluorescence Assays (IFA) result indicates a visual depletion of endogenous SNAPIN signal in HeLa cells after *snapin* siRNA transfection. (E, F) Giemsa-stained infected HeLa cells transfected with (E) the control siRNA or (F) a pool of snapin siRNA. White halo surrounding the parasites indicates the location inside the cell otherwise outside. Results are representative of two independent experiments.

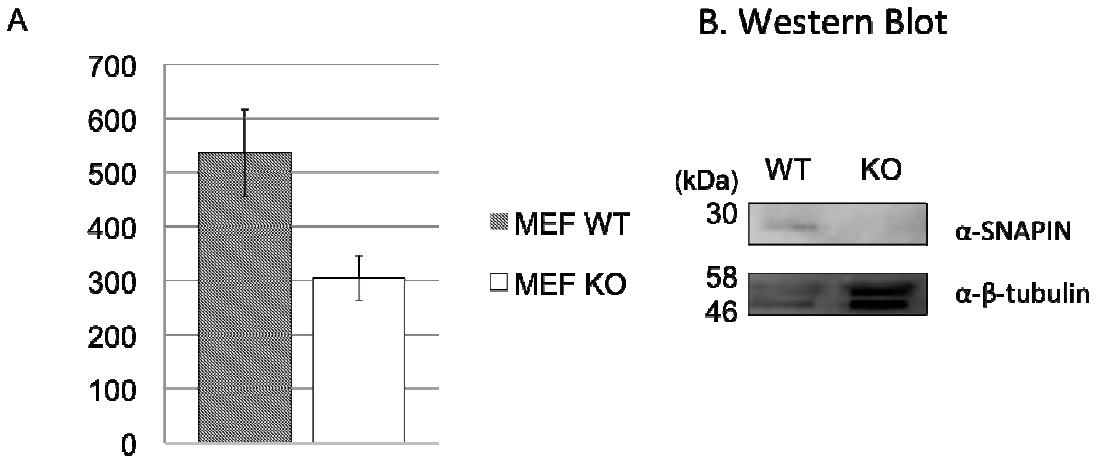

Figure 3-3. Deletion of *snapin* results in the *T. cruzi* infection inhibition. (A) SNAPIN WT and KO MEF cells were infected with Y strain tissue-culture derived trypomastigotes (TCTs) and incubated for 20 minutes followed by extensive wash with PBS. Infected MEF cells were stained with Giemsa and mounted on the microscope for the inspection. The number of intracellular parasites in 200 MEF cells was counted twice under the microscope and averaged. Parasite invasion rate was reduced by *snapin* deletion in SNAPIN KO MEF cells when compared to that in SNAPIN WT MEF cells. (B) The immunoblot analysis of SNAPIN WT MEF and SNAPIN KO MEF total cell lysates confirms the absence of SNAPIN protein expression in MEF cells when probed with rabbit polyclonal SNAPIN antibodies. β-tubulin was used as a loading control. Results are representative of two independent experiments.

this *T. cruzi* invasion assay. A similar invasion experiment was conducted using Snapin$^{+/+}$ and *snapin*$^{-/-}$ MEF cells where Western blot analysis confirmed the ablation of SNAPIN expression (Figure 3-3 B). Under the same condition, the number of intracellular parasites in *snapin*$^{-/-}$ MEF cells dropped greatly by 45% when compared to that in Snapin$^{+/+}$ MEF cells which is consistent with our previous RNAi data. In two independent experiments, SNAPIN was demonstrated to be involved in the *T. cruzi* invasion process. Particularly, SNAPIN-deficient cells resulted in an increased resistance to *T. cruzi* invasion. The plausible reason that we observed a moderate infection reduction in the *snapin*$^{-/-}$ MEF cells (45%) compared to that in SNAPIN-depleted cells (66%) might be due to a compensatory pathway partially counteracting the loss of SNAPIN in the *snapin*$^{-/-}$ MEF cells.

3.3.2 Recruitment of SNAPIN to the parasite surface and the subcellular localization of SNAPIN to the late endosomes and lysosomes

We next sought to determine the subcellular localization of SNAPIN during *T. cruzi* invasion of HeLa cells. Immunostaining of endogenous SNAPIN in HeLa cells revealed an intracellular perinuclear and punctate pattern (Figure 3-4 B) so we colocalized endogenous SNAPIN with several endosomal markers such as the recycling endosomal marker (Rab11-YFP), the early endosomal marker (Rab5-YFP), the late endosomal marker (Rab9-YFP), and the lysosomal marker (Lgp120-YFP or adenovirus encoding LAMP1-RFP) while *T. cruzi* Y strain infective trypomastigote is invading the HeLa cell. HeLa cells were either transfected with each plasmid encoding an endosomal marker or transduced with an adenovirus encoding a lysosomal marker protein and incubated with *T. cruzi* CL Brener strain metacyclic

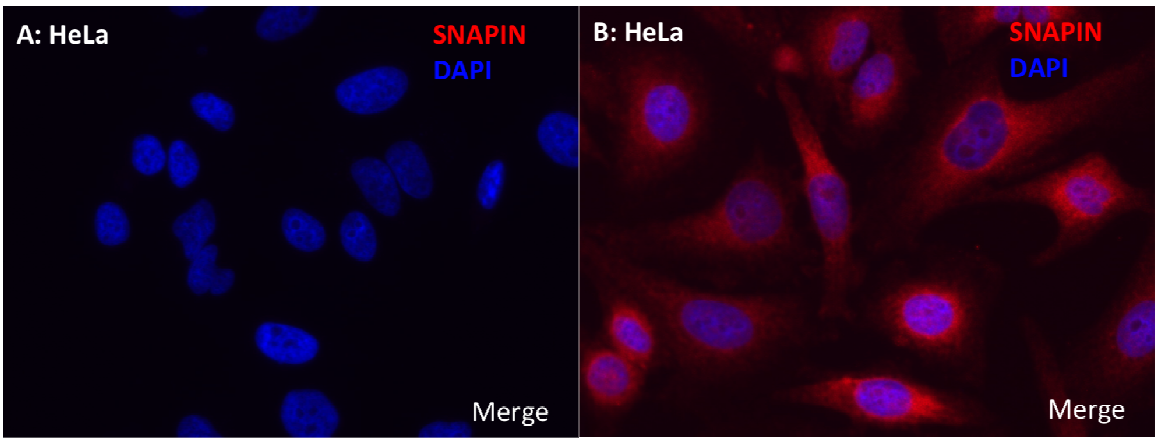

Figure 3-4. The immunostaining of SNAPIN in HeLa cells. Endogenous SNAPIN proteins in HeLa cells were immunostained (B) with or (A) without mouse anti-SNAPIN monoclonal antibodies coupled with rabbit anti-mouse Alexa594 antibodies (DAPI in blue).

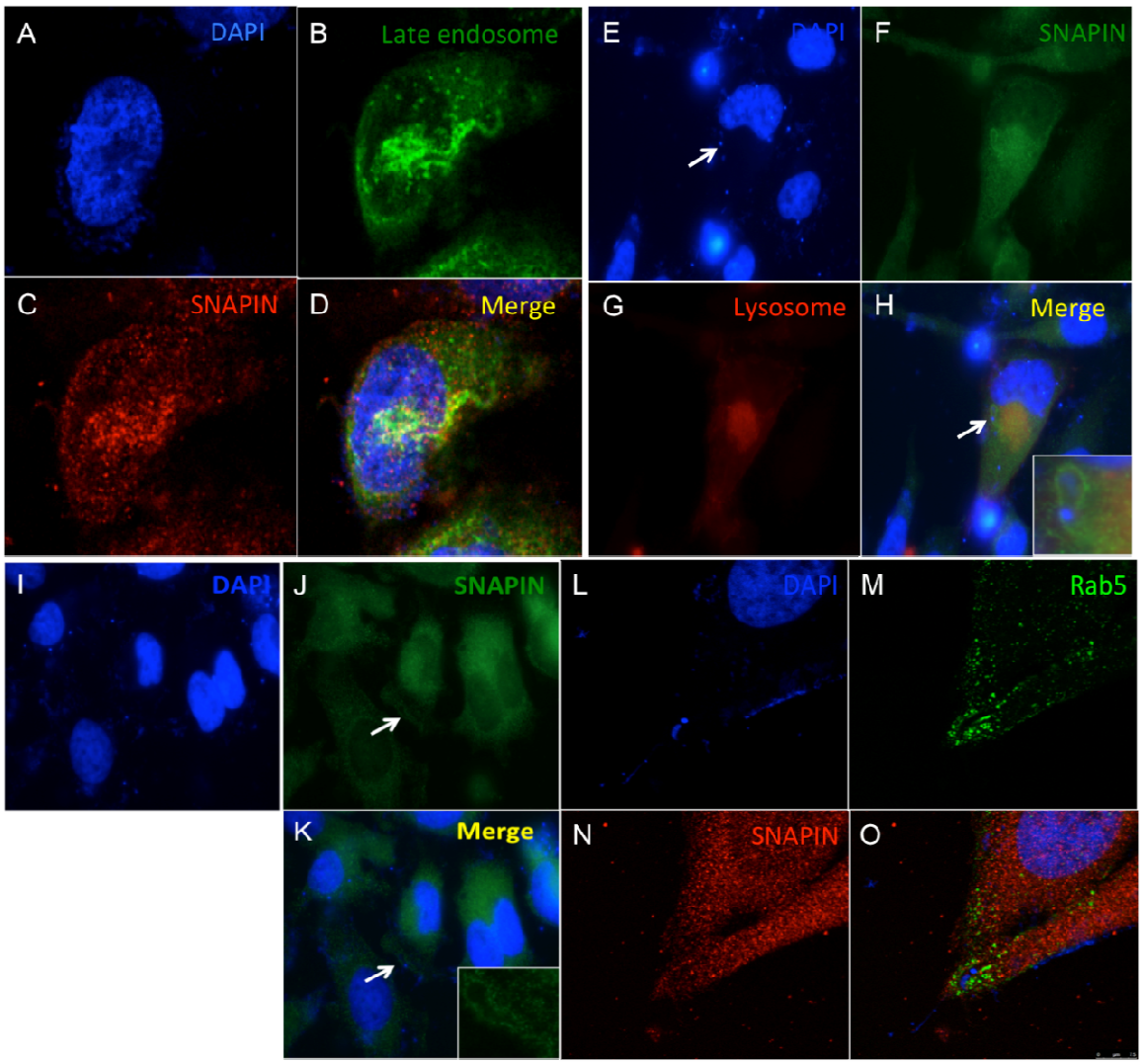

Figure 3-5. SNAPIN is recruited to the parasite and colocalized with the late endosomes and lysosomes. HeLa cells overexpressing Rab9-YFP (A-D) or LAMP1-RFP (E-H) were infected with Y strain metacyclic trypomastigotes (MTs) cells for 60 minutes. Infected HeLa cells were fixed and stained with mouse monoclonal anti-SNAPIN antibodies followed by anti-mouse Alexa594 or anti-mouse Alexa488 antibodies respectively for the inspection on the microscope (A-D; Leica SP5X, E-H; Nikon E200). (A and E) Nucleus of HeLa cells and the nucleus and kinetoplast DNA of the parasite are stained with DAPI shown in blue. (B and G) subcellular

localization of Rab9 (the late endosomal marker) in green and LAMP1 (lysosomal marker) in red respectively. (C and F) Endogenous SNAPIN subcellular localization in HeLa cells shown in red and green respectively. (D and H) Merged image reveals the colocalization of SNAPIN with the late endosomes and lysosomes respectively especially on the surface of the parasite shown in yellow (enlarged image is embedded).

HeLa cells were infected with Y strain TCTs for 60 minutes and stained with mouse monoclonal anti-SNAPIN antibodies followed by rabbit anti-mouse Alexa488 antibodies for endogenous SNAPIN localization during *T. cruzi* invasion. (I) DAPI staining in blue. (J) Endogenous SNAPIN (green) was recruited to the parasite surface. (K) Merged image.

HeLa cells overexpressing Rab5-YFP were infected with Y strain TCTs for 60 minutes and stained with mouse monoclonal anti-SNAPIN antibodies followed by rabbit anti-mouse Alexa594 antibodies. (L) DAPI staining in blue. (M) The early endosomes in green. (N) endogenous SNAPIN in red. (O) Merged image.

trypomastigotes for 60 minutes 48 hours post transfection or transduction. Subsequently, cells were fixed with 4% fresh PFA, permeabilized and stained with mouse anti-SNAPIN monoclonal antibodies and inspected on the confocal microscope. Indeed, SNAPIN was recruited to the parasite surface (Figure 3-5) and largely col-localized with the late endosomes (Rab9) and lysosomes (adenovirus encoding LAMP1-RFP) as previously reported (Figure 3-5 A-H) (Lu, Cai et al. 2009; Cai, Lu et al. 2010). We also were able to observe that the early endosomes (Rab5) were recruited to the point of parasite entry (Figure 3-5 L-O) as previously shown elsewhere (Baud, Lovis et al. 2001) but not colocalized with endogenous SNAPIN. This data indicates that SNAPIN is associated with the parasite invasion process, more specifically a lysosome-dependent entry process rather than a non-lysosome dependent entry process engaging the early endosomes.

3.3.3 Poor host lysosome recruitment to the parasite in SNAPIN-deficient MEF cells

Abnormal accumulation and atypical subcellular distribution of immature lysosomes in *snapin*$^{-/-}$ neuron cells due to the defects in late endocytic trafficking were reported previously (Lu, Cai et al. 2009; Cai, Lu et al. 2010). We also have observed the similar phenotypes in *snapin*$^{-/-}$ MEF cells when compared to Snapin$^{+/+}$ MEF cells (Figure 3-6). To visually examine how SNAPIN affects a lysosome-dependent *T. cruzi* invasion process, we performed the invasion assays by infecting Snapin$^{+/+}$ and *snapin*$^{-/-}$ MEF cells with *T. cruzi* Y strain tissue-culture derived trypomastigotes expressing GFP for 0, 20, and 40 minutes after extensive washing following an initial 20-minute incubation in order to synchronize the parasite entry. Infected MEF cells

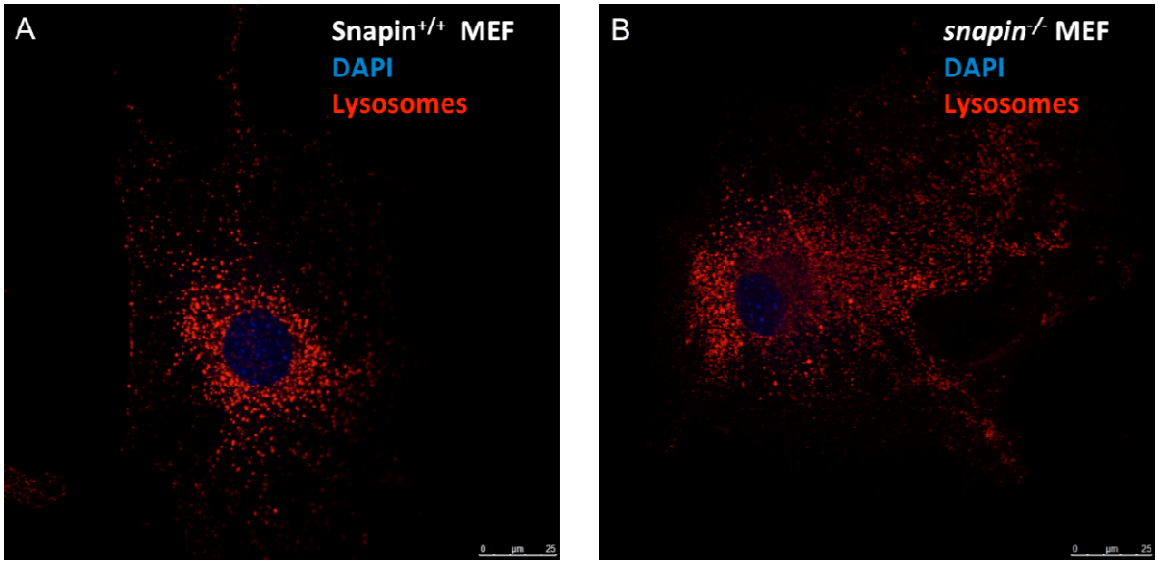

Figure 3-6. SNAPIN KO MEF cells display aberrant lysosome distribution.

SNAPIN WT MEF cells (A) and SNAPIN KO MEF cells (B) were stained with mouse anti-LAMP1 (lysosomal marker) antibodies followed by rabbit anti-mouse Alexa594 antibodies and inspected on the confocal microscope (Leica SP5X). (A) SNAPIN WT MEF cell displays a typical perinuclear lysosomal staining pattern. (B) SNAPIN KO MEF cell shows strikingly increased amount of lysosomes spread over the cell. DAPI in blue.

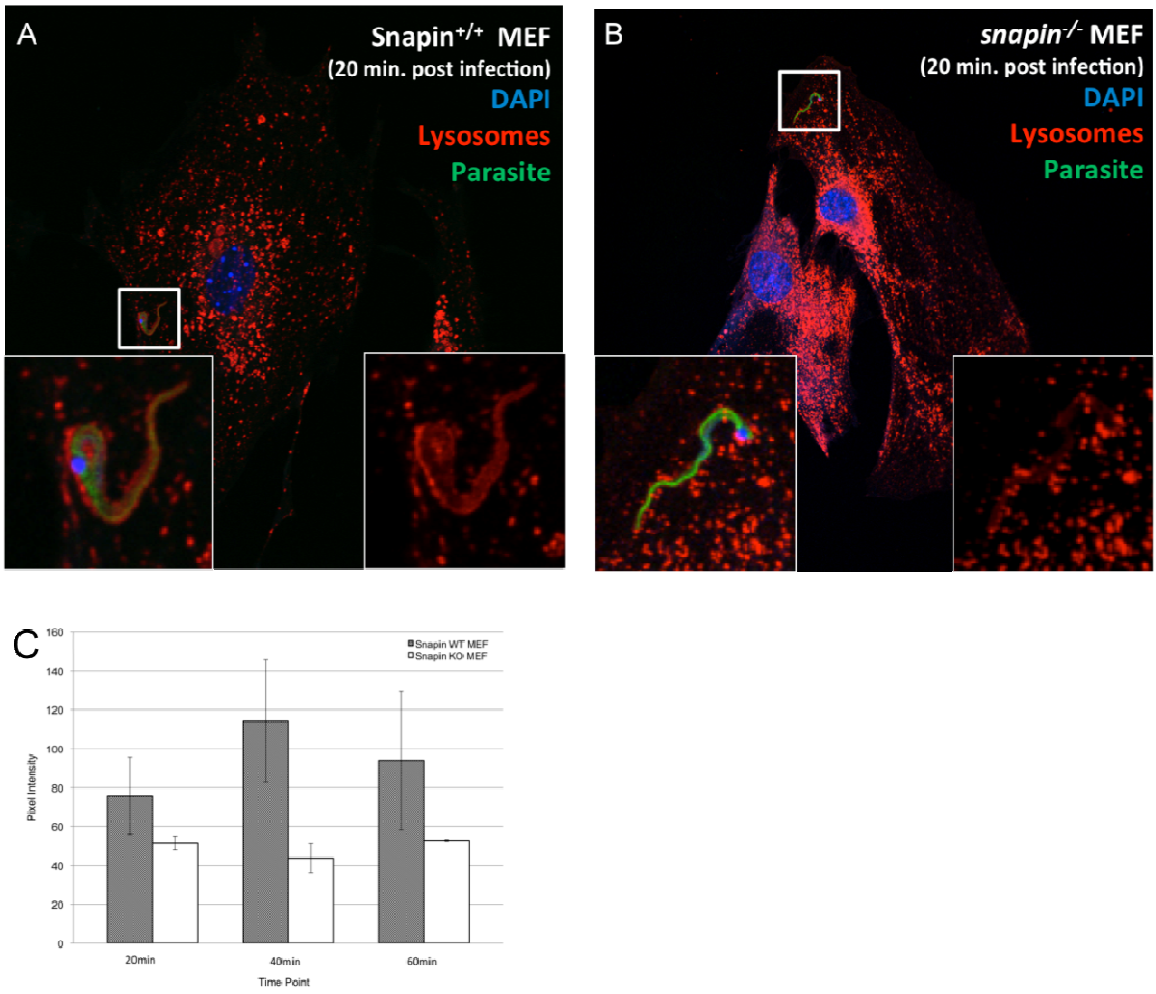

Figure 3-7. SNAPIN KO MEF cells display poor host lysosome recruitment to the parasites. SNAPIN WT MEF and KO MEF cells infected with Y strain tissue-culture derived trypomastigotes (TCTs) expressing GFP for 20 minutes were washed extensively in order to synchronize the entry of the parasite and fixed after 0 minute, 20 minute, 40 minute further incubation. MEF cells were stained with mouse anti-LAMP1 antibodies followed by rabbit anti-mouse Alexa594 antibodies and examined on the confocal microscope (Leica SP5X). (A) SNAPIN WT MEF cell shows normal recruitment of lysosomes (red) to the parasites surface 20 minutes post infection. DAPI in blue. (B) SNAPIN KO MEF cells display poor recruitment of lysosomes to the parasites surface compared to SNAPIN WT MEFs 20 minutes post infection. (C)

Lysosome pixel intensity surrounding the parasites in SNAPIN WT MEF (hashed column) and SNAPIN KO MEF (white column) cells was quantified and compared at each time point. Results are presented as means ± SE from 20 parasites invading either SNAPIN WT or KO MEF cells at each time point.

were fixed and labeled with anti-LAMP1 antibodies to monitor lysosomes at each time point. The mean pixel intensity of lysosomes surrounding a parasite invading the MEF cells was measured on the confocal microscope and analyzed. Interestingly not only the number of the intracellular parasites was significantly reduced in the *snapin*$^{-/-}$ MEF cells as we previously observed (Figure 3-3) but also poor host lysosomal recruitment to the parasites was displayed compared to the that of Snapin$^{+/+}$ MEF cells over time despite the fact that substantially increased amount of lysosomes present in *snapin*$^{-/-}$ MEF cytosol was observed (Figure 3-7). *T. cruzi* is well known to use unusual mechanisms to invade the cell by exploiting the recruitment and fusion of host lysosomes with the plasma membrane at the point of parasite entry (Tardieux, Webster et al. 1992) and the poor host lysosome recruitment to the parasite may explain why *T. cruzi* invasion was significantly reduced in SNAPIN-deficient cells. Furthermore, a failure of the parasites to reside in the lysosome-like parasitophorous vacuoles (Andrade and Andrews 2004) may possibly lead to the critical defect in differentiation into the intracellular amastigotes, and intracellular survival eventually.

3.3.4 Reduced calcium-dependent lysosome exocytosis in *snapin*$^{-/-}$ MEF cells

It was very intriguing that the parasites showed an impaired recruitment of host lysosomes in *snapin*$^{-/-}$ MEF cells despite the massive accumulation of LAMP1-positive lysosomes and its distribution spread throughout the cell cytosol. Host lysosome recruitment and fusion to the plasma membrane is a required event for *T. cruzi* to gain entry to the host cells (Tardieux, Webster et al. 1992). To figure out why the parasite invading the *snapin*$^{-/-}$ MEF cells was not able to exploit the host

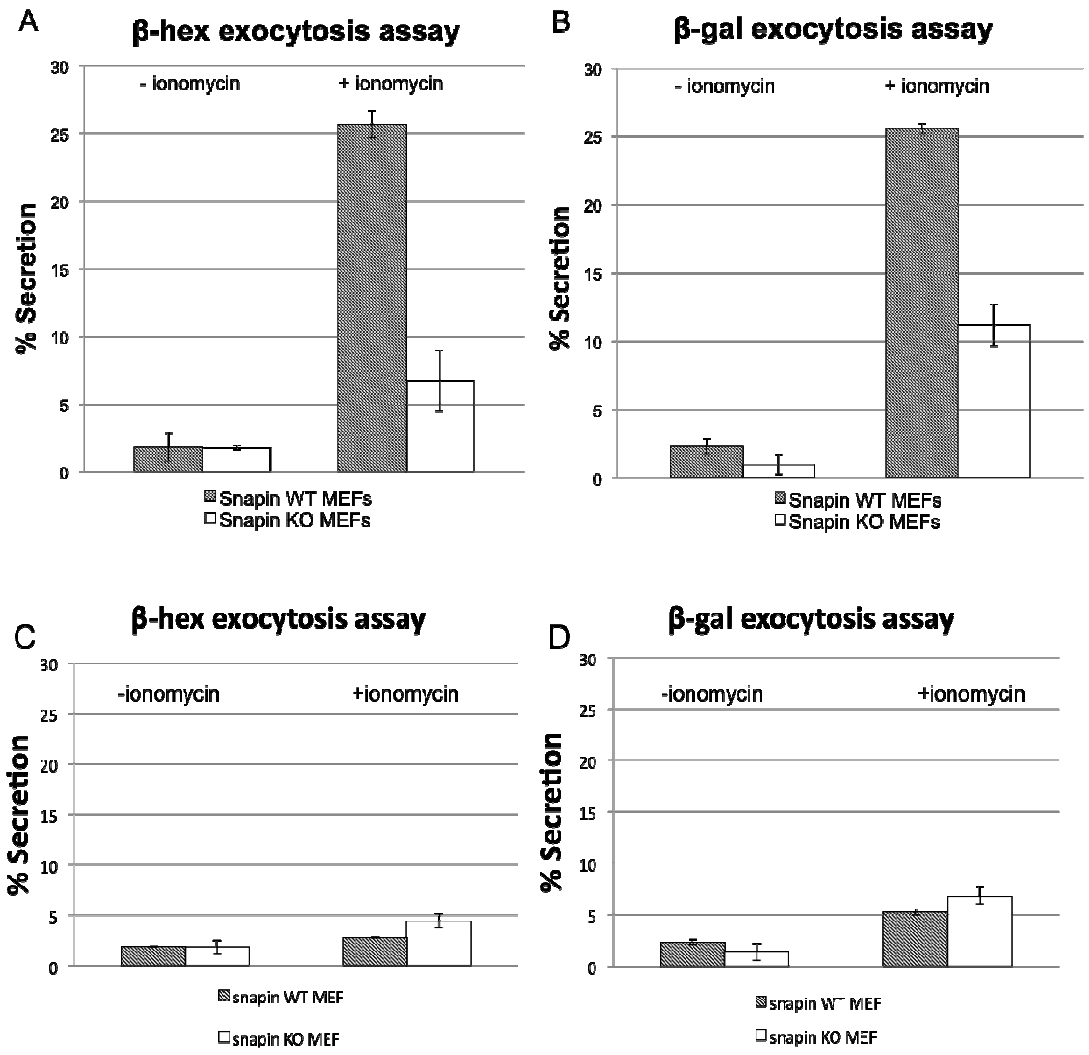

Figure 3-8. SNAPIN KO MEFs are impaired in calcium dependent lysosomal exocytosis. Calcium-dependent lysosomal exocytosis in SNAPIN WT and KO MEF cells was assayed and compared in two independent experiments using different lysosomal enzymes, β-hexosaminidase and β-galactosidase, respectively. (A) SNAPIN KO MEF cells show a great reduction in the rate of β-hexosaminidase secretion after 10 μM ionomycin treatment compared to the SNAPIN WT MEF cells. (B) β-galatosidase secretion was also significantly inhibited in SNAPIN KO MEFs when the cells were treated with 10 μM ionomycin compared to the SNAPIN KO

MEF cells. (C and D) MEF cells do not display lysosomal exocytosis upon 10 µM ionomycin treatment in the absence of calcium in the culture media. Results are representative of three independent experiments.

lysosomes present in the cell, we examined the rate of calcium-dependent lysosomal exocytosis using two distinct lysosomal enzymes: β-hexosaminidase and β-galactosidase. Both Snapin$^{+/+}$ MEF cells and *snapin*$^{-/-}$ MEF cells were incubated in the presence or absence of 10 μM ionomycin and the amount of secreted lysosomal enzyme was measured using a colorimetric assay coupled with an appropriate substrate to each lysosomal enzyme. Ionomycin is a calcium ionophore that allows transporting calcium across biological membrane and thus increasing the intracellular calcium level. The amount of secreted enzyme resulting from a calcium-dependent lysosomal exocytosis was normalized over the entire amount of the enzyme in the total cell lysates and compared. When compared to Snapin$^{+/+}$ MEF cells, *snapin*$^{-/-}$ MEF cells revealed significantly reduced amounts of β-hexosaminidase and β-galactosidase, 75% and 55%, respectively, that are secreted in the culture media upon ionomycin treatment in both independent experiments (Figure 3-8). This indicates that SNAPIN deficiency leads to an impaired calcium-dependent lysosomal exocytosis in the host cells and provides a clue how SNAPIN impacts the lysosome-dependent parasites invasion process. This is interesting because SNAPIN-deficient cells display increased amount of LAMP-1 positive lysosomes, yet the vast majority of these LAMP-1 positive lysosomes is not functional for a calcium-dependent exocytosis. This data is in agreement with a previous study (Tian, Wu et al. 2005) showing SNAPIN deletion in neuron impairs calcium-dependent exocytosis. It was previously shown that *snapin*$^{-/-}$ neuron exhibits accumulation of immature lysosomes with impaired lysosomal function such as reduced clearance of autolysosomes (Cai, Lu et al. 2010) and this report along with our data may suggest SNAPIN regulates the

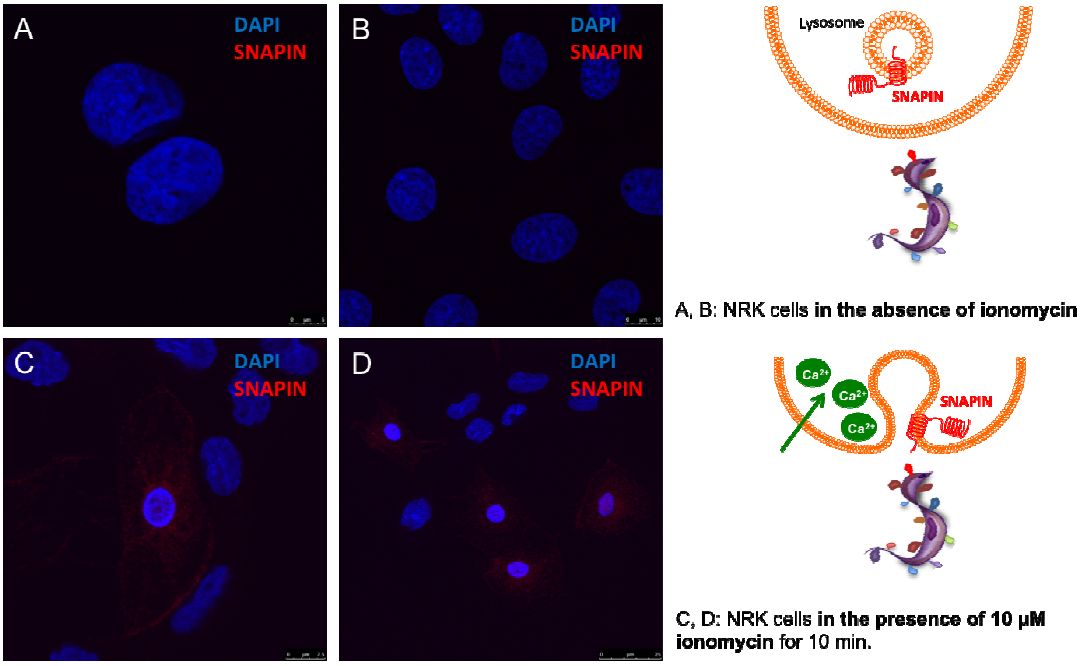

Figure 3-9. SNAPIN is translocated to the plasma membrane and exposed to the extracellular space. NRK cells were treated with 10 µM ionomycin for 10 minutes and kept unpermeabilized when being stained with polyclonal anti-SNAPIN antibodies. (A, B) In the absence of ionomycin, NRK cells do not expose SNAPIN to the extracellular space. (C, D) SNAPIN (in red), in a subset of NRK cells, was translocated to the plasma membrane and exposed to the extracellular space in the presence of ionomycin.

lysosome maturation and only the mature functional lysosome pool is used for a calcium-dependent exocytosis that will eventually benefit the parasite entry. The absence of SNAPIN accumulates the immature lysosomes that are not functional for a calcium-dependent exocytosis thus inhibits the parasite invasion. We had also observed a reduced GFP signal from several parasites expressing GFP that reside in the LAMP-1 positive parasitophorous vacuoles in Snapin$^{+/+}$ MEF cells (Figure 3-7 A) whereas the parasite invading the *snapin*$^{-/-}$ MEF cells was expressing the bright GFP (Figure 3-7 B). It is very plausible that GFP was quenched by the low pH in the functional and mature lysosomes and the LAMP-1 positive lysosomes in the *snapin*$^{-/-}$ MEF cells are immature and not acidic enough to quench the GFP proteins in the invading parasite.

3.3.5 SNAPIN is translocated and exposed to the extracellular space upon calcium influx

The topology of SNAPIN in the endosomal membrane is yet to be fully understood but according to the previous *in silico* analysis (Gowthaman, Silvester et al. 2006), SNAPIN is predicted to have two helical domains, one of them at its far C-terminus is most likely to be a coiled-coil domain based on PARCOIL analysis (Figure 3-10). This coiled-coil domain was demonstrated to be responsible for most interactions with SNARE proteins and other proteins (Buxton, Zhang et al. 2003; Chen, Lucas et al. 2005; Bao, Lopez et al. 2008; Wei, Xu et al. 2010), hence is presumed to be facing towards the cytosol. Although we found that TMHMM failed to predict a potential transmembrane domain in SNAPIN, several biochemical and cellular studies demonstrated the existence of cytosolic SNAPIN as well as membrane-associated

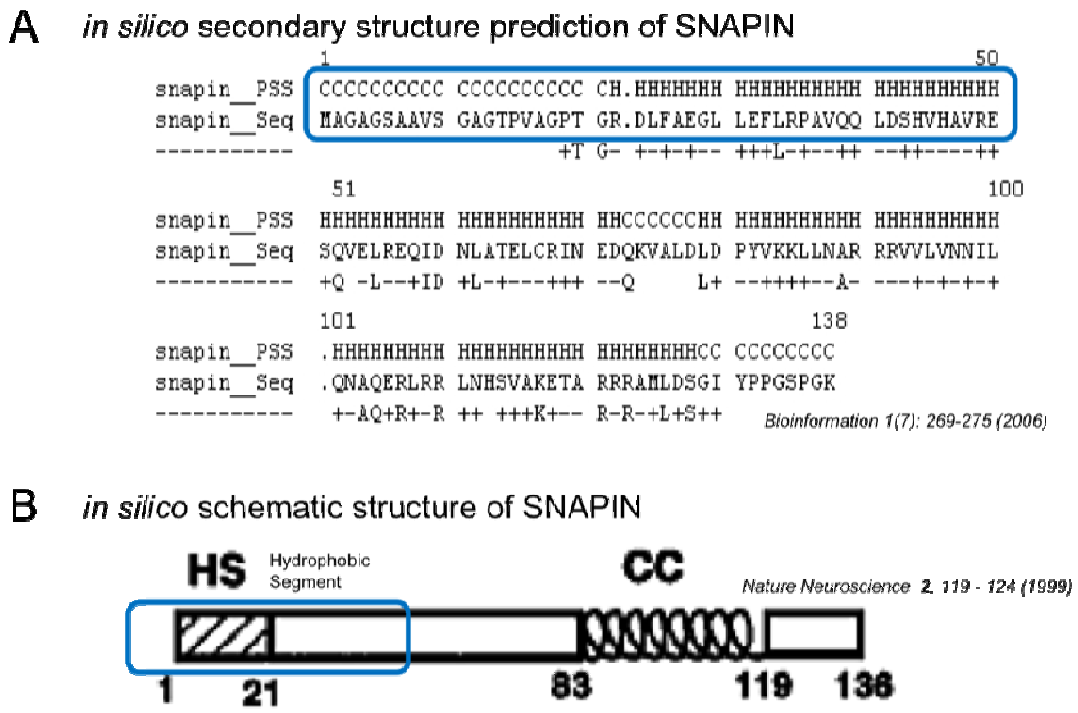

Figure 3-10. Schematic representation of SNAPIN structure. (A) *in silico* prediction of SNAPIN secondary structure and (B) protein motifs were represented. Hydrophobic segment (HS, in blue box) and coiled coil (CC) indicated (modified from 2006 Gowthaman *et al.* Bioinformation and 1999 Ilardi *et al.* Nature Neuroscience).

A

Bait	Prey	Interaction results
MASP1	N-terminal fragment SNAPIN	X
MASP4		X

B

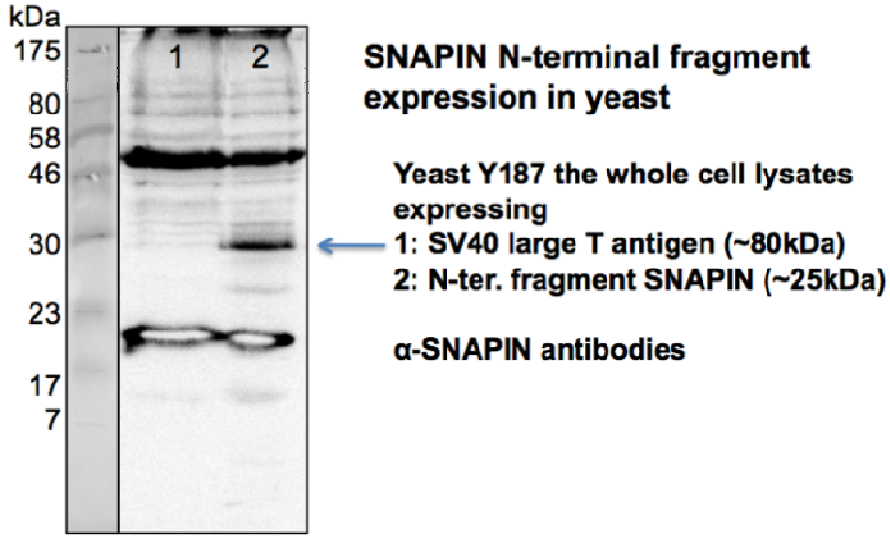

Figure 3-11. A pairwise interaction between MASP and the luminal domain of SNAPIN by yeast two-hybrid (A) Both MASP1 & MASP4 and the N-terminal fragment of SNAPIN do not interact in the yeast two-hybrid system. B) Western blot analysis revealed the expression of the N-terminal fragment of SNAPIN in yeast (lane 2).

SNAPIN (Buxton, Zhang et al. 2003; Chen, Lucas et al. 2005; Ruder, Reimer et al. 2005; Suzuki, Morishima et al. 2007). This prediction posed a topological issue for us since we initially identified SNAPIN as a putative MASP interactor (Figure 2-5) that is on the surface of the parasites. We hypothesized that the luminal domain of SNAPIN is exposed to the extracellular space as a result of a calcium-dependent lysosomal exocytosis. To test this hypothesis, NRK cells were stimulated with 10 µM ionomycin for 10 minutes and labeled with anti-SNAPIN antibodies under conditions not permitting cell permeabilization. NRK cells were selected since those cells are easily elicited by ionomycin and exhibit a better lysosomal exocytosis. We were able to observe the massive translocation of SNAPIN to the plasma membrane upon calcium influx (Figure 3-7 C and D) under the nonpermeabilized condition indicating the luminal domain of SNAPIN is exposed to the extracellular space due to a calcium-dependent lysosomal exocytosis event. This result confirms our earlier observation that SNAPIN is associated with lysosomes (Figure 3-5 E-H). Also this unravels the putative role of SNAPIN in *T. cruzi* invasion process possibly by providing the parasite the anchor or the target point for its entry. It is also worth noting that not all NRK cells responded to the stimulus and exposed SNAPIN to the extracellular space. This is in agreement with the observation that *T. cruzi* selectively invades a subset of cells and the distribution of *T. cruzi* infection obeys the negative binomial distribution rather than the Poisson-distribution (Dvorak and Hyde 1973; Fernandes, Cortez et al. 2011).

We tested the interaction between MASP proteins and the N-terminal domain of SNAPIN using a pairwise Y2H assay. Amino acid 1-50 of SNAPIN (Figure 3-10)

was cloned in pGADT7g Y2H expression vector by Gateway® cloning system and the expression in yeast cell was validated and confirmed by the standard immunoblotting analysis using anti-SNAPIN antibodies after transfection into yeast Y187 strain haploid cell. Unfortunately we were unable to show MASP1 nor MASP4 interacting with the N-terminal domain of SNAPIN in Y2H system. This might be one of a false negative that is one of disadvantages of Y2H system or may reflect the shortcoming of validating the protein-protein interaction in the heterologous system.

3.4 Conclusions and significance

SNAPIN seems to play a role in *T. cruzi* invasion process as *T. cruzi* infection is inhibited in SNAPIN-deficient cells. As we expected from MASP-SNAPIN interaction, SNAPIN was recruited to the parasite surface during the invasion process and associated with the late endosomes and lysosomes suggesting that SNAPIN is involved in the lysosome-dependent parasite entry process. SNAPIN deletion led to an accumulation of immature and nonfunctional lysosomes in the cell cytosol and a decrease in host lysosome recruitment to the parasite surface due to an impaired calcium-depenent lysosome exocytosis. Upon induced calcium influx, SNAPIN is translocated to the plasma membrane of the cells and the luminal domain is exposed to the extracellular space that may provide an anchor to the parasite for its entry although the interaction between MASP and the N-terminal domain of SNAPIN was tested as negative. A set of experiments shown in this chapter gives the clues about not only the roles of SNAPIN in the context of cellular biology but also the functions of SNAPIN in the parasite invasion process and how parasites utilize the host proteins to gain better access to the cell. Also, this demonstrates the loss-of-function study in

host cells can infer the function of parasite counterpart proteins and how useful this can be in *T. cruzi* gene annotation where 50% of the genes are still unannotated and genetic tools are very limited.

Chapter 4: The investigation of a putative function for MASP in host cell invasion

4.1 Objective of Study

The overall objective of this study was to characterize the putative function of the MASP family utilizing molecular genetics tools and cellular biological techniques. In Chapter 3, human interacting partner protein of MASP1 and MASP4, SNAPIN, was demonstrated to be involved in the *T. cruzi* invasion process by mediating the host lysosome maturation and calcium-dependent lysosomal exocytosis. In Chapter 4, we aimed to determine the role of MASP1 and MASP4 in the context of calcium-dependent lysosomal exocytosis where SNAPIN was implicated via generating transgenic parasites that constitutively overexpresses recombinant MASP proteins in the kinetoplastid protozoan parasite, *Leishmania tarentolae*, not only the non-pathogenic but also incapable to host cell invasion and down-regulating the MASP expression in *T. cruzi* by blocking the translation initiation site with the modified complementary oligomers. Even though we are focusing on only two MASP members out of 1,377 copies in the genome, the putative function determined from this study may apply to other members if MASP1 and MASP4 turn out to share the common role in *T. cruzi* invasion process.

4.2 Materials and Methods

4.2.1 Materials

Materials	Catalogue numbers	Sources
LEXSYcon2 Expression Kit	EGE-1300sat	Jena Bioscience
Nourseothricin (NTC)	AB-102L	
Hemin	H9039	Sigma-Aldrich
*Bgl*II	R0144S	New England Biolabs
*Nhe*I	R0131S	
*Not*I	R0189S	
*Swa*I	R0604S	
Triton X-114 (TX-114)	80057-670	Calbiochem®
G418 Sulfate	345810	
Pfx50™ DNA polymerase	12355012	Invitrogen
pDONR™/Zeo	12535035	
Phosphatidylinositol-Specific Phospholipase C (PI-PLC)	P-6466	
Fluo-4 Direct™ Calcium Assay Kit	F10471	
Ni-NTA agarose resin	R901-01	
pDEST-CMV-c-Myc vector		Dr. Sunghak Kim (National Research Laboratory for Cancer Epigenetics, Cancer Research Institute, Seoul, Korea)
pENTR-Zeo-Bcl2		Dr. Michael Waisberg (National Institute of Allergy and Infectious Diseases (NIAID), National Institutes of Health (NIH)
Propidium iodide (PI)	P4170	Sigma-Aldrich
Mouse anti-c-Myc antibodies	631206	Clontech
Lab-Tek™ Chamber Slide™ System	177437	Thermo
Horse Serum	14-403E	Lonza
Basic Parasite Nucleofector® Starter Kit	VMI-1101	
CellTiter 96 AQueous Non-Radioactive Cell Proliferation Assay	G5421	Promega
GP72 morpholino	Custom-made	Gene Tools LLC.
Mouse anti-His monoclonal antibodies	34660	Qiagen
BSA-coated Polystyrene Particles	BP-08-10	Spherotech
Polystyrene Particles	PP-08-10	

4.2.2 Methods

Host cells and Parasites: HeLa cells (CCL-2.1) and LLC-MK_2 (Rhesus Monkey Kidney Epithelial) cells were maintained in Dulbecco's Modification of Eagle's Medium (DMEM) supplemented with 10% heat inactivated Fetal Bovine Serum (FBS) at 37ºC with 5% CO_2. *Trypanosoma cruzi* epimastigotes (CL Brener and Y strains) were maintained in Liver Infusion Tryptose (LIT) medium with 10% heat inactivated FBS at 28ºC. Metacyclic trypomastigotes (MTs) of *T. cruzi* were purified from 10-day old LIT culture by ion-exchange chromatography (DEAE cellulose) and Tissue-culture derived trypomastigotes (TCTs) were obtained from infected LLC-MK_2 cells. *Leishmania tarentolae* P10 strain (Jena Bioscience) was cultivated in Brain Heart Infusion (BHI) medium supplemented with 5 µg/ml Hemin at 26ºC.

Over-expression of MASP in the L. tarentolae system: Pairs of restriction enzymes *Bgl*II & *Nhe*I and *Bgl*II & *Not*I were used to clone GFP and full-length internally 6xHis-tagged MASP1 & MASP4 proteins into pLEXSY-sat2 vector respectively. The constructs were linearized with *Swa*I for the genomic integration into the chromosomal 18S rRNA locus and $5x10^7$ *L. tarentolae* P10 strain in mid-log phase was electroporated using Gene Pulser II system (Bio-Rad) according to the manufacturer's instructions. Twenty-four hours after electroporation, the transgenic populations were selected under 100 µg/mL Nourseothricin (NTC) for the generation of stable population.

Purification of GPI-anchored recombinant MASP from L. tarentolae: GPI-anchored recombinant MASP proteins were purified from the transgenic *L. tarentolae* membrane using a modified Triton X-114 partition method described elsewhere (Ko

and Thompson 1995; Anez-Rojas, Garcia-Lugo et al. 2006; Rojas, Garcia-Lugo et al. 2008). The transgenic parasites were resuspended in a 10 mM Tris–HCl, 150 mM NaCl pH 7.4 buffer (TBS) with 2% Triton X-114 and incubated for 1 hour at 0ºC. The suspension was then centrifugated and the supernatant was kept at -20ºC for 24 hours. The frozen supernatant was thawed at room temperature and incubated at 32ºC for 12 minutes to obtain the partition. The partition was spun at 3,000x g for 3 minutes and the aqueous phase containing hydrophilic proteins was stored at -20ºC for the downstream analysis. The detergent phase was further washed in 3 volumes of TBS pH 7.4 contianing 0.06% Triton X-114 and kept at 0ºC for 10 minutes. The partition process was repeated once more, the aqueous phase was discarded and the detergent phase was mixed with 3 volumes of TBS pH 7.4 containing 0.06% Triton X-114 again. The suspension was incubated at 0ºC for 10 minutes and cleared by centrifugation at 13,000x g, 0ºC for 15 minutes. The pellet containing hydrophobic proteins was kept at -20ºC for the downstream analysis and the supernatant fraction was subjected to another partition. The detergent phase containing GPI-anchored proteins was precipitated with 4 volumes of cold acetone and resuspended in PI-PLC buffer (25 mM HEPES pH 7.5, 0.1% sodium deoxycholate). GPI-anchored proteins were cleaved by 1U PI-PLC (Invitrogen) for 3 hours at 37ºC. 6xHis-tagged MASP proteins in the aqueous phase were purified by Ni-NTA agarose resin. The proper fractionation and purification of 6xHis-tagged MASP proteins were confirmed by performing SDS-PAGE analysis followed by the standard immunoblotting analysis using mouse anti-His monoclonal antibodies.

Leishmania tarentolae pull-down assay: Purified 6xHis-tagged *L. tarentolae* recombinant MASP protein was used as bait and the c-Myc-tagged full-length SNAPIN, N-terminal fragment of SNAPIN, and Bcl-2 recombinant proteins were expressed in HeLa cells and used as prey. The c-Myc plasmids were constructed by Gateway® recombination. Open reading frames (ORFs) of full-length *snapin*, N-terminus of *snapin, bcl-2* were amplified by the polymerase chain reaction using the *Pfx50*™ DNA polymerase using the primers (See Appendix B.1 for sequence) with *att*B overhang sequences that served as the recombination sites. Amplicons were cloned into the pDONR™/Zeo vector and then the inserts were shuttled to pDEST-CMV-c-Myc vector by LR reaction (Invitrogen) according to the manufacturer's instructions. The interaction pairs, 6xHIS-baits (6xHIS-MASP1 and 6xHIS-MASP4) and c-Myc-preys (c-Myc-Bcl2, c-Myc-SNAPIN and c-Myc-Luminal SNAPIN) were incubated for 1 hour at 4ºC. The complexes were purified by Ni-NTA agarose resin and analyzed by SDS-PAGE and the standard immunoblotting techniques with mouse anti-His antibodies and mouse anti-c-Myc antibodies.

Immunofluorescence: LLC-MK_2 cells infected by *T. cruzi* were fixed with 4% fresh paraformaldehyde (PFA) for 10 minutes at room temperature, washed with PBS 3 times, and quenched with 15 mM NH_4Cl. The samples were then blocked with 2% BSA-containing PBS for 1 hour at room temperature. Cells on the glass coverslip were permeabilized with 0.1% Saponin for 10 minutes if necessary. The samples were incubated with mouse anti-His monoclonal antibodies for 1 hour followed by anti-mouse Alexa Fluor 488 secondary antibody incubation. Images were acquired using the confocal microscope (Leica SP5 X) in the imaging core facility (University

of Maryland, College Park). For *L. tarentolae*, the cells were fixed in 4% fresh PFA and washed with PBS 3 times followed by 50 mM NH_4Cl. The fixed cells were spotted on a glass slide and allowed to dry for 30 minutes at room temperature. The dried cells were rehydrated with PBS twice for 10 minutes each and blocked for 1 hour with 3% BSA in PBS. The slide was incubated with mouse anti-6xHis monoclonal antibodies at 1:100 dilution for 1 hour with no cell permeabilization step and then with anti-mouse Alexa Fluor 594 secondary antibodies at 1:500 dilution. The samples on the slide were inspected on the confocal microscope (Leica SP5 X) in the imaging core facility (University of Maryland, College Park).

Live cell imaging and calcium transient analysis: HeLa cells ($1x10^5$) were seeded on Lab-Tek™ Chamber Slides and preloaded with the green-fluorescent calcium indicator, Fluo-4 for 30 minutes at 37ºC followed by another 30 minutes at room temperature on the following day. The Fluo-4-preloaded cells in the chamber slides were incubated with $2x10^7$ *T. cruzi* CL Brener strain trypomastigotes, *L. tarentolae* P10 strain, and transgenic P10 strains expressing MASP1 or MASP4. For the experiments with polystyrene beads, Fluo-4-preloaded HeLa cells were incubated with BSA-coated polystyrene particles, MASP1-coated polystyrene particles, and MASP4-coated polystyrene particles. Cells were live-imaged every 213 ms over 300 sec on the confocal microscope (Leica SP5 X) in the imaging core facility (University of Maryland, College Park). Intracellular calcium transients in 100 HeLa cells (color-coded) were monitored and plotted over time using the Leica LAS AF Lite software (version 2.4.1). Video was compressed and played at 45 frames per second.

MASP proteins-coated particles were prepared by passive adsorption. Purified recombinant MASP proteins were incubated with 0.1M phosphate buffer (pH 7.4) and 5% w/v 0.7~0.9 µm polystyrene particles. The mixture was incubated for one hour at room temperature. The supernatant was removed carefully after centrifugation for 15 minutes at 3,000x g. Isotonic Buffered Saline (IBS) was added and the mixture was vortexed well. The supernatant was once again removed by centrifugation for 15 minutes at 3,000x g. The particles were resuspended with IBS and the suspension was used for the experiments. The efficiency of passive adsorption was confirmed by immunofluorescence assays using mouse anti-His mono clonal antibodies coupled with Alexa Fluor 594 secondary antibodies and inspected under Nikon epifluorescence microscope (E200).

Cell wounding assay: HeLa cells ($2x10^6$) were incubated with *L. tarentolae* wild-type P10 strain, or transgenic P10 strains expressing MASP1 or MASP4, in the absence of Ca^{2+} in DMEM with 25 µg/ml propidium iodide (PI) for 30 minutes at 37ºC. Cells were fixed with 4% fresh PFA for 10 minutes and stained with DAPI (4',6-diamidino-2-phenylindole). The plasma membrane integrity was inspected on Nikon epifluorescence microscope (E200) by counting PI-positive cells.

MASP adhesion assay: **Transgenic** *L. tarentolae* cells ($6x10^7$) expressing MASP1 or MASP4, along with wild-type *L. tarentolae* were incubated with $2x10^6$ HeLa cells (MOI=30) for 1 hour and washed extensively with PBS 5 times. The cells were fixed in Bouin's fixative for 20 minutes at room temperature and washed with PBS 5 times thoroughly. Cells were stained with Giemsa solution overnight and mounted on the slide for the quantification of the parasites attached to 200 HeLa cells.

Cell protection from complement lysis assay: *L. tarentolae* P10 strain and transgenic parasites expressing MASP1 or MASP4 were incubated in BHI medium with 10% Horse Serum for 2 hours or 4 hours. The number of viable cells was determined by CellTiter 96 AQueous Non-Radioactive Cell Proliferation Assay at each time point according to the manufacturer's instructions.

Knock-down attempts of GP72 in T. cruzi using morpholino: Morpholino oligo sequence (5'-TGAAAACATCACGTCCAAGACGGGA-3') was synthesized according to the manufacturer's recommendation to efficiently block the translation of *T. cruzi* GP72 by targeting from 16 bases upstream of start codon to 9 bases downstream of start codon. 100 µM of GP72 morpholino oligomers was transfected into $5x10^7$ mid-log phase *T. cruzi* CL Brener strain epimastigotes with Basic Parasite Nucleofector® Starter Kit by Nucleofector™ II Device, program U-033 (Lonza). The same amount of Nucleofector® solution without morpholino oligomers was used as a negative control. The morphology of the transfected parasites was monitored up to 48 hours on Nikon epifluorescence microscope (E200).

4.3 Results and Discussion

4.3.1 The overexpression of MASP in *Leishmania tarentolae*

Recombinant MASP proteins used in our earlier assays were expressed in a variety of heterologous systems (Figure 2-1). Our attempts to overexpress recombinant MASP proteins *in T. cruzi* resulted in very low expression levels observed by immunoblotting (data not shown) and immunostaining analyses (Figure 5-6 A), presumably due to its tight regulation depending on the life cycle. For instance,

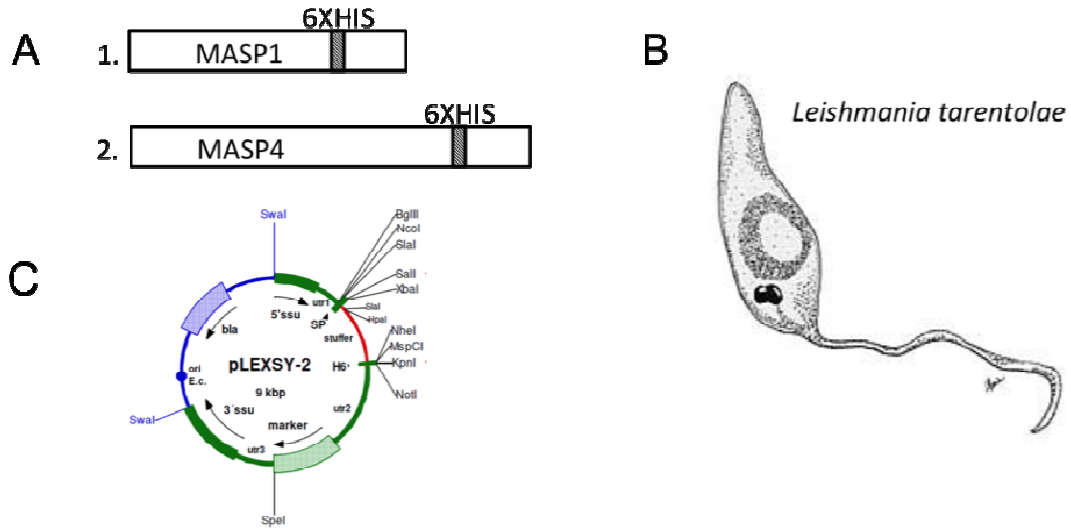

Figure 4-1. *Leishmania tarentolae* expression system (LEXSY). (A) Internally 6xHis-tagged *masp1* and *masp4* ORFs were cloned in pLEXSY-2 vector and tranfected into (B) *Leishmania tarentolae* P10 strain. (C) pLEXSY-2 vector was used to overexpress MASP in *L. tarentolae*. utr1, utr2 and utr3 contain efficient trans-splicing as well as poly-adenylation signals for the proper transcript processing. 5' and 3' ssu are for genomic integration of the linearized construct by homologous recombination events.

TcDHH1 protein, a DEAD box RNA helicase, was recently implicated to regulate the expression of MASP in the epimastigote stage, by directly binding to MASP transcripts and inhibiting the translation of MASP in the epimastigote stage (Holetz, Alves et al. 2010). Therefore, it was very tricky to work with recombinant MASP proteins in *T. cruzi* because MASP expression seemed to be strictly controlled in the replicative epimastigote form and even under one of the strongest promoters, ribosomal DNA, the expression of MASP was not detectable in the epimastigote form. Although MASP expression was found in the trypomastigote form, considering multiple endogenous MASP proteins already present in the surface of wild-type trypomastigotes, it was not ideal to compare the transgenic trypomastigotes expressing MASP protein to wild-type trypomastigotes.

Thus, we evaluated recombinant MASP proteins overexpression in a related kinetoplastid, *L. tarentolae* as this is a well-established overexpression system for trypanosome proteins and represents a relatively homologous system (Breitling, Klingner et al. 2002; Heise, Singh et al. 2009; Bolhassani, Taheri et al. 2011) to *T. cruzi*. *L. tarentolae* belongs to the *Leishmania* genus and the Trypanosomatidae family where *T. cruzi* is included. Unlike other pathogenic *Leishmania spp.* and trypanosomes, *L. tarentolae* is non-human pathogenic and lives predominantly as an extracellular promastigote form in lizard (Baud, Lovis et al. 2001). *L. tarentolae* overexpression system has several advantages over others that we have tried in the previous studies including a large quantity protein yield, and a much better likelihood of correct protein folding and 'native' post-translational modifications (Breitling, Klingner et al. 2002). Furthermore, transgenic *L. tarentolae* expressing MASP protein

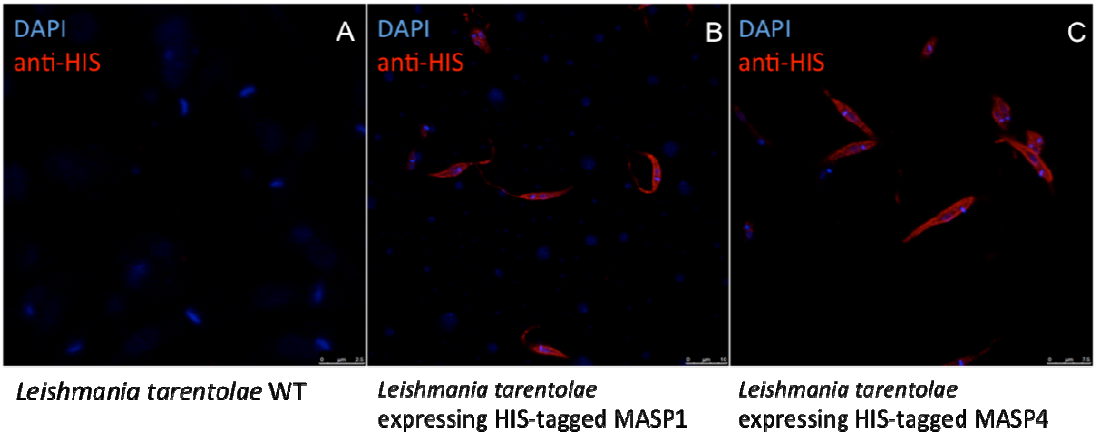

Figure 4-2. Recombinant MASP expression in *Leishmania tarentolae.* (A) 6xHIS-tagged MASP1 and MASP4 were expressed in *Leishmania tarentolae* P10 strain. Each fraction was analyzed by Western blot revealing that MASP proteins are enriched in a GPI-anchored protein fraction. (B) GPI-anchored protein enriched fraction was prepared by Triton X-114 fractionation protocol described in the materials and methods. (C) The subcellular localization of recombinant MASP proteins was assessed by IFA and appeared to be on the plasma membrane presumably by GPI-anchor.

on the plasma membrane can be used along with wild-type *L. tarentolae* and compared to each other to investigate the putative function of MASP as recombinant MASP protein is expressed constitutively in the promastigote form and has no orthologs in *L. tarentolae.* Hence we introduced *L. tarentolae* expression system (LEXSY) in order to obtain reliable amount of recombinant 6xHis-tagged MASP proteins presumably folded and modified in a very similar fashion to that in *T. cruzi* (Figure 4-1 A). The full-length *masp1* and *masp4* harboring 6xHis-tag in the hypervariable region were cloned into pLEXSY-sat2 expression vector. The wild-type *L. tarentolae* P10 strain (Figure 4-1 B) was transfected with the linearized DNAs for the genomic integration and the transgenic parasites expressing MASP proteins were selected using Nourseothricin (NTC). Stable population of *L. tarentolae* P10 strain expressing 6xHis-tagged MASP1 and MASP4 were subjected to the immunofluorescence assay using mouse anti-His monoclonal antibodies and the cellular localization was clearly confirmed to the plasma membrane, presumably by GPI-anchor whereas no 6xHis-tagged protein expression was detected in *L. tarentolae* P10 strain as expected (Figure 4-2). This *L. tarentolae* expressing MASP proteins on the surface became a powerful tool in our hands allowing production of large amounts of MASP proteins and providing us with a live transgenic trypanosomatid expressing MASP. The purification of recombinant MASP proteins was performed by Triton X-114 (TX-114) fractionation (Figure 4-3) (Ko and Thompson 1995; Anez-Rojas, Garcia-Lugo et al. 2006; Rojas, Garcia-Lugo et al. 2008). Triton X-114 is a unique mild nonionic detergent that not only solubilizes membrane proteins but also separates them from hydrophilic proteins by phase

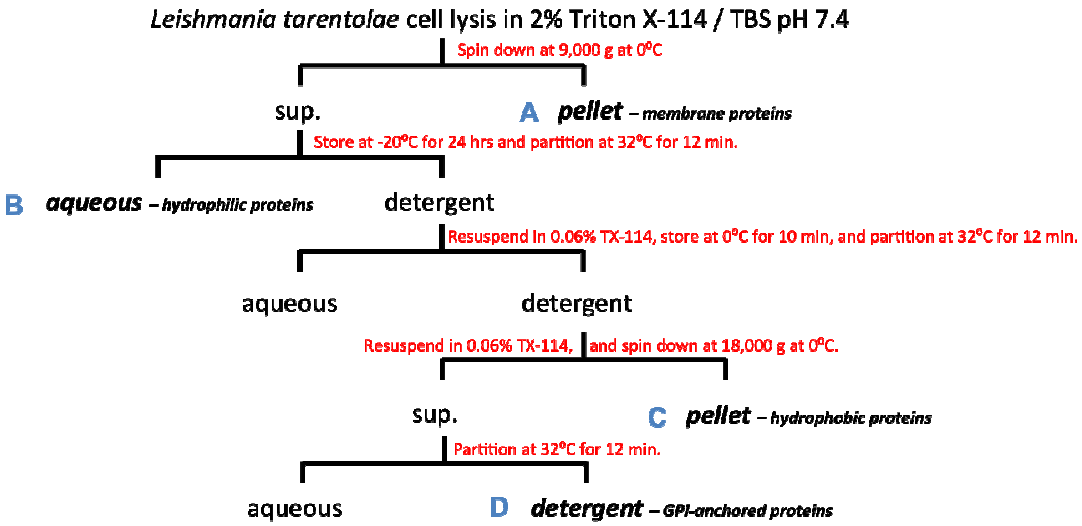

Figure 4-3. GPI-anchored protein partitioning pipeline using Triton X-114 (modified from 1995 Ko *et al.* BJ). *L. tarentolae* expressing MASP were lysed in TBS containing 2% Triton X-114 (TX-114) and the cell lysates were spun down to separate membrane proteins (A). Supernatant was transferred to the new tube and partitioned at 32ºC into aqueous phase (B: hydrophilic proteins) and detergent phase. The detergent phase was washed in TBS containing 0.06% TX-114 and further partitioned. The aqueous phase was discarded and the detergent phase was centrifugated to separate hydrophobic proteins (C). The supernatant was transferred to a fresh tube and partitioned once more to obtain detergent phase enriched with GPI-anchored protein (D).

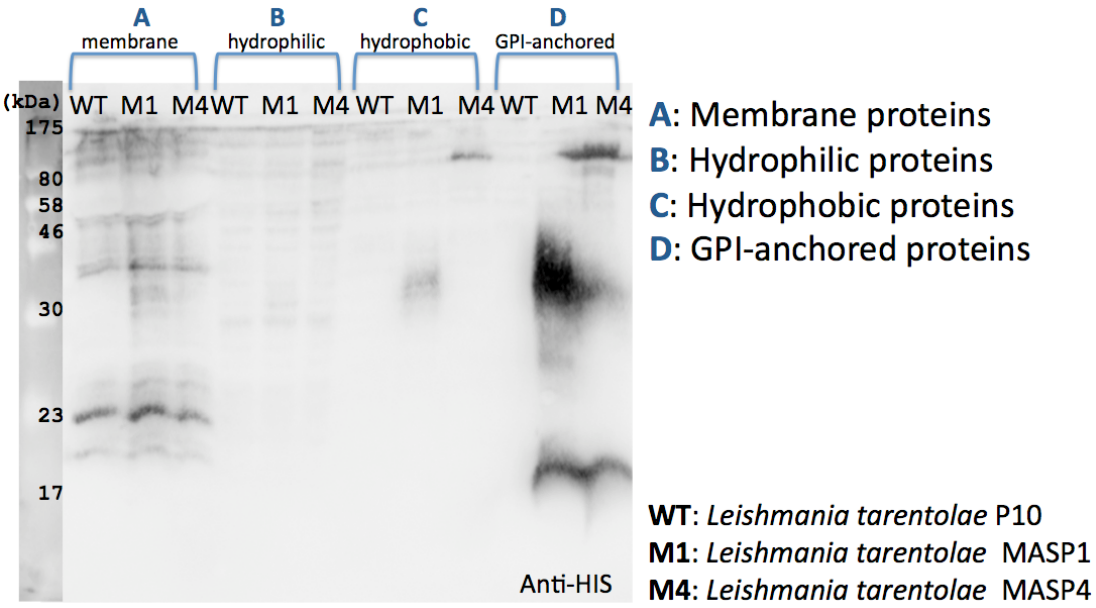

Figure 4-4. Immunoblotting analysis of each fraction from Triton X-114 partitioning. Membrane (A), hydrophilic (B), hydrophobic (C) and GPI-anchored proteins (D) of *L. tarentolae* wild-type, *L. tarentolae* expressing MASP1 and MASP4 were probed with mouse anti-His antibodies.

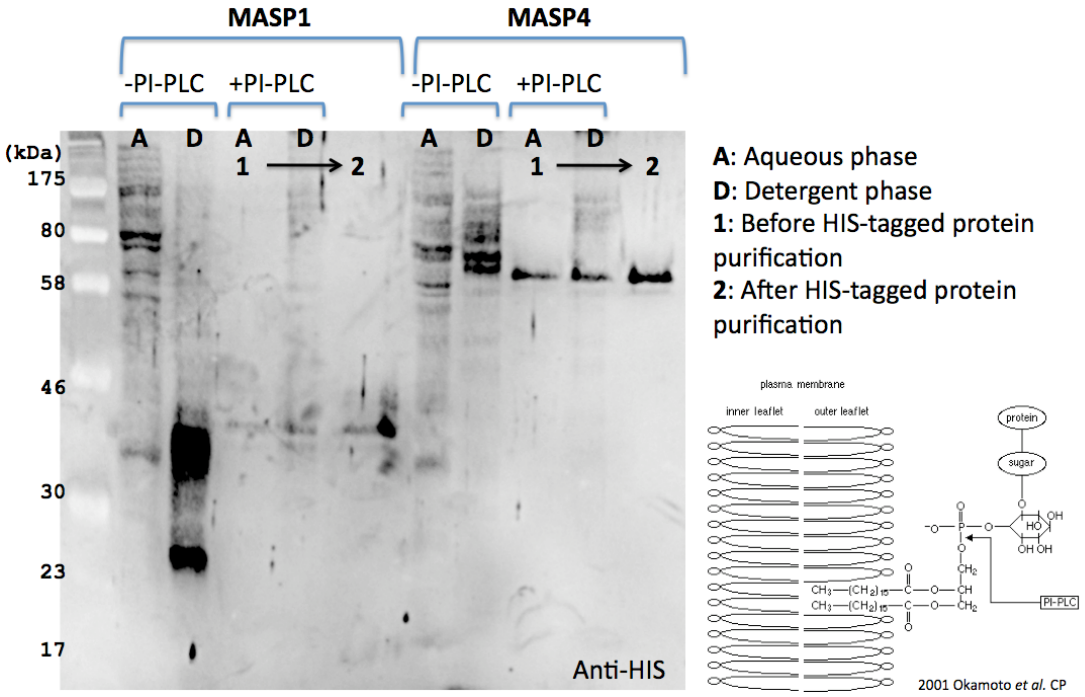

Figure 4-5. Purification of GPI-anchored MASP proteins. GPI-anchored MASP proteins were cleaved by PI-PLC enzyme to be released from the detergent phase (D) to the aqueous phase (A) and further purified with Ni-NTA agarose resin.

partitioning at room temperature. This is very useful for protein fractionation because TX-114 solution is homogeneous at 0ºC as a clear micellar solution but separates into an aqueous phase and a detergent phase above 20ºC as micellar aggregates form and the solution turns turbid. With increased temperature, phase separation proceeds until two clearly separated phases are formed where hydrophilic proteins are enriched in the upper aqueous phase and hydrophobic proteins are enriched in the bottom detergent phase. First, *L. tarentolae parasites* were lysed in 2% TX-114 solution and membrane proteins were solubilized. The total cell lysates were partitioned into membrane, hydrophilic, hydrophobic and GPI-anchored protein fractions (See Methods for a detailed preparation steps) (Figure 4-3). Each fraction obtained from TX-114 fractionation was analyzed by the standard immunoblotting technique using anti-His antibodies. As expected, the vast majority of 6xHis-tagged MASP proteins (MASP1 and MASP4) were detected in the GPI-anchored protein enriched fraction (Figure 4-4 D) indicating MASP proteins were processed properly in *L. tarentolae* overexpression system. However, small amounts were found in hydrophobic protein fraction (Figure 4-4 C) demonstrating MASP proteins are hydrophobic presumably because they are still anchored to the outer leaflet of the plasma membrane by GPI-anchor. GPI-anchored MASP proteins were not present in membrane protein fraction confirming the efficiency of TX-114 in solubilizing and enriching GPI-anchored proteins (Figure 4-4 A). In order to make our MASP proteins soluble, MASP protein pellet from acetone precipitation step was resuspended in PI-PLC buffer and incubated with 1U of PI-PLC enzyme for 3 hours at 37ºC. PI-PLC cleaves a phosphatidylinositol (PI) of GPI-anchored proteins that is linked on the outer leaflet

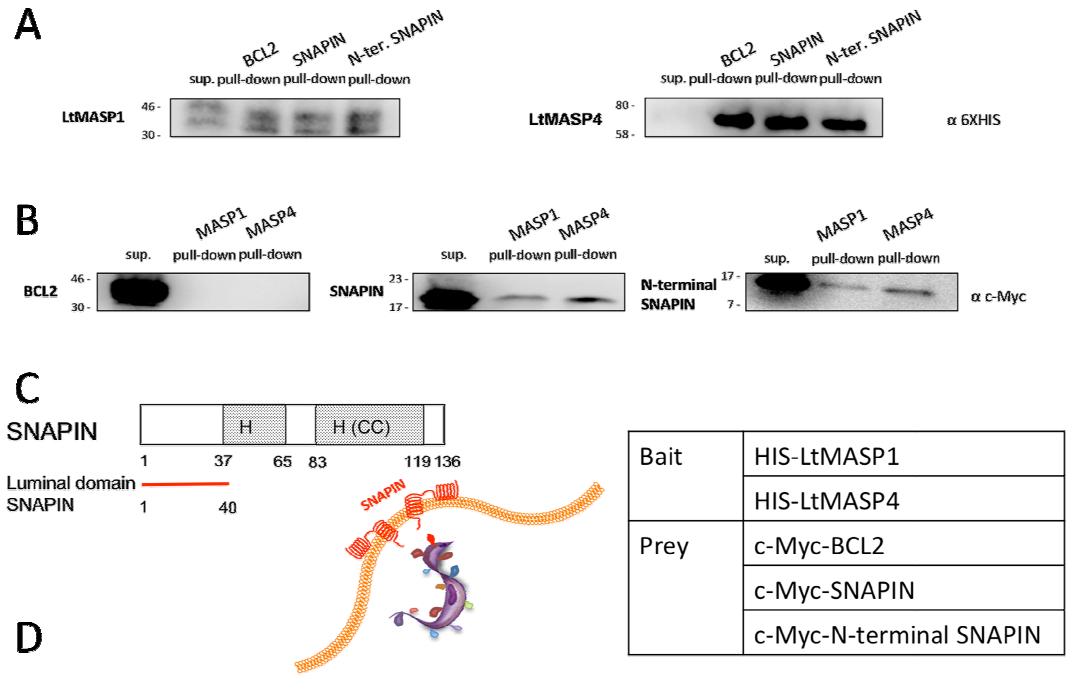

Bait	HIS-LtMASP1
	HIS-LtMASP4
Prey	c-Myc-BCL2
	c-Myc-SNAPIN
	c-Myc-N-terminal SNAPIN

Figure 4-6. A luminal domain of SNAPIN is interacting with MASP proteins.

6xHIS-tagged MASP1 and MASP4 proteins (baits) expressed in *Leishmania tarentolae* were prepared as described earlier and incubated with the HeLa cell lysates where c-Myc-tagged BCL2, SNAPIN and a luminal domain of SNAPIN (preys) were overexpressed respectively for 1 hour. The protein complex was purified with Ni-NTA agarose and analyzed by the standard immunoblotting analysis. (A) 6xHIS-tagged MASP1 and MASP4 were expressed and present in each protein complex. (B) The expression and detection of c-Myc-fusion proteins in each protein complex were probed with anti-c-Myc antibodies. (C) Domain map of SNAPIN showing two helical domains predicted *in silico* with the second region (83-119) higher possibility of a coiled-coil structure. A luminal domain of SNAPIN used in the pull-down assay in red. H: helix, CC: coiled-coil. (D) Biologically relevant configuration between MASP on *T. cruzi* and the luminal domain of SNAPIN interaction.

of the membrane bilayer. For both MASP1 and MASP4 proteins, we were able to observe the shift from the detergent phase to the aqueous phased after PI-PLC treatment (Figure 4-5) and soluble 6xHis-tagged MASP1 and MASP4 proteins were further purified by Ni-NTA agarose resin to remove other endogenous GPI-anchored proteins present in the membrane of *L. tarentolae* from GPI-anchored protein enriched fraction. PI-PLC treatment clearly showed the release of soluble MASP proteins from the plasma membrane indicating recombinant MASP proteins were indeed GPI-anchored (Figure 4-4 and 4-5).

4.3.2 The luminal domain of SNAPIN interacts with the MASP proteins

Purified and soluble recombinant MASP proteins expressed in *L. tarentolae* were used to evaluate their interaction with the luminal domain of c-Myc-tagged SNAPIN expressed in HeLa cells simulating the most biologically and topologically relevant environment for the host-parasite interaction. A pair of MASP and SNAPIN or a luminal domain of SNAPIN was mixed and incubated at 4ºC overnight. The protein complex was purified by Ni-NTA agarose resin and subjected to the standard immunoblotting analysis. The results demonstrate both MASP1 and MASP4 interact with the luminal domain of SNAPIN as well as the full-length SNAPIN (Figure 4-6 B) but not with BCL2, a negative control. This contrasts with the results that we got from Y2H system where we were not able to detect an interaction between MASP1 or MASP4 and the luminal domain of SNAPIN (Figure 3-11). Interestingly, both MASP proteins also interact with the C-terminal fragment of SNAPIN, which contains the cytosolic coiled-coil domain (data not shown). This may suggest other roles for SNAPIN when the parasite escapes the parasitophorous vacuole to the cytosol and

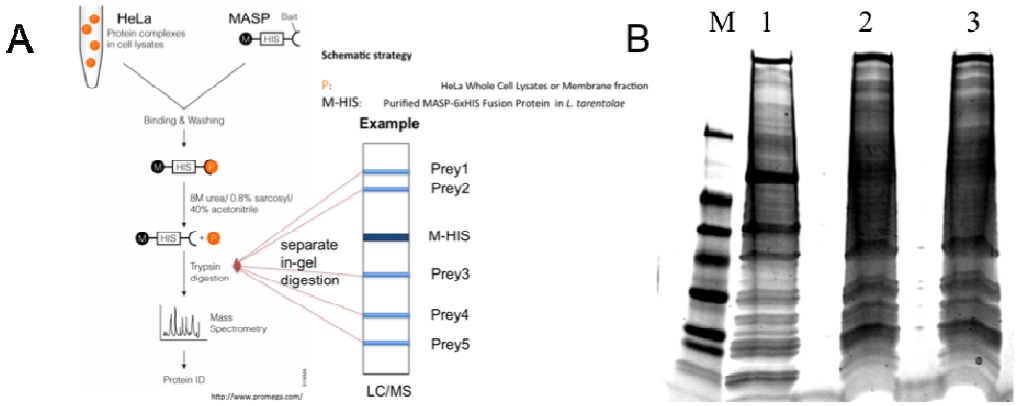

Figure 4-7. Preliminary *in vitro* pull-down assay strategy and result. (A) Purified 6-His-tagged MASP proteins were incubated with precleared HeLa total cell lysates for 1 hour. Protein complexes were purified by Ni-NTA agarose resin and analyzed by SDS-PAGE. (B) Coomassie blue staining of SDS-PAGE loaded with 1: Precleared HeLa total cell lysates, 2: MASP1 interacting proteins and 3: MASP4 interacting proteins.

modulate the lysosome exocytosis or when the parasite redifferentiates into the trypomastigote after nine rounds of binary division. Purified MASP proteins were also used for *in vitro* pull-down assays with human total cell lysates followed by mass spectrometry so we can confirm the interaction identified from Y2H screens and discover novel interactions (Figure 4-7 A). HeLa cells were lysed and incubated with Ni-NTA agarose resin to eliminate non-specific bindings to the resin in the absence of MASP proteins. Then, each MASP protein was incubated with the pre-cleared HeLa cell lysates at 4ºC overnight. The protein complex was recovered by Ni-NTA agarose resin and analyzed on SDS-PAGE. Even with the extensive clearance of non-specific bindings in HeLa cell lysates, Coomassie blue staining of PAGE gel revealed multiple bands in MASP pull-down lanes (Figure 4-7 B, lane 2 and 3) that are shown to be non-specific bindings when compared to the lane where pre-cleared HeLa total cell lysates were loaded (Figure 4-7 B, lane 1). This indicated that the further optimization was being required.

4.3.2 MASP expressed in *Leishmania tarentolae* triggers calcium transients, probably by wounding the host cell membrane

T. cruzi-specific MASP family was speculated to play a major role in the interaction of the parasite with the host cell, as *T. cruzi* has the unique characteristics to actively invade any nucleated cells among the Tritryps (Schenkman, Robbins et al. 1991; El-Sayed, Myler et al. 2005). Also MASP is preferentially expressed in the infective form of *T. cruzi* on the surface (Bartholomeu, Cerqueira et al. 2009). In my earlier experiments in Chapter 3, MASP's putative human partner protein, SNAPIN, was shown to be involved in *T. cruzi* invasion process, at least in the early stage, by

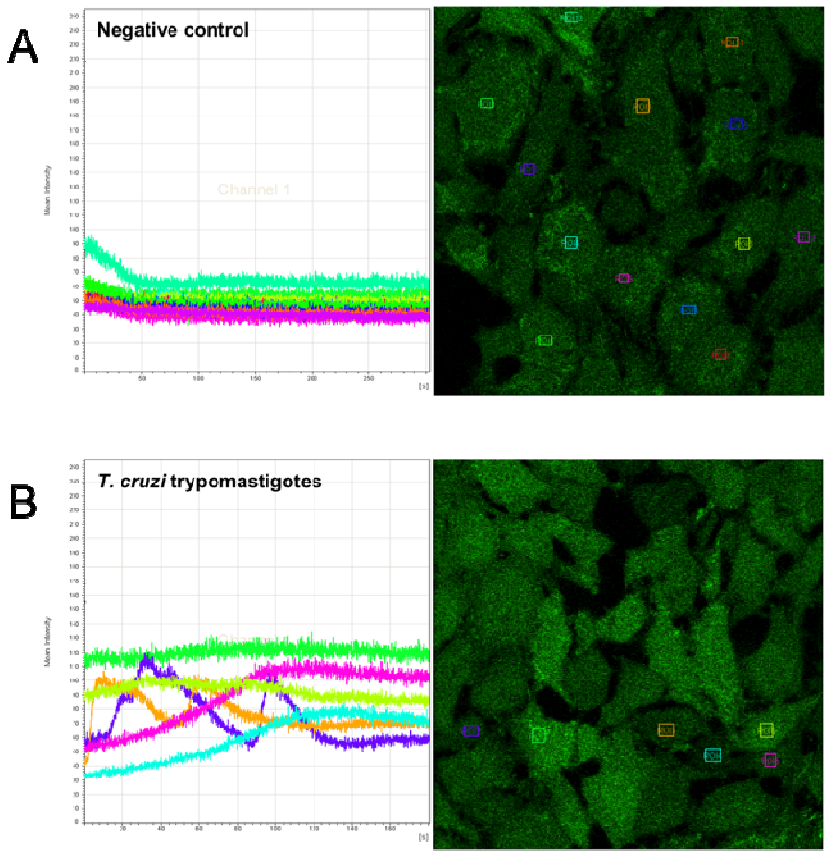

Figure 4-8. *T. cruzi* trypomastigotes induce a calcium transient in HeLa cells. HeLa cells were preloaded with Fluo-4, a green fluorescent calcium sensor, and incubated with (A) DMEM media alone and (B) CL Brener stain trypomastigotes. Cells were imaged live every 200 ms over 5 minutes. Intracellular calcium concentration was monitored in each cell (color-coded) and plotted over time.

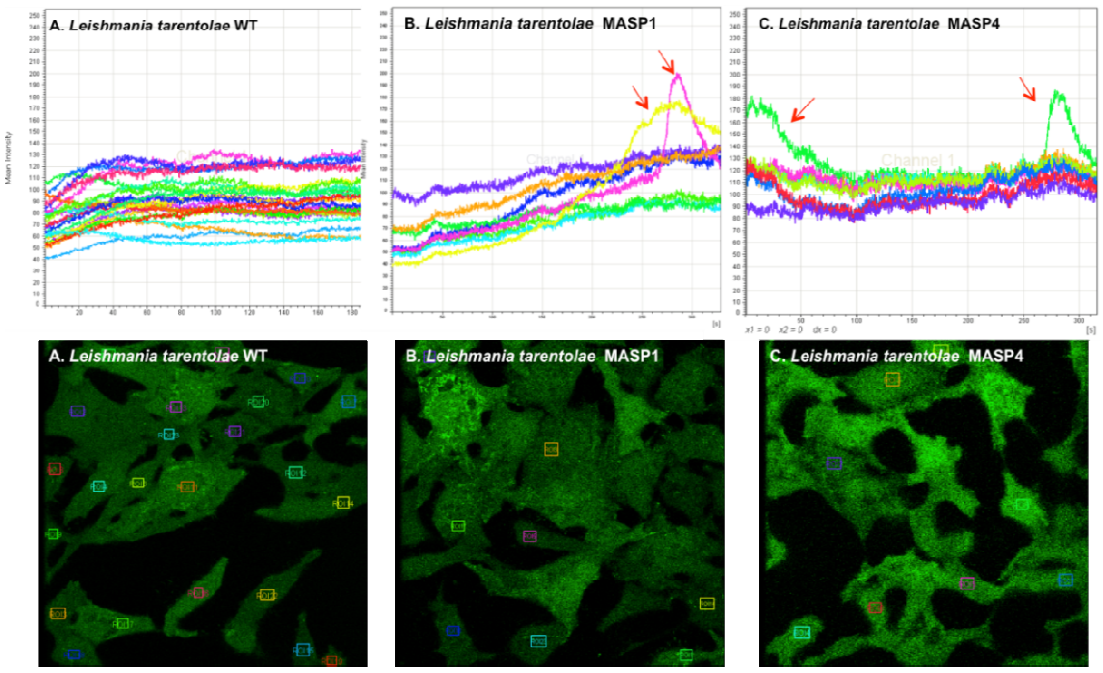

Figure 4-9. MASP triggers intracellular free calcium $[Ca^{2+}]_i$ transient in the host cell. HeLa cells were preloaded with Fluo-4, a green fluorescent calcium sensor, and incubated with (A) *Leishmania tarentolae* P10 strain, (B) P10 strains expressing 6xHIS-tagged MASP1 and (C) MASP4 respectively. Cells were imaged live every 200 ms over 5 minutes. Intracellular calcium concentration was monitored in each cell (color-coded) and plotted over time.

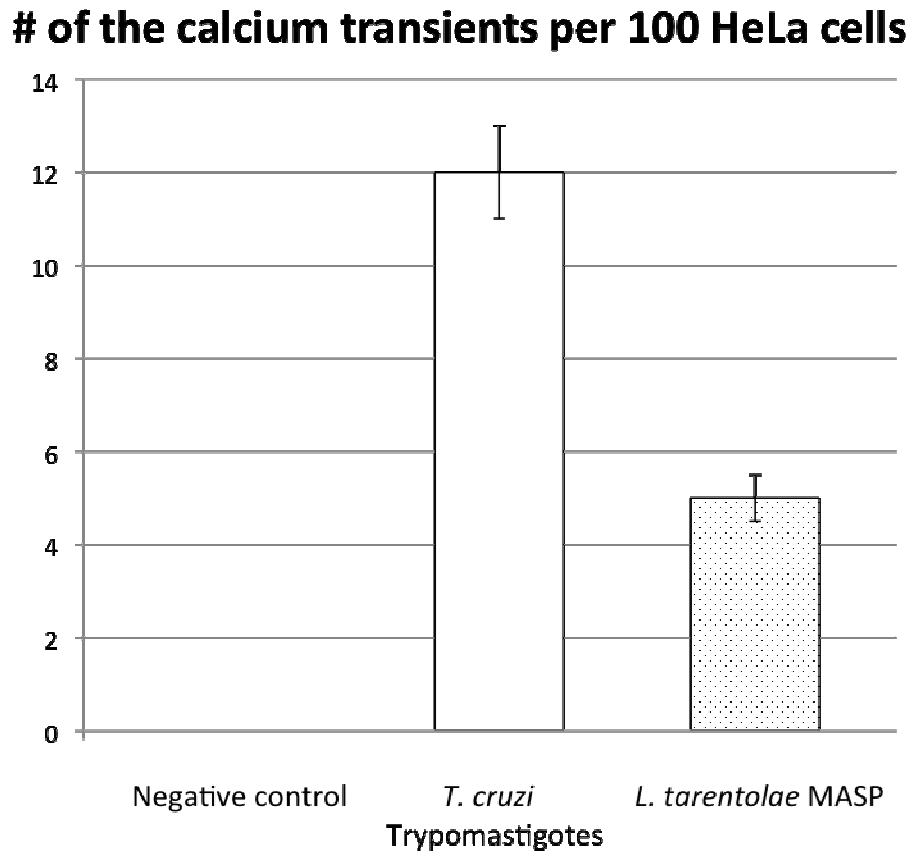

Figure 4-10. *T. cruzi* trypomastigotes trigger a calcium transient more frequently than *L. tarentolae* expressing MASP. The frequency of trypomastigotes inducing the calcium transients in HeLa cells (12 out of 100 HeLa cells) was higher than that of *L. tarentolae* expressing MASP (5 out of 100 HeLa cells). Results are representative of at least two independent experiments.

regulating a calcium-dependent lysosomal exocytosis. We next examined if transgenic *L. tarentolae* expressing GPI-anchored MASP proteins on the surface can trigger intracellular free calcium transient. Intracellular calcium increase was shown to be an event required for the host lysosomal exocytosis (Caler, Vaena de Avalos et al. 1998; Rodriguez, Martinez et al. 1999). HeLa cells were preloaded with Fluo-4, a fluorescent calcium indicator, 1 hour prior (30 minutes at 37ºC and another 30 minutes at room temperature protected from the light) to the experiment and incubated with either wild-type parasites or the transgenic parasites expressing recombinant MASP proteins (MOI=200). Intracellular calcium concentration in each field (around 20 HeLa cells per field) was monitored by live imaging over 5 minutes on the confocal microscope (Leica SP5X). Interestingly, calcium transients were only observed in HeLa cells incubated with the transgenic *L. tarentolae* overexpressing MASP proteins in a frequency of around 1 out of 20 HeLa cells monitored for 5 minutes (5%) whereas none were observed when the cells were exposed to wild-type parasites (0%) in the same conditions (Figure 4-9). Among 500 HeLa cells surveyed, 25 times of the calcium transients were observed when incubated with the transgenic *L. tarentolae* overexpressing MASP proteins. These results implicate MASP as the likely cause of the observed intracellular free calcium transients in the host cells since wild-type *L. tarentolae* did not evoke any calcium transients in 500 HeLa cells that were monitored in the same experimental conditions. This observation is reminescent of similar transients observed when *T. cruzi* CL Brener strain trypomastigotes were incubated with Fluo-3-preloaded HeLa cells and triggered a calcium transient in HeLa cells (Tardieux, Nathanson et al. 1994). In order to compare our results with

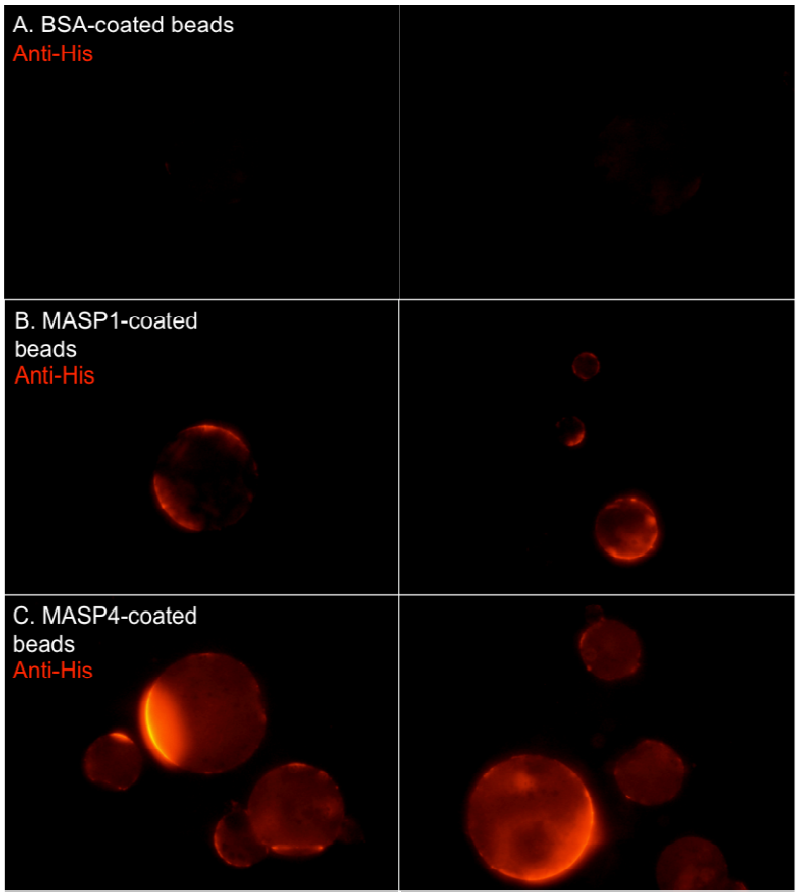

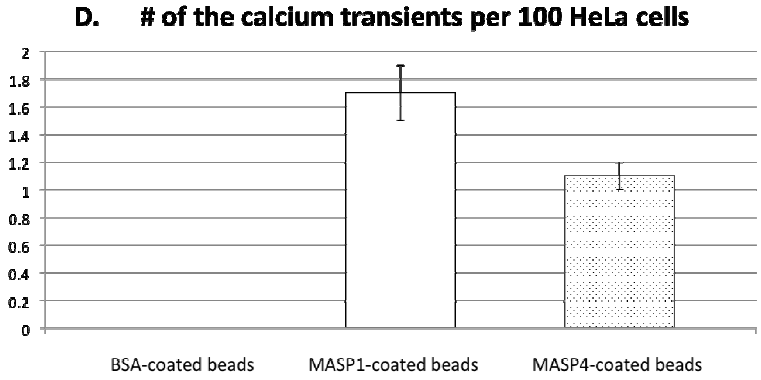

Figure 4-11. MASP-coated polystyrene beads induced the calcium transients in the host cells. Immunostaining images of A) BSA-coated polystyrene particles (0.7~0.9 µm) B) MASP1-coated polystyrene particles (0.7~0.9 µm) and C) MASP4-coated polystyrene particles (0.7~0.9 µm) with mouse anti-His monoclonal antibodies

and Alexa Fluor 594 secondary antibodies. D) The number of Fluo-4 preloaded HeLa cells showing the calcium transients per 100 HeLa cells observed.

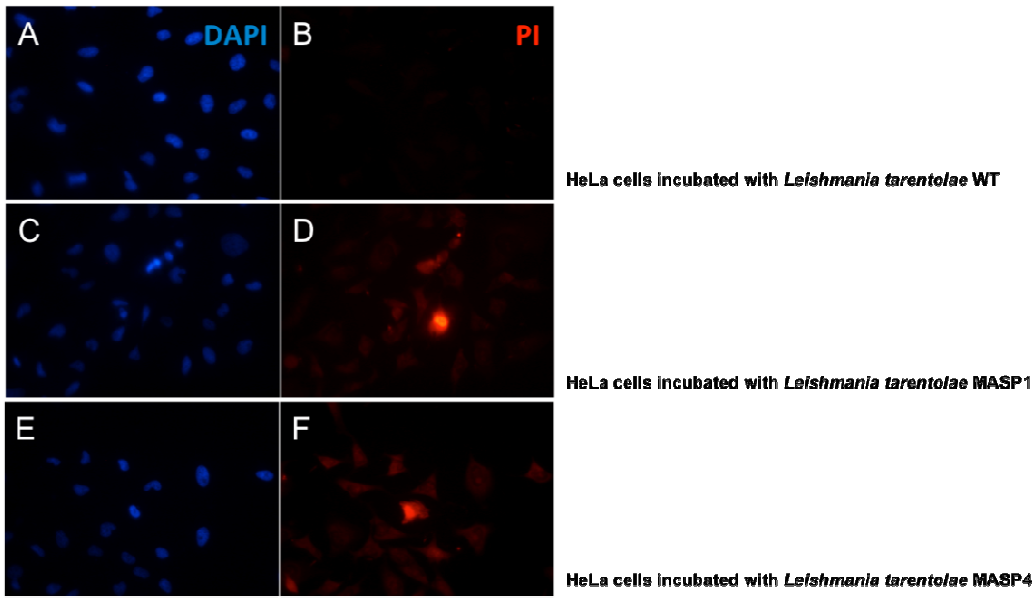

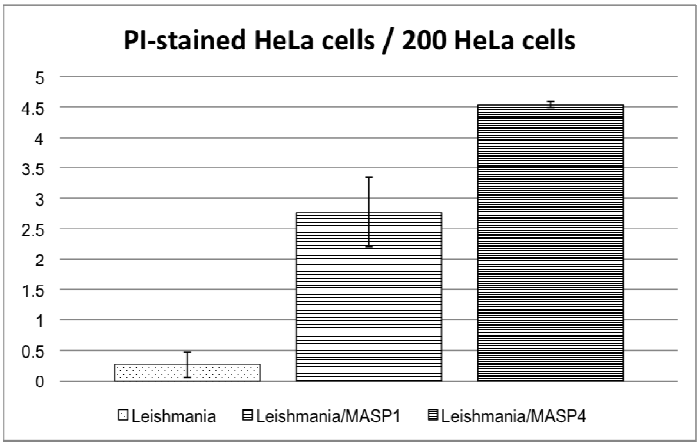

Figure 4-12. MASP may wound the host cell plasma membrane. HeLa cells were preloaded with 25ug/ml PI in calcium-free DMEM and incubated with (A and B) *Leishmania tarentolae* P10 strain (C and D) P10 strains expressing 6xHIS-tagged MASP1 and (E and F) MASP4 respectively for 30 minutes. Fixed cells were inspected under the epifluorescent microscope (E200) and the number of PI-stained cells per 200 HeLa cells was counted. DAPI in blue and PI in red. Results are representative of two independent experiments.

observations in the *T. cruzi* trypomastigotes where multiple endogenous MASP members are present on the surface, we incubated Fluo-4-preloaded HeLa cells with *T. cruzi* CL Brener strain trypomastigotes (MOI=200) and monitored the changes in an intracellular calcium concentration over 5 minutes. Compared to that induced by the transgenic *L. tarentolae* overexpressing MASP proteins, much more frequent calcium transients were observed when HeLa cells were incubated with the trypomastigotes at a rate of 1 out of 8 HeLa cells (12%) (Figure 4-8 and 4-10). The difference (12% and 5%) between *T. cruzi* trypomastigote-induced calcium transient frequency and transgenic *L. tarentolae* expressing MASP-induced calcium transient frequency was expected and can be attributed to the fact that *T. cruzi* is still likely to express and fold its native MASP proteins more accurately, among multiple other MASP proteins in their proper context and other *T. cruzi*-specific surface proteins. To investigate a more direct connection between MASP proteins and the calcium transients in the host cells, MASP1 and MASP4-coated beads were prepared by passive adsorption using the purified recombinant MASP proteins overexpressed in *L. tarentolae.* The efficiency of the passive adsorption coating was validated by the immunofluorescence assays with anti-His antibodies and bovine serum albumin (BSA)-coated beads were purchased and included as a negative control (Figure 4-11 A-C). MASP-coated and BSA-coated control beads were incubated with Fluo-4-preloaded HeLa cells and the intracellular calcium concentration in the HeLa cells was monitored for 5 minutes. As expected, BSA-coated beads did not trigger any calcium transients. However, the calcium transients were observed in HeLa cells where MASP1 and MASP4-coated beads were incubated (Figure 4-11 D)

demonstrating that MASP may be the direct cause of the calcium transients in the host cells. In each experiment with protein-coated beads, 250 HeLa cells were monitored and no transient intracellular calcium increase was observed with BSA-coated beads (0%) whereas 1.7 in 100 HeLa cells (1.7%) and 1.1 in 100 HeLa cells (1.1%) displayed the calcium transients by MASP1-coated beads and MASP4-coated beads, respectively. The frequency of the host calcium transients caused by MASP-coated beads was lower than that of transgenic *L. tarentolae* expressing recombinant MASP proteins-induced calcium transients (around 5 occurrences in 100 HeLa cells, Figure 4-10). This demonstrates that MASP protein itself is sufficient to trigger the calcium transients in the host cells even at a low rate but the active motility of the parasites may help increase the efficiency of the calcium transients caused by MASP proteins. Or further optimization of extensive MASP coating might be necessary (Figure 4-11 B, C) to increase the frequency of the calcium transients.

To further determine whether this intracellular free calcium transient is caused by calcium influx from the extracellular space or calcium release from the internal store, we validated the plasma membrane integrity while HeLa cells were incubated with the parasites. HeLa cells were incubated with the parasites in the calcium-free media (plasma membrane non-repair condition) containing 25 µg/mL propidium iodide (PI), a membrane-impermeable dye (Fernandes, Cortez et al. 2011). The calcium was intentionally omitted from the culture media to prevent host cells from resealing the injury through a calcium-dependent lysosomal exocytosis (Tam, Idone et al. 2010; Fernandes, Cortez et al. 2011). HeLa cells incubated with transgenic *L. tarentolae* expressing MASP1 and MASP4 were PI-stained (1.9% and 2.2% respectively)

indicating recombinant MASP proteins are mechanically wounding the cell membrane whereas almost none (0.1%) were PI-stained when incubated with *L. tarentolae* wild-type parasites (Figure 4-12 A-F). All together this set of data demonstrates that MASP may trigger intracellular free calcium transients presumably by injuring the host cell membrane to initiate the calcium-dependent lysosome exocytosis. Calcium release from internal stores as a result of calcium influx from the extracellular space (calcium-induced calcium release) cannot be ruled out. Two consecutive calcium transients observed in our previous experiments using Fluo-4 support the possibility (Figure 4-8 B, left panel). This calcium-dependent lysosome exocytosis will lead to the exposure of the luminal domain of SNAPIN to the extracellular space for the interaction with MASP on *T. cruzi* to occur. This may provide an anchor for *T. cruzi* to stay in vicinity of the host cell for its entry.

4.3.3 Examination of other putative functions of MASP

In addition, the parasites expressing MASP proteins were showing significantly higher adherence to the host cells (around 90 parasites per 200 HeLa cells) than the wild-type parasites (around 43 parasites per 200 HeLa cells) when they were incubated with HeLa cells (Figure 4-13). This confirms the *in silico* prediction of multiple glycosylation sites on the MASP sequence and suggests *T. cruzi* may utilize the glycosylated MASP protein as an adhesion molecule such as gp82 to better attach to the host cells. Trans-sialidases (TSs) are the largest gene family in *T. cruzi* and one of their known functions is providing protection against the host complement lysis pathway by binding to complement factors C3b and C4b and inactivating them. We also tested if MASP on the surface of the parasite may confer the protection from the

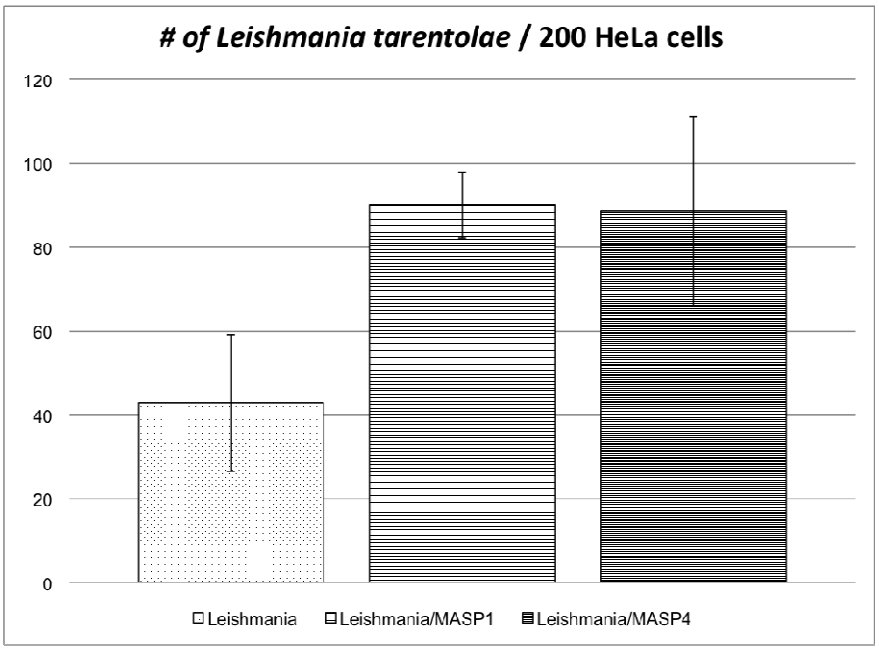

Figure 4-13. MASP enhances the adherence to the host cells. *L. tarentolae* wild-type and *L. tarentolae* expressing MASP proteins were incubated with HeLa cells. After extensive washing, the number of parasites attached to 200 HeLa cells were counted and compared to each other.

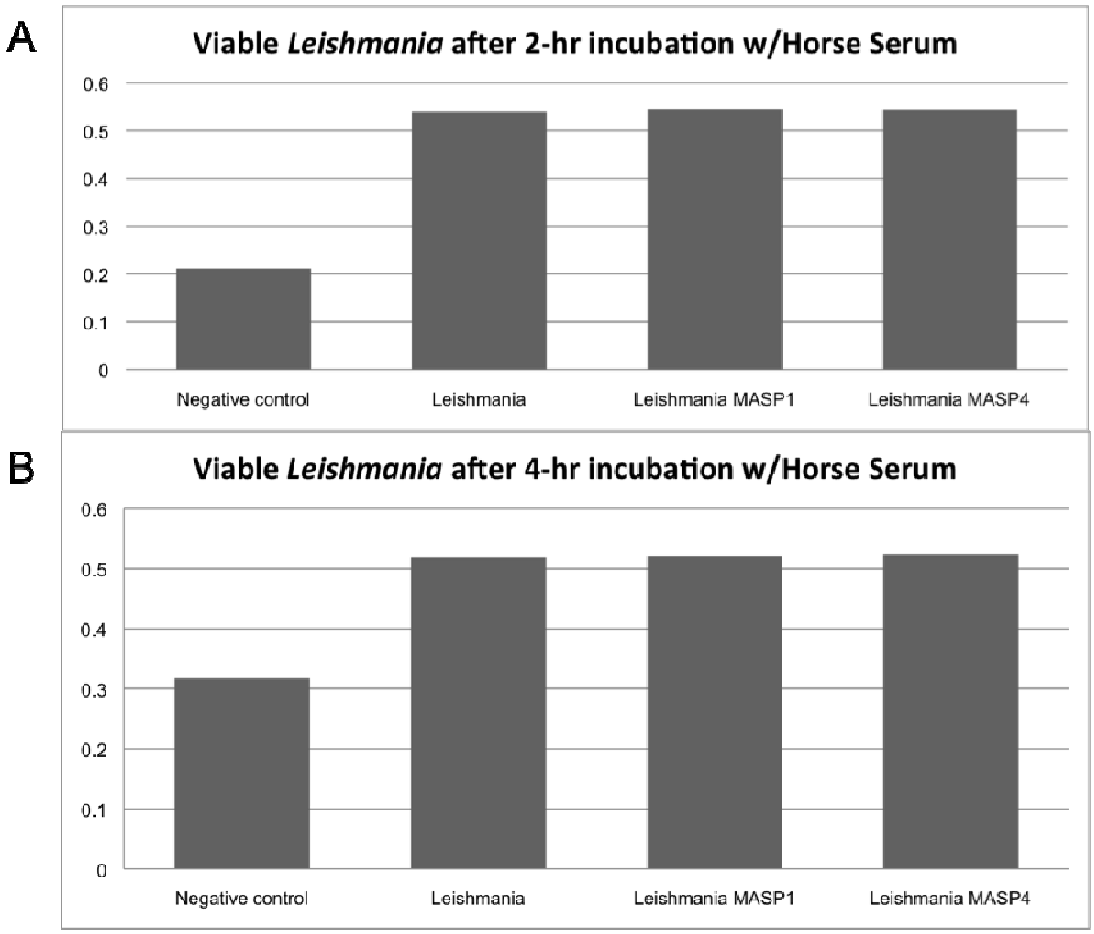

Figure 4-14. MASP does not seem to protect the parasite from the complement lysis. *L. tarentolae* wild-type and *L. tarentolae* expressing MASP proteins were incubated with 10% horse serum for (A) 2 hours and (B) 4 hours respectively and the viable *Leishmania* were measured and compared to each other.

complement lysis as MASP is predominantly expressed in the bloodstream form of *T. cruzi*. Wild-type *L. tarentolae* and transgenic *L. tarentolae* expressing MASP proteins were incubated in BHI media in the presence of 10% Horse Serum for 2 hours and 4 hours. The number of viable parasites were measured by the colorimetric assays and compared to each other (Figure 4-14). It turned out that *L.tarentolae* expressing MASP proteins does not confer significant resistance to the complement lysis when compared to wild-type *L. tarentolae* suggesting MASP does not provide the protection to the parasites from the host complement lysis.

4.3.4 Gene down-regulation in *T. cruzi* by morpholino oligomers

In an effort to down-regulate the expression of MASP family in *T. cruzi*, we decided to try morpholino oligomers which are antisense modified nucleic acid analogs to block access of ribosomes to the translation initiation site. Although there are no reports of utilizing morpholino oligomers in *T. cruzi*, the approach was succesfully used in *T. brucei* as a comparison to downregulation by RNAi. To examine if morpholino works in *T. cruzi*, we chose a gene that has a visible knock-down phenotype and tested it before its application to MASP family. GP72 is *T. cruzi* surface glycoprotein which phenotype was previously described by gene deletion experiments. A null mutant parasite had a detached flagellum and this abnormal flagellar phenotype persisted during the life cycle. We synthesized the morpholino oligomers targeting the gp72 translation initiation site from 16 bases upstream of start codon to 9 bases downstream of start codon and transfected into epimastigotes. Twenty-four hours post transfection, the parasites were inspected under the microscope. Several atypical detached flagellum phenotypes were observed when the


A


B

Figure 4-15. The morpholino pilot study in *T. cruzi*. The morphology of *T. cruzi* epimastigotes 24 hours after transfection. (A) *T. cruzi* transfected with the equal amount of the transfection solution. (B) *T. cruzi* transfected with 100 μM of morpholino. Red circle indicates the interesting phenotypes.

morpholino was delivered but similar phenotype was also found in the negative control where the same amount of transfection solution was transfected (Figure 4-15 A, B). It is likely that the observed abnormal morphologies are simply the result of the transfections, which typically seem to stress *T. cruzi.* It was therefore difficult to draw the conclusion that the phenotype shown by the parasites transfected with the morpholino oligomers is directly connected to targeted gene, gp72. Hence, the morpholino technology seems to be not feasible for *T. cruzi* unless there are improvements in *T. cruzi* transfection or delivery methods.

4.4 Conclusions and significance

MASP seems to be triggering a calcium transient presumably by directly wounding the host cell membrane. Intracellular calcium increase either by calcium influx or calcium induced calcium release from the internal stores initiate the calcium dependent lysosome exocytosis leading to the exposure of the SNAPIN luminal domain to the extracellular space. With the aid of interaction between MASP and a luminal domain of SNAPIN, *T. cruzi* may be able to stay in the vicinity of the host lysosome exocytosis site and better take advantages of complement endocytosis for its entry into the cells. It remains unclear how MASP protein can directly injure the host cell membrane. The structural study using crystallized MASP protein may be able to help us understand the mechanism.

The function of MASP was not documented before and only speculated based on the genomic context and we were able to unravel a putative role for MASP in the

invasion process by exploiting non-pathogenic *L. tarentolae* overexpression system and molecular/cell biological experiments.

Chapter 5: A preliminary study of the expression profile of *masp* family genes and novel regulatory element(s) within *masp* coding sequence

5.1 Objective of Study

In addition to the massive expansion of the *masp* family in *T. cruzi*, suggesting an important role of MASP in *T. cruzi* biology, the ability of *T. cruzi* to invade any nucleated cell demonstrates a strategy to invade and adapt to different the host cell environments. Our previous data, including the trypomastigote cDNA library study and the immunofluorescence assay using anti-MASP peptide 7 antibodies (Bartholomeu, Cerqueira et al. 2009), strongly suggest that MASP expression includes only a subset of members at a time. We aimed to investigate the MASP expression profile in distinct host cells and determine if it correlates with the host cell selection via the trypomastigote cDNA library screening both in a small-scale and a large-scale studies using a conventional Sanger sequencing method and next-generation sequencing technology.

MASP expression was shown to be tightly regulated (Bartholomeu, Cerqueira et al. 2009; De Pablos, Gonzalez et al. 2011; De Pablos and Osuna 2012) and recently TcDHH1, a DEAD box RNA helicase, was demonstrated to play a role in differential expression of MASP in the epimastigote stage (Holetz, Alves et al. 2010). We aimed to identify the regulatory element(s) involved in differential expression of MASP. The following works are incomplete, yet significant, experiments to be further explored but not within the scope of our work presented here.

5.2 Materials and Methods

5.2.1 Materials

Materials	Catalogue numbers	Sources
T. cruzi CL Brener strain (DTU TcVI lineage) epimastigotes		
T. cruzi CL Brener metacyclic trypomastigotes		
HeLa ATCC CCL-2.1		Dr. Norma Andrews' lab (University of Maryland, College Park)
Rhesus Monkey Kidney Epithelial Cells (LLC-MK_2)		
DEAE cellulose	D3764	Sigma
Dulbecco's Modification of Eagles Medium (DMEM)	MT-15-013-CM	Cellgro
Dulbecco's Phosphate-Buffered Salt Solution (DPBS)	MT-21-031-CM	
SuperScript® II Reverse Transcriptase	18064-014	Invitrogen
TRIzol® Reagent	15596-026	
RNase H	18021-071	
Zero Blunt® TOPO® PCR Cloning Kit	450245	
One Shot® TOP10 Chemically Competent *E. coli*	C4040-03	
SuperScript® III Reverse Transcriptase (SS® III RT)	18080-044	
Penicillin-Streptomycin solution	15070-063	
DNase I (RNase-free)	M0303L	New England Biolabs
T4 DNA ligase	M0202S	
DNA Polymerase I	M0209L	
DEPC (Diethylpyrocarbonate) -treated water	786-117	G-Biosciences
Heat-inactivated Fetal Bovine Serum (FBS)	BW14-503F	Lonza
RNeasy Mini Kit	74104	Qiagen
NucleoSpin® Plasmid	740588	Macherey Nagel
TruSeqTM RNA sample preparation kit		Illumina
Library Quantification Kit - Illumina/LightCycler® 480	KK4854	KAPA Biosystems
pTREXneo-*gfp* vector		Dr. Santuza Teixeira (Federal University of Minas Gerais, Brazil)

*Xba*I	R0145	New England Biolabs
*Xho*I	R0146	
All other chemicals		VWR Scientific or Fisher Scientific.

5.2.2 Methods

Preparation of the parasites and the host cells: A 10-day old *T. cruzi* CL Brener strain epimastigote culture in LIT media at 28ºC was used for the purification of metacyclic trypomastigotes (MT) by DEAE cellulose affinity chromatography. Semiconfluent HeLa ATCC CCL-2.1 and LLC-MK_2 cells were passaged on the monolayer in DMEM media supplemented with 10% heat-inactivated FBS and 1X Penicillin-Streptomycin solution. The cells were cultured at 37ºC in a humid atmosphere with 5% CO_2.

T. cruzi infection: Purified MTs were counted on the hemocytometer and prepared in a concentration of $1x10^7$ tryps/mL in DMEM suspension. HeLa cells and LLC-MK_2 cells with 90% confluency were infected with $1x10^7$ tryps for 1 hour. Subsequently, the cultures were washed with DPBS and the infected cells were incubated at 37ºC with 5% CO_2 for 5 days. Tissue-culture derived trypomastigotes (TCTs) emerging from HeLa and LLC-MK_2 cell cultures were collected separately and spun down at 4,000x g for 10 minutes. The cell pellet was resuspended in DMEM and the number of TCTs was counted on the hemocytometer. Equal number of purified MTs was collected and used as a control.

Total RNA preparation: Total RNA was extracted using TRIzol® (Invitrogen) and chloroform followed by DNase I (NEB) treatment to remove possible genomic DNA

contamination. Extracted total RNA was purified by RNeasy Mini Kit (Qiagen) according to the manufacturer's instructions and resuspended in 60 µL DEPC-treated water. The quality and quantity of total RNA from MTs (A260/280 ratio: 2.0, concentration: 40 ng/µL), TCTs emerging from HeLa cells (A260/280 ratio: 2.1, concentration: 170 ng/µL) and LLC-MK_2 cells (A260/280 ratio: 2.1, concentration: 140 ng/µL), were measured using a NanoDrop ND-1000 spectrophotometer.

1st strand cDNA synthesis: MASP 3'UTR-specific oligomer (MASP 3RT: 5'-GTGTGCTTCGTGGGGTGAGGTG-3') was used for oligomer priming in the reactions (See Appendix A.1 for a detailed description of the reaction). The tubes were heated to 65ºC for 5 minutes and incubated on ice for 1 minute and continued to the 1st strand synthesis (See Appendix A.2 for a detailed description of the reaction). After mixing the reaction, the tubes were incubated at 55ºC for 1 hour and the reaction was heat-inactivated at 70ºC for 15 minutes.

2nd strand cDNA synthesis: On ice, the 2nd strand synthesis reaction followed the 1st strand synthesis immediately (See Appendix A.3 for a destailed description of the reaction). The tubes were gently mixed and incubated for 2 hours at 16ºC. After the reaction, 3.3 µL (10 U) of T4 DNA Polymerase was added to each tube and continued to incubate at 16ºC for another 5 minutes. The reaction was stopped by placing the tubes on ice and adding 10 µL of 0.5 M EDTA.

Double-stranded cDNA purification: For the separation of nucleic acids and proteins, 160 µL of Phenol:Chloroform:Isoamyl Alcohol (25:24:1, v/v) was added, the mixture was vortexed thoroughly and spun at room temperature for 5 minutes at 14,000x g. 140 µL of the upper aqueous layer was removed and transferred to a fresh 1.5 mL

tube. For the precipitation, 15 µL of 3M sodium acetate (NaOAc) was added, followed by another 400 µL of ice-cold 100% ethanol (EtOH). The tube was vortexed thoroughly and immediately centrifuged at room temperature for 20 minutes at 14,000x g. The supernatant was carefully removed and the pellet was washed with 400 µL of ice-cold 70% EtOH. The tube was centrifuged for 2 minutes at 14,000x g and the supernatant was discarded. The double-stranded cDNA pellet was dried at 37ºC for 10 minutes to evaporate residual EtOH and dissolved in 4 µL distilled water (ddH_2O).

TOPO blunt-end cloning: The double-stranded cDNAs were added to the sequencing vector, pCR™II-Blunt-TOPO® vector, for TOPO blunt-end cloning and mixed thoroughly (See Appendix A.3 for a detailed description of the reaction). The reaction was incubated for 30 minutes at room temperature. ***E. coli transformation:*** The TOPO ligates were transformed into One Shot® TOP10 Chemically Competent cells according to the manufacturer's instructions and the transformants were plated on Lysogeny Broth (LB) agar plates containing 50 µg/mL Kanamycin and incubated inverted overnight at 37ºC.

Sequencing: The colonies were taken from the LB agar plates and cultured in 5 mL LB liquid media containing 50 µg/mL Kanamycin overnight at 37ºC, 225 rpm on a shaker. The plasmids were isolated by NucleoSpin® Plasmid kit according to the manufacturer's instructions. Each recovered plasmid was sequenced using SP6 forward sequencing primer (5'-ATTTAGGTGACACTATAG-3') on Applied Biosystems 3730xl DNA Analyzer and the sequenced insert from plasmids was identified by NCBI Basic Local Alignment Search Tool (BLAST).

Illumina cDNA library preparation: Total RNA from $2x10^8$ CL Brener trypomastigotes was provided by Dr. Burleigh's lab (Harvard University). The quantity and quality of total RNA were evaluated on NanoDrop ND-1000 spectrophotometer and Agilent 2100 Bioanalyzer respectively. For cDNA library conversion, the llumina TruSeq™ RNA sample preparation kit was used according to manufacturer's instructions. Briefly mRNA was purified from 4µg of total RNA by oligo(dT)-conjugated magnetic beads and fragmented. The first strand cDNA was synthesized from fragmented mRNA using SuperScript® II Reverse Transcriptase (Invitrogen) with random primers. The second strand cDNA was further generated using DNA polymerase I with random primers. Double-stranded (ds) cDNA library was end-repaired and single adenylated. After ligation of adaptors and purification reactions, cDNA library was amplified 15 times and quantified by KAPA Library Quantification Kit (KAPA Biosystems).

Illumina sequencing: Quantified cDNA library was diluted to 15 pmoles/L and sequenced in Genome Analyzer IIx (Illumina, Inc.) in the Institute for Genome Sciences (University of Maryland, Baltimore). Twenty-six million 75-nucleotide pair-ended reads were produced.

Data analysis and Visuallization: Reads were aligned to the *T. cruzi* reference genome by TopHat (The University of Maryland Center for Bioinformatics and Computational Biology) (WHO 2002; Quaglia, Ostacolo et al. 2009) and the transcripts were assembled by Cufflinks (The University of Maryland Center for Bioinformatics and Computational Biology) (WHO 2002; Ancizu, Moreno et al. 2009). The output file, BAM, along with the annotation file, GTF, downloaded from

TriTrypDB (http:// http://tritrypdb.org/tritrypdb/) was visualized on Integrated Genome Viewer (IGV, Broad Institute) (Beard, Cordon-Rosales et al. 2002; WHO 2010).

Overexpression of MASP1 in T. cruzi: 6xHis sequence was internally inserted into *masp1* open reading frame by Splicing by Overlap Extension (SOE) PCR using two pairs of primers, MASP1SPXba5 & MASP1His3 and MASP1His5 & MASP1GPIXho3 (See Appendix B.1 for sequence). The final amplicons were gel-purified and cloned into the linearized pTREXneo-*gfp T. cruzi* overexpression vector, digested by *Xba*I and *Xho*I, to replace the GFP sequence with 6xHis-tagged *masp1*. The pTREXneo-*masp1* plasmids were transfected into $5x10^7$ mid-log phase *T. cruzi* CL-Brener strain epimastigote forms. pTREXneo-*gfp* vector was used as a control for the generation of the transgenic parasite expressing cytosolic GFP. The transfectants were selected by 200 µg/mL G418 24 hours post transfection. Metacyclic trypomastigotes (MTs) of transgenic parasites were purified by DEAE cellulose and incubated with LLC-MK_2 cells for 20 minutes for the infection (MOI=250). MTs that did not invade the host cells were washed for 5 times with PBS and infected LLC-MK_2 cells were further incubated at 37ºC with 5% CO_2. At each time point, 24, 48, 72, 96, 120 hours post infection, infected LLC-MK_2 cells were prepared for IFA to examine the differential expression of MASP1 in the infected host cells.

5.3 Results and Discussion

5.3.1 Expression profile of *masp* members in the parasite population emerging from distinct host cells

It was previously reported that the expression of *masp* members in a trypomastigote cDNA library is biased towards a particular *masp* subgroup (Bartholomeu, Cerqueira et al. 2009). Given the selective pressure to expand and maintain around 1,377 copies of *masp* in the *T. cruzi* genome and the ability of *T. cruzi* to invade any nucleated cells, we hypothesized that a subset of *masp* members correlates with the host cell selection. To test this hypothesis, we infected three different host cells (HEK293T, HeLa and LLC-MK_2) with the infective MTs purified from the old epimastigote culture using DEAE cellulose and harvested as TCTs emerged from each infected host cell line. Infected HEK293T cells detached from the culture plates before releasing the trypomastigotes so excluded from the study (Figure 5-1). Total RNA was extracted from purified $1x10^7$ MTs and TCTs emerging from two distinct host cells that were initially infected with MTs. The 1st strand cDNA was synthesized using a primer specific to 3'UTR of MASP in order to enrich MASP transcripts in the library as the 3'UTR of MASP family is extremely conserved (Figure 1-9) and the 2nd strand cDNA was generated using DNA polymerase I. The library of blunt-ended double-strand cDNA was directly cloned into the sequencing vector, pCR®Blunt II-TOPO® Vector, using topoisomerase I to avoid introduction of any possible bias during the PCR amplification step. After transformation of ligated clones into *E. coli*, 70 to 90 positive colonies were picked from each library, cultured overnight.

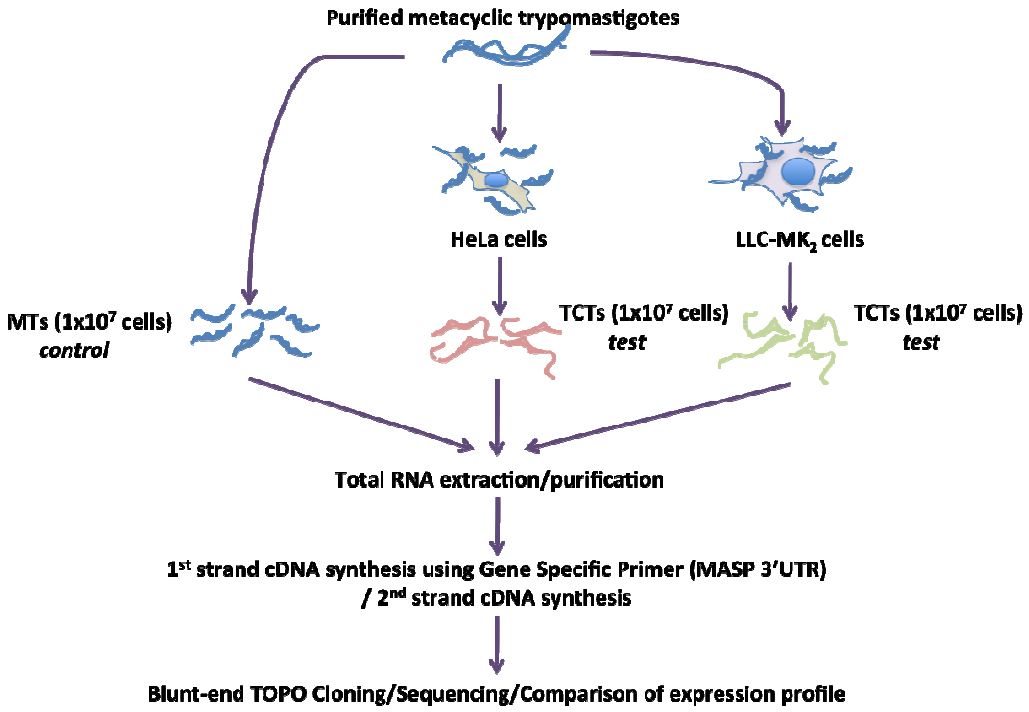

Figure 5-1. Protocol for MASP expression profiling. A schematic diagram of the protocol for MASP expression profiling is illustrated. See Method for detailed reactions.

The plasmids from each *E. coli* liquid culture were isolated and the insert in each plasmid was sequenced and identified by NCBI BLAST.

The sequencing result from this small-scale MASP expression pilot study revealed *masp* transcripts in each library as well as MASP-like protein transcripts and many hypothetical protein transcripts (Figure 5-2). Six *masp* members were identified in the metacyclic trypomastigotes (MT, control) along with one MASP-like protein and the expression of one specific *masp* member (Reference Sequence number, RefSeq: XM_805143) was relatively enriched (Figure 5-2). Nine *masp* members and four MASP-like proteins were detected in the TCT population emerging from HeLa cells, only three (RefSeq: XM_805143, XM_816319, and XM_808786) of nine *masp* members overlapped with *masp* members detected in the MT population. Other six *masp* members were exclusively expressed in this population. Seven *masp* members and three MASP-like proteins were identified in the TCT population emerging from infected LLC-MK_2 cells and only one *masp* (RefSeq: XM_805143) of them was shown as commonly expressed in all three trypomastigote populations. The expression of other six *masp* members seems to be specific to this population emerging from LLC-MK_2 cells. This study demonstrated, inconclusively, that there exists a different *masp* expression pattern in distinct host cells (Figure 5-3). Also unlike the VSG expression in *T. brucei* clonal population, multiple MASP members seem to be expressed in *T. cruzi* trypomastigote population indicating very different gene regulation mechanisms and invasion/survival strategies in *T. brucei* and *T. cruzi*.

MT population

MASP	6
MASP-like protein	1
hypothetical protein	18
empty vector	30
Total	73

TCT population emerging from HeLa cells

MASP	9
MASP-like protein	4
Mucin	1
Mucin-like protein	1
hypothetical protein	12
empty vector	27
Total	76

TCT population emerging from LLC-MK_2 cells

MASP	7
MASP-like protein	3
hypothetical protein	13
empty vector	29
Total	85

Figure 5-2. Overall *masp* profile sequencing result. The identification of inserts in each cDNA library was shown after NCBI BLAST searches.

MASP in MTs	MASP in TCTs emerging from HeLa	MASP in TCTs emerging from LLCMK2
XM_805143	XM_805143	XM_805143
XM_805143	XM_816319	XM_811466
XM_816319	XM_808786	XM_814152
XM_808786	XM_799185	XM_805457
XM_813431	XM_804074	XM_810315
XM_816314	XM_809922	XM_815646
	XM_806047	XM_808790
	XM_799407	
	XM_800009	

Figure 5-3. Overall MASP distribution. The members of MASP expressed in each trypomastigote population are shown. Accession numbers (RefSeq) in red, blue and green indicate the identical MASP members otherwise all different.

Hypothetical protein transcripts detected in this study are speculated to possess a very similar sequence within the transcripts thus get selected for the 1st stand synthesis template when we used a conserved MASP 3' UTR region as a primer or they might represent chimeric transcripts containing the 3' UTR region of MASP that was already reported previously in the trypomastigote cDNA library screen.

T. cruzi is well-known for its polycistronic transcription therefore its post-transcriptional regulation has been suspected to play a major role in gene regulation. This finding hints that MASP and these hypothetical proteins identified in this screen might be post-transcriptionally regulated by means of a similar RNA binding protein (RBP). Preliminary RNA-seq data obtained in the context of another ongoing project in the lab aimed at profiling the *T. cruzi* transcriptome, shows additional evidence that multiple MASP members were expressed in the trypamostigote population (Figure 5-4). This RNA-seq analysis allowed us to detect hundreds of MASP member expression in the trypomastigote population, validating the superior sensitivity of the system over the conventional cDNA screening. I continue expanding the previous experiment by taking advantage of next generation sequencing (NGS) to overcome the limitation and bias inherent in the traditional cloning and sequencing, as means of determining the *masp* family expression profile more conclusively.

Figure 5-4. *T. cruzi* trypomastigote RNA-seq data. An example of the *T. cruzi* trypomastigote RNA sequencing reads mapped to several *masp* loci on the genome. (A) *masp* gene loci with TcMUC group II gene (B) *masp* gene loci with trans-sialidase gene. (Red boxes: annotated coding genes of *T. cruzi*, blue arrows: *masp* genes and grey boxes: sequencing reads).

5.3.2 MASP is differentially expressed during the life cycle of *T. cruzi* and the regulatory element might reside within the coding region

While attempting to overexpress recombinant MASP proteins in *T. cruzi* for the eventual generation of MASP antibodies, we constructed 6xHis-tagged MASP. 6xHis tag was internally inserted in the hypervariable region of *masp1* coding sequence by Splicing Overlap Extension (SOE) PCR. The 6xHis-tagged *masp1* amplicon was cloned in the pTREXneo expression vector under ribosomal promoter. This expression vector harbors several elements ensuring constitutive expression and proper processing of the recombinant proteins in *T. cruzi*. For instance, HX1 located upstream of 6xHis-tagged *masp1* is very efficient in trans-splicing event. The *gapdh* intergenic segment downstream of 6xHis-tagged *masp1* includes a poly-adenylation signal and ensures the constitutive expression in all life cycles of *T. cruzi* (Figure 5-5). pTREX-*masp1* was transfected into *T. cruzi* CL Brener epimastigotes and the stable population of transgenic parasites followed by a clonal cell line was established. The clonal transgenic parasites expressing recombinant MASP1 proteins were subjected to the immunofluorescence assay (IFA) to validate the expression in *T. cruzi* epmastigotes. Even though expression of *masp1* was driven by ribosomal promoter that is one of the strongest promoters in *T. cruzi* and under *gapdh* 3'UTR control, we were only able to observe very low level of MASP expression in a punctate pattern in the epimastigote stage (Figure 5-6 A), which were contrary to our prediction. TREXneo-*gfp* was transfected into epimastigotes as a transfection control and the transgenic parasites expressing GFP was inspected as well (Figure 5-6 A). LLC-MK_2 cells were infected by transgenic parasites expressing MASP or GFP in parallel and

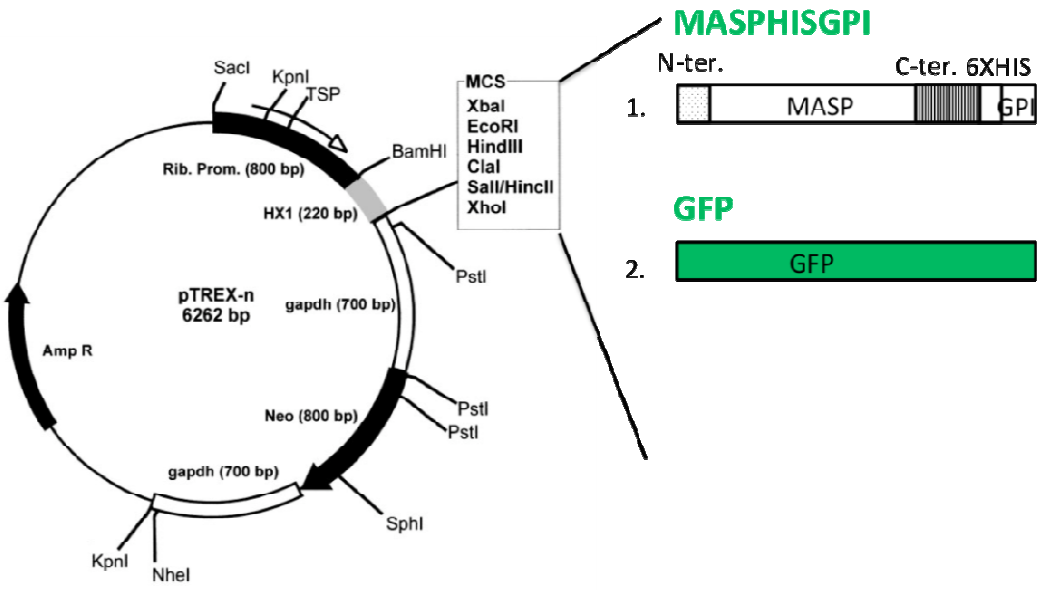

Figure 5-5. MASP overexpression in *T. cruzi* 1) Internally 6xHis-tagged *masp1* construct was cloned into pTREXneo-*gfp* by replacing *gfp* open reading frame with *masp1*. 2) pTREXneo-*gfp* was used as a transfection and negative control

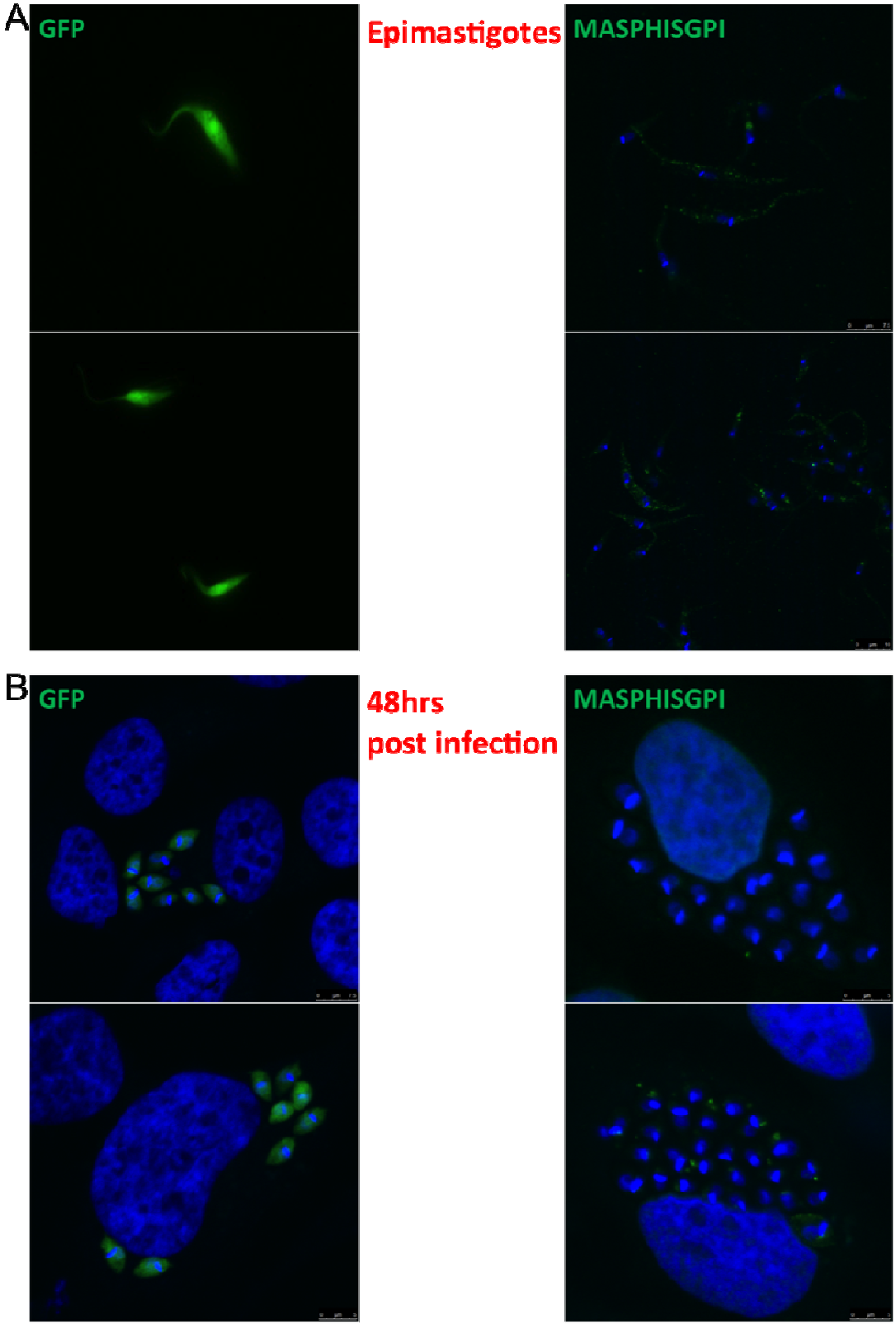
A
GFP
Epimastigotes
MASPHISGPI
B
GFP
48hrs
post infection
MASPHISGPI

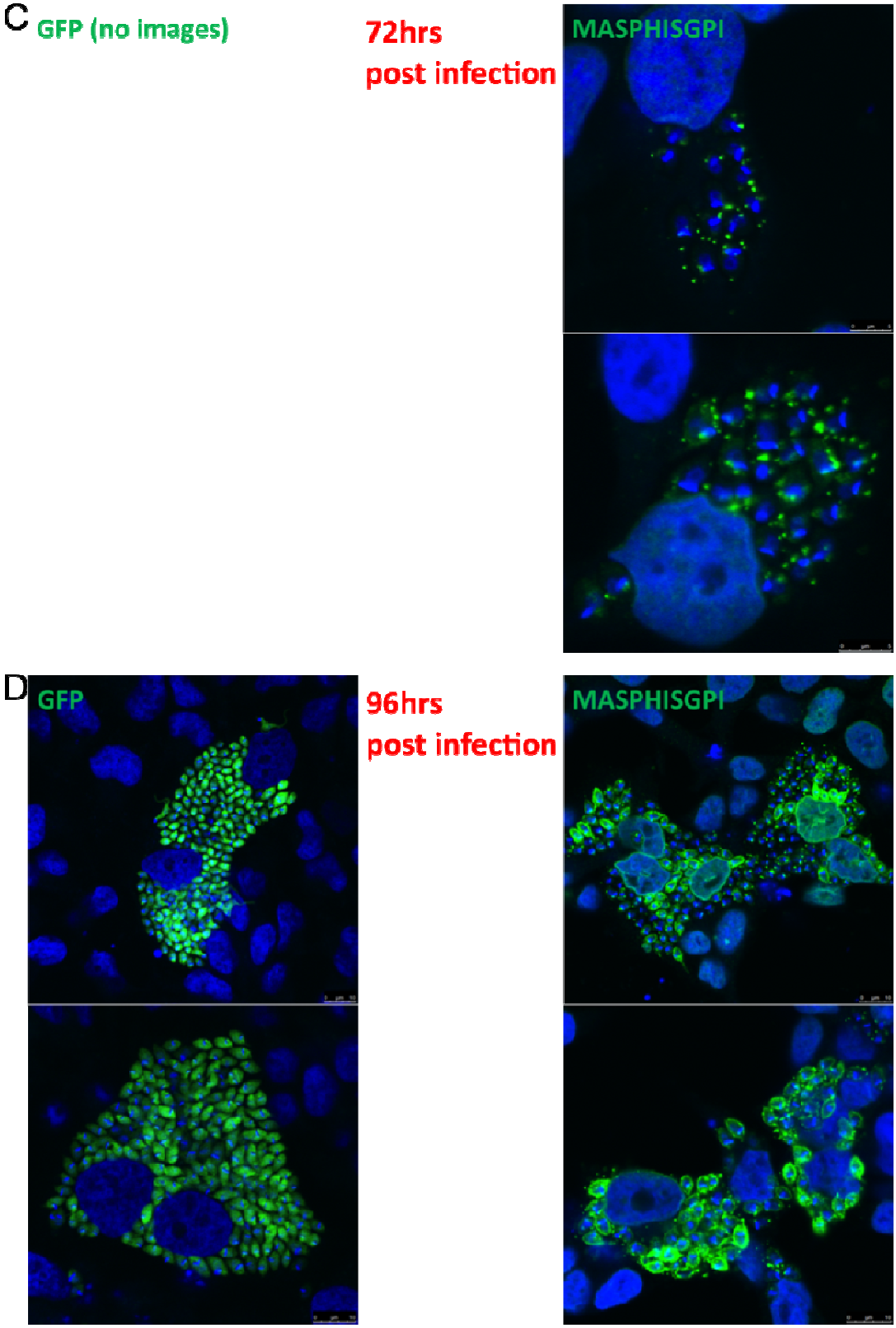
C
GFP (no images)
72hrs
post infection
MASPHISGPI
D
GFP
96hrs
post infection
MASPHISGPI

E

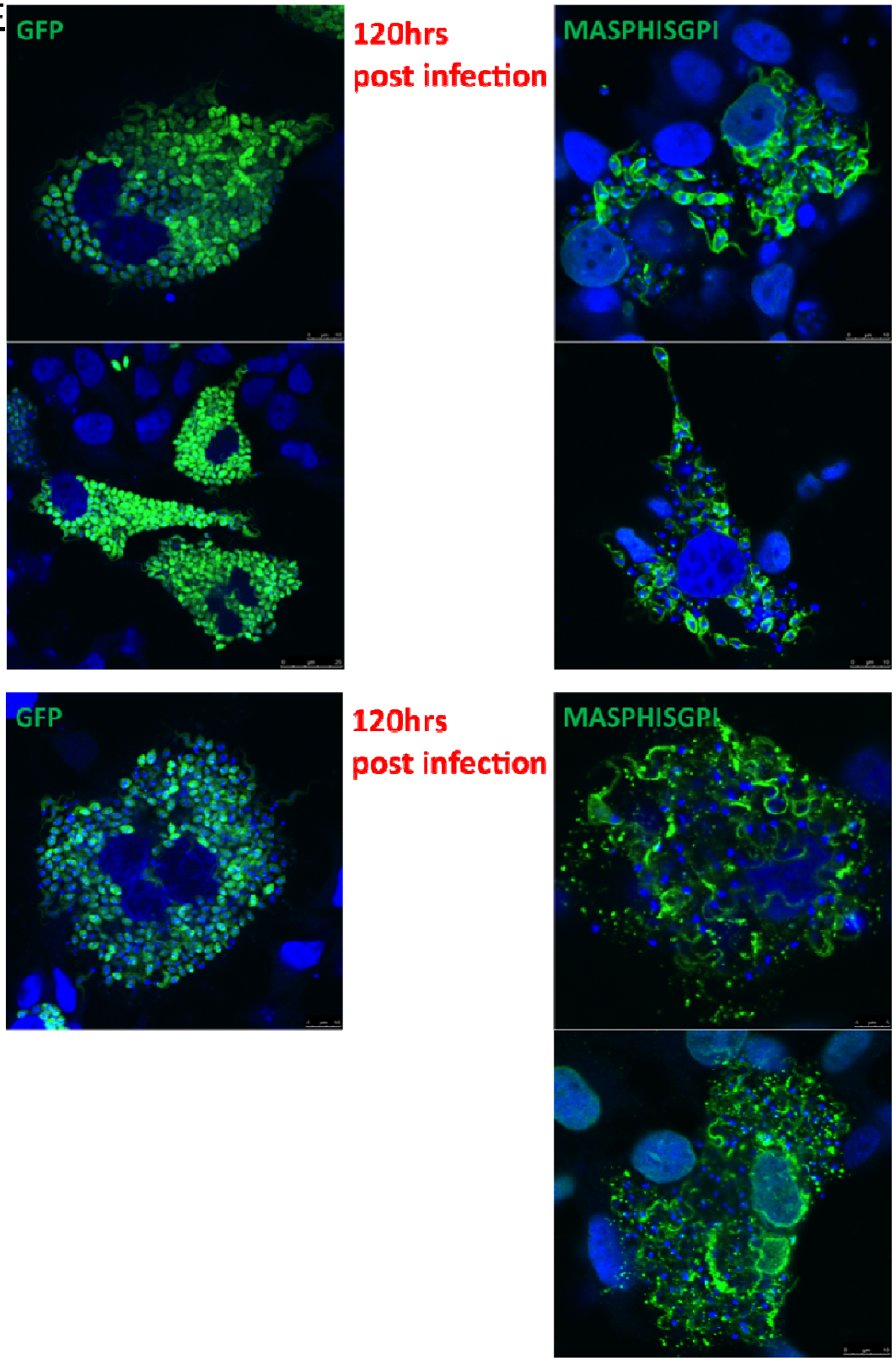
GFP
120hrs
post infection
MASPHISGPI
GFP
120hrs
post infection
MASPHISGPI

Figure 5-6. Differential expression of MASP during the life cycle. (A) *T. cruzi* CL Brener strain epimastigotes expressing GFP (left panel) and MASP1 (right panel). (B) Infected LLC-MK_2 cells with the parasites expressing GFP (left panel) and MASP1 (right panel) 48 hours post infection. (C) Infected cells with the parasites expressing MASP1 (right panel) 72 hours post infection. (D) Infected cells with the parasites expressing GFP (left panel) and MASP1 (right panel) 96 hours post infection, (E) 120 hours post infection. DAPI in blue, GFP and 6xHis-tagged MASP proteins in green.

infected cells were subjected to IFA every 24 hour until 120 hours post infection. LLC-MK_2 cells are monkey kidney epithelial cells and tougher to *T. cruzi* infection than other epithelial cells such as HeLa and HEK293T cells thus ideal for a long-term (120 hour) infection study. Up to 48 hours, the transgenic parasites expressing 6xHis-tagged MASP1 did not show any signals when probed with anti-His antibodies whereas the transgenic parasites expressing GFP constituvely expressing a bright green signal all the time demonstrating indeed the *gapdh* sequence drives the constitutive expression and does not affect the differential expression of gene in the upstream. Forty-eight (48) hours post infection, the transgenic parasites expressing MASP1 started to display recombinant proteins. By 96 hours, the subcellular localization of MASP1 was clearly on the surface indicating the proper processing of the recombinant GPI-anchored proteins in *T. cruzi* (Figure 5-6 D, E). This was very intriguing because it has been believed that the gene expression in *T. cruzi* is regulated by the elements in UTR especially in 3' UTR (Page, Rassias et al. 2001; Rassiat, Ragonnet et al. 2001; Rassin 2001). This is the first discovery that a regulatory element in MASP coding sequence can likely override strong ribosomal promoter and the signals in 3'UTR. Since the differential expression of MASP was not observed when *masp* was cloned in pLEXSY-sat (Figure 4-1 C) and overexpressed in *L. tarentolae* promastigotes (Figure 4-2), it seems like that there could be transcriptional/translational factors uniquely present in *T. cruzi* genome and these factors recognize the regulatory elements within the coding sequence and control the differential expression. It will be interesting to figure out what the regulatory elements are by mutagenesis studies.

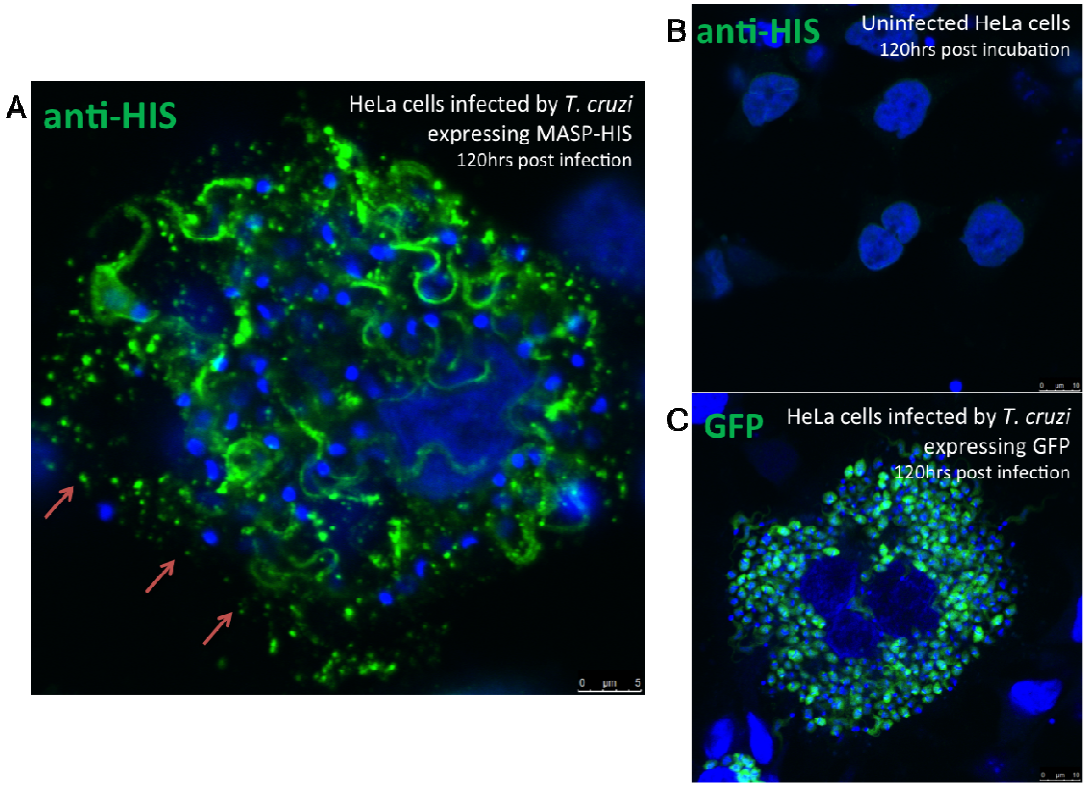

Figure 5-7. MASP proteins are shed or secreted into the media. A) *T. cruzi* trypomastigotes expressing MASP are about to rupture HeLa cells 120 hours post infection. Shed or secreted MASP proteins are indicated by arrows. B) Uninfected HeLa cells probed by anti-His antibodies. C) HeLa cells infected by *T. cruzi* trypomastigotes expressing GFP 120 hours post infection.

We also observed the evidence of shed or secreted MASP1 when the transgenic parasites expressing MASP1 were about the rupture the cells after redifferentiation into trypomastigotes (Figure 5-7). This is consistent with the previously published immunoblotting data showing the presence of MASP proteins in the culture media (Bartholomeu, Cerqueira et al. 2009) especially in the presence of the host cells (De Pablos, Gonzalez et al. 2011) indicating the interaction between the parasite and the host cells is important. This phenomenon may be related to the putative function of MASP in triggering extracellular calcium influx (described in Chapter 4) possibly forming a pore on the membrane after being shed or secreted from the surface of the parasite. TcTox, *T. cruzi* hemolysin active at pH 5.0~5.5, is a well-characterized pore-forming protein and known to be responsible for the parasitophorous vacuole disruption by forming a large pore (~10 nm) (Himle, Rassi et al. 2001; Kouvaraki, Gorgoulis et al. 2001; Rassin, Diepstraten et al. 2001; Wall and El Rassi 2001). It will be interesting to assay if MASP can form a pore on the membrane and also is active at physiological pH unlike TcTox that is only active at lower pH.

5.4 Conclusions and Significance

My small-scale pilot study indicates that a subset of *masp* expression correlates to the host cell types thus MASP might be involved in host cell targeting. Further examination of *masp* expression profile in the biologically relevant cells and tissues such as smooth muscle cells and cardiomyocytes using NGS will unravel the selective pressures to maintain a large *masp* gene family in *T. cruzi* genome and the putative function of MASP as well. The future study may lead to identification of a subset of MASP members that play an important role in the tissue tropism found in Chagas

disease. And the subsequent intervention targeting on specific MASP members will help treat the disease based on the clinical manifestations found in the patients.

In addition, the regulatory element(s) within *masp* CDS seem to overcome the signals from the promoter and UTR. To my knowledge, this may be the first evidence to show the existence of such things in *T. cruzi* where post-transcriptional regulation via UTR was considered to be dominated. This novel regulatory element within CDS might represent the whole new strategy for *T. cruzi* to regulate differential gene expression depending on the host environment that is very important for *T. cruzi* biology.

Chapter 6: General discussion

The comparative genomic analysis of three related trypanosomes, the Tritryps, revealed a subset of gene clusters shared by all three organisms representing a valuable opportunity to design drugs to target the all of the Tritryps (Figure 1-6 B), considering around 2,000 gene clusters do not share human orthologs (El-Sayed, Myler et al. 2005). This comparative analysis also identified species-specific gene clusters encoding proteins responsible for the distinct nature of the diseases, particularly pointing to different mechanisms of survival and immune evasion used in each organism. A unique feature of *T. cruzi* among the Tritryps is a massive expansion of species-specific gene clusters where most of the large gene families encoding surface antigens and many hypothetical proteins were found (El-Sayed, Myler et al. 2005; El-Sayed, Myler et al. 2005). The second largest multigenic family (771 members/1,377 copies) in *T. cruzi* and the largest *T. cruzi*-specific gene family, corresponding to ~6% of the coding genes, were first discovered in the areas downstream of TcMUCII genes and upstream of gp85/TS-like superfamily and thus were named mucin-associated surface proteins (MASP) (El-Sayed, Myler et al. 2005). In addition to having a high copy number, MASP family is preferentially expressed in the infective trypomastigote stage, has a GPI-anchored surface localization, and is predicted to have heavy glycosylations (four O-glycosylation sites and three N-glycosylation sites per sequence in average) (El-Sayed, Myler et al. 2005; Bartholomeu, Cerqueira et al. 2009). This evidence strongly suggests that MASP plays a major role in a host-pathogen interaction, especially during *T. cruzi* invasion and persistence in the host cells, which is unique to the biology of *T. cruzi* among the

Tritryps. Interestingly, a previous examination of the expression profile of *masp* genes revealed a bias towards a subset of *masp* members in individual parasite populations suggesting another possible role of *masp* in host cell selection (Bartholomeu, Cerqueira et al. 2009).

One of the aims of this dissertation was to characterize the function of *T. cruzi masp* protein family by identifying and investigating the human interacting partner proteins of MASP proteins. In order to achieve this, in Chapter 2, we have established a robust high-throughput platform for screening protein-protein interactions between the trypanosomatid and human proteomes using a Y2H system. We included two different MASP proteins as baits against the human proteome to investigate a putative role for MASP in the interface of human and the parasite. Our work proved that an automated high-throughput Y2H screen could detect a biologically meaningful interaction in combination with several biochemical PPI assays. Further optimization of our high-throughput Y2H system will facilitate the emergence of the genome-wide host-pathogen interactome (infectome) taking advantage of the automated workflow and deep sequencing technology for rapid interactome profiling (Yu, Tardivo et al. 2011).

Human SNAPIN was identified as one of the major interacting partner proteins of two MASP proteins we selected as baits in our Y2H screens. SNAPIN was originally described as a SNAP-25 binding protein in neuronal cells and reported as functionally critical in vesicle priming and synchronized fusion events (Ilardi, Mochida et al. 1999; Pan, Tian et al. 2009). Later SNAPIN was demonstrated to be ubiquitously expressed in non-neuronal cells (Buxton, Zhang et al. 2003) and to have at least 20 interacting

partner proteins such as SNAP-23 (Buxton, Zhang et al. 2003), biogenesis of lysosome-related organelle complex-1 (BLOC-1) (Starcevic and Dell'Angelica 2004), ryanodine receptor (Zissimopoulos, West et al. 2006), EHD1 (Wei, Xu et al. 2010), Exo70 (Bao, Lopez et al. 2008), and cypin (Chen, Lucas et al. 2005). This indicates multiple roles for human SNAPIN protein depending on cell types. Several lines of evidence in various cells implicated the function of SNAPIN in a calcium-dependent exocytosis (Tian, Wu et al. 2005), endocytic trafficking (Lu, Cai et al. 2009; Cai, Lu et al. 2010), autophagy-lysosomal regulation (Cai, Lu et al. 2010) and calcium influx signal pathways (Hunt, Edris et al. 2003; Zissimopoulos, West et al. 2006; Suzuki, Morishima et al. 2007; Wang, Lin et al. 2009). The possible involvement of SNAPIN in these pathways caught our attention because *T. cruzi* was known to use unusual mechanisms to gain entry into the cells (Schenkman, Robbins et al. 1991; Tardieux, Nathanson et al. 1994; Burleigh and Andrews 1995; Andrade and Andrews 2004; Fernandes, Cortez et al. 2011). Unlike the entry of many other intracellular parasites that involve a host actin polymerization mediated phagocytosis, *T. cruzi* was shown to exploit a host calcium-dependent lysosome exocytosis for its entry (Andrews 1995). Other studies propose that this atypical calcium-dependent lysosome-mediated exocytosis may be a housekeeping mechanism in mammalian cells for repair of injured plasma membranes (Idone, Tam et al. 2008; Tam, Idone et al. 2010; Fernandes, Cortez et al. 2011), and is consistent with the observation that *T. cruzi* can penetrate any nucleated cells. This may also explain the tissue tropism that *T. cruzi* prefers to invade muscle cells prone to frequent injuries due to repeated contraction and relaxation cycles. Recently it was shown that *T. cruzi* trypomastigote wounds the

plasma membrane mechanically to trigger a plasma membrane repair process involving a calcium-dependent lysosomal exocytosis followed by complement endocytosis of the parasite (Tam, Idone et al. 2010; Fernandes, Cortez et al. 2011). It still remains unclear which parasite-derived molecule causes the physical wounding on the host plasma membrane to trigger this response. It was shown that a parasite glycoprotein, GP82, induces the intracellular calcium increase by PLC-mediated calcium release from the internal stores such as ER and SR (Manque, Neira et al. 2003).

In this study, we demonstrated a putative MASP interacting partner protein, human SNAPIN is playing a critical role in the *T. cruzi* invasion process by regulating host lysosome maturation and directly interacting with *T. cruzi* MASP proteins thus anchoring motile flagellated parasites to the vicinity of the plasma membrane injury site for its entry during complement endocytosis of the host cell. Indeed, SNAPIN deficiency resulted in a reduction in *T. cruzi* infection rate by 66% in SNAPIN depleted cells and 45% in SNAPIN knockout cells respectively compared to SNAPIN wild-type cells. It is plausible that the reason we observed a moderate infection reduction in the *snapin*$^{-/-}$ MEF cells compared to that in SNAPIN depleted cells was possibly due to the presence of a complementary pathway in *snapin*$^{-/-}$ MEF cells that compensated for the loss of SNAPIN. All together, these results indicate that SNAPIN participates the process of *T. cruzi* invasion, at least in the early stage, although we cannot yet determine the role of MASP in this process.

SNAPIN was shown to be present in both cytosolic and membrane-bound fractions (Buxton, Zhang et al. 2003). We determined the subcellular localization of

membrane-bound SNAPIN with several endosomal markers and confirmed that it is colocalized with late endosomes and lysosomes, which is consistent with previous reports (Lu, Cai et al. 2009; Cai, Lu et al. 2010). Also SNAPIN was found to be enriched near the invading parasite confirming the recruitment of host SNAPIN to the parasite surface via the interaction with the parasite surface antigens, presumably MASP. Early endosomes recruited to the point of parasite penetration did not overlap with SNAPIN, suggesting that SNAPIN is involved in a lysosome-dependent parasite entry pathway, the major *T. cruzi* entry mechanism.

The drastic accumulation of immature lysosomes in SNAPIN deficient cells confirmed the recent finding (Cai, Lu et al. 2010) that SNAPIN plays a role in late endocytic transport and lysosome maturation. We observed relatively weak GFP signal in parasites trapped in host lysosomes in Snapin$^{+/+}$ cells, whereas the parasite in wild type cells retained a strong GFP signal. We attribute this to quenching of the GFP signal by the low pH in the mature lysosomes, and would be consistent with poor recruitment of host mature lysosomes to the parasite surface in *snapin*$^{-/-}$ cells. Low pH in the host lysosomes is critical for the retention and differentiation of parasites for intracellular parasite survival, so SNAPIN deficiency may interfere with this process by allowing the reversible *T. cruzi* exit to the extracellular space and blocking the differentiation of the trypomastigotes into amastigotes and both lead to an unsuccessful infection. Furthermore, a lysosomal enzyme release assay confirmed that SNAPIN deletion in cells causes a reduction in a calcium-dependent exocytosis of lysosomes that is required for parasite invasion. We cannot yet determine whether SNAPIN is the only factor affecting the lysosome-dependent parasite entry pathway

or not. Nonetheless, SNAPIN appeared to be a critical player impacting the *T. cruzi* invasion process by regulating the late endocytic pathway and autophagy-lysosome function in the host cells thus determining the size of available pool for mature lysosomes. Autophagosomes were recently shown to replace the role of host lysosomes in *T. cruzi* invasion process (Romano, Arboit et al. 2009).

L. tarentolae is a well-established model organism for the eukaryotic protein overexpression system and has been extensively used in trypanosomes for recombinant protein production (Breitling, Klingner et al. 2002; Heise, Singh et al. 2009; Bolhassani, Taheri et al. 2011). It provides several advantages including a robust production of eukaryotic recombinant proteins and relatively homologous post-translational modifications. Expression of only one member of MASP family on the surface of the non-pathogenic parasite allowed us an opportunity to examine the function of MASP in a way that was not feasible in a native homologous system, *T. cruzi*. The expression of recombinant MASP proteins in *T. cruzi* epimastigotes seems to be strictly regulated and many other surface antigens, possibly including other members of MASP proteins, are present on the surface of the trypomastigotes naturally. In addition, these transgenic parasites maintain the motility that may contribute to energy-driven active invasion resembling *T. cruzi* expressing the MASP proteins. MASP protein expressed in *L. tarentolae* was localized on the surface by GPI-anchor indicating the overexpressed recombinant protein was properly processed. Moreover, it was shown to interact with SNAPIN protein, in particular with the luminal domain of SNAPIN, which was expressed in HeLa cells, simulating the most biologically relevant environment. Interestingly, SNAPIN C-terminal fragment

containing a coiled-coil domain previously determined as responsible for several protein-protein interactions (Ilardi, Mochida et al. 1999; Buxton, Zhang et al. 2003; Gowthaman, Silvester et al. 2006) also binds to MASP proteins raising the possibility that SNAPIN – MASP interaction may have a multivalent role after the trypomastigote form of *T. cruzi* escapes the parasitophorous vacuole or before *T. cruzi* ruptures the host cell.

The vast majority of the *T. cruzi* invasion process is not yet characterized at the molecular level. It has been recently proposed that *T. cruzi* trypomastigote, not epimastigote, can mechanically damage the plasma membrane integrity to exploit the universal repair mechanism of mammalian cells and gain entry into the cells (Fernandes, Cortez et al. 2011). The exact parasite-derived molecules responsible for the wounding are not identified thus far, however the MASP-mediated host calcium transients that we observed in this work suggest that MASP may contribute to this process. We also suspect a similar role for MASP in the process of escaping the parasitophorous vacuole or rupturing the cells in combination with trans-sialidase and TcTox (Andrews 1990; Andrews, Abrams et al. 1990; Schenkman, Jiang et al. 1991; Buschiazzo, Amaya et al. 2002). We still do not have a good understanding on the mechanism how MASP could trigger host calcium transients. 3D crystal structure analysis using the purified recombinant MASP proteins expressed in *L. tarentolae* will answer many relevant questions including not only how two substantially different MASP members can interact with SNAPIN but also potential mechanisms by which they can induce the calcium influx. For example, the observation that GPI-anchored MASP can be shed/secreted into the culture media (Bartholomeu, Cerqueira

et al. 2009; De Pablos, Gonzalez et al. 2011) points to the possibility that MASP can be embedded in the plasma membrane of the host cell and breaks the membrane integrity like TcTox and triggers the calcium transients. It is worth noting that shed/secreted MASP can be found only when the parasites are interacting with the host cells, not when they are incubated themselves in the culture media in the absence of the host cells. This supports the hypothesis that *T. cruzi* is interacting with non-phagocytic cells, actively injuring the plasma membrane and that MASP is contributing to this phenomenon. Interestingly it turned out the parasite motility plays an important role in inducing the calcium transients in the host cells effectively thus strengthening our working model that MASP on *T. cruzi* surface initiate extracellular calcium influx by actively wounding the cell membrane during the invasion process. MASP-coated polystyrene beads triggered the calcium transients despite at a lower frequency whereas BSA-coated polystyrene beads failed to do so, showing that MASP is a molecule responsible for the intracellular free calcium increase in the host cells and allowing us to speculate that the motility of the parasite aids the injury of the host cell membrane via MASP or helps MASP to be shed while interacting with the host cells. We have observed less severe cell membrane injury when cells were incubated with *L. tarentolae* expressing MASP1 and MASP4 compared to cells incubated with *T. cruzi* trypomastigote in similar conditions. This can be explained by the presence of multiple surface antigens, including multiple members of MASP, on the surface of *T. cruzi* trypomastigote whereas only one MASP member being present on the surface of *L. tarentolae* in our experiments.

Our work demonstrates that shed or secreted MASP may injure the plasma membrane of the host cell by yet unknown mechanism and trigger a calcium-dependent lysosomal exocytosis that translocates lysosome-associated SNAPIN proteins to the plasma membrane resulting in the exposure of the luminal domain of SNAPIN to the extracellular space. Our work describes, for the first time, the possibility of the exposed luminal domain of SNAPIN serving as an anchor for holding *T. cruzi* near the host entry sites to be internalized by complement endocytosis. This line of work provides a plausible mechanism for previously observed events in the early stages of the *T. cruzi* invasion process (Figure 6-1).

Our attempt to constitutively overexpress MASP proteins in *T. cruzi* was not successful due to the strict gene regulation during the life cycle. On the other hand, this experiment uncovered a novel feature of *masp* gene, suggesting that putative regulatory element(s) in the *masp* coding sequence may be governing the expression of MASP over other cis-elements such as signals from a ribosomal promoter or UTR. This was very surprising because trypanosomes have a unique polycistronic transcription system and mainly 3'UTR was shown to play a role in controlling gene regulations. This could be the first evidence that the elements within the CDS override other regulatory signals in *T. cruzi* although extensive control experiments have to be carried out to confirm the interesting observation. Of course, the following work will focus on identifying the sequence(s) responsible for this by the mutagenesis tools.

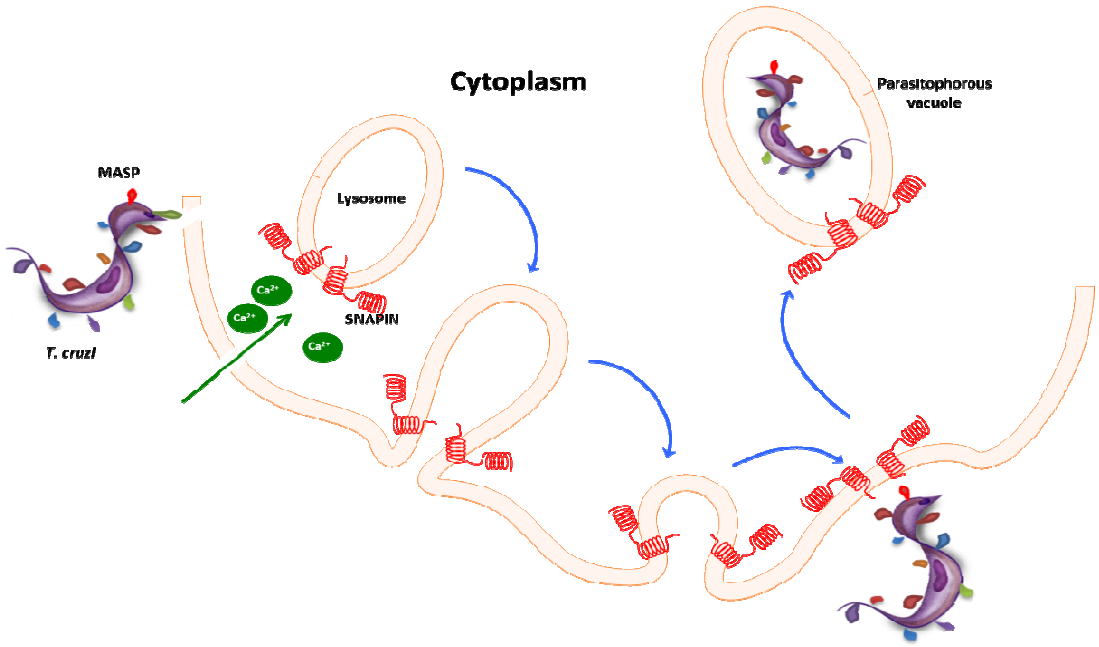

Figure 6-1. Working model. Trypomastigote pokes and breaks the membrane integrity, in turn, triggering the calcium influx into the host cells. A calcium-dependent lysosome exocytosis will follow and expose a luminal domain of SNAPIN to the extracellular space. Trypomastigote will anchor to a luminal domain of SNAPIN via the interaction with MASP proteins on the parasite surface and stay in the vicinity of the host cell so that it could gain entry into the cell when complement endocytosis occurs on the host cell membrane.

One of the challenges that confound the characterization of MASP was the lack of loss-of-function system such as RNAi in *T. cruzi* due to incomplete RNAi machinery in the genome (El-Sayed, Myler et al. 2005). Another option that is to delete the gene and generate the null mutant by a homologous recombination was not feasible for a multigenic protein family such as MASP. To overcome this, we introduced morpholino oligomers (Angerer, Oleksyn et al. 2001; Ahn, Kourakis et al. 2002; Branford and Yost 2002) which were never applied in *T. cruzi* system before and only tested in *T. brucei* as a down-regulation comparison to RNAi system (Shi, Tschudi et al. 2007; Shi, Chamond et al. 2009). We tested the morpholino against GP72, the gene with a well-characterized phenotype and a single copy presence in the *T. cruzi* genome to validate if it is working in *T. cruzi* (de Jesus, Cooper et al. 1993; Haynes, Russell et al. 1996; Shi, Chamond et al. 2009). Since *masp* transcripts show very highly conserved N-terminus and C-terminus as well as 5'UTR and 3'UTR, it was feasible to design a morpholino oligomer to target the vast majority of 771 MASP translation initiation sites if the system turned out to be working as expected. However, due to the lack of proper transfection method for *T. cruzi,* it was difficult to attribute abnormal morphologies to the effect of morpholino. Also the detection of an endogenous GP72 down-regulation was not possible because anti-GP72 antibodies were not available. Once the appropriate transfection methods are developed for *T. cruzi,* the validation of morpholino system in *T. cruzi* should be continued.

Lastly, the expression profile of MASP was of our particular interest as this might explain the evolutionary pressure resulting in the massive expansion of 771 *masp* genes in the *T. cruzi* genome. Differential expression was previously shown with

Northern blot analysis but expression level of individual *masp* gene was unclear (Bartholomeu, Cerqueira et al. 2009). I conducted a small-scale screening to get an idea about how the expression of *masp* is changed upon infection to different host cells. Apparently unlike VSG protein in *T. brucei* where only one member of family is expressed at a time (Turner 1997; Barry and McCulloch 2001; Marcello and Barry 2007), multiple MASPs were expressed in the population, which is in consistent with previous report. The expression was also biased toward a different subset depending on the host cells. The following investigation was expanded and the results are being analyzed by deep sequencing technology to elucidate if a subset of MASP members correlates with the distinct host cells in much deeper coverage. The data obtained from this analysis will answer if a small subset of MASP members displayed by the trypomastigote population emerging from the same re-infected host cells will be more enriched than the one emerging from the original host cells thus confers host tissue-tropism by *T. cruzi* that is one of the characteristics of Chagas chronic disease.

Acknowledgement

We thank Drs. Zu-Hang Sheng and Qian Cai at National Institutes of Health for generating and providing SNAPIN Knock-out MEF cells; Drs. Norma Andrews and Cecilia Fernandes at the Department of Cell Biology and Molecular Genetics for helping cellular biological experiments; Amy Beaven of the at the Department of Cell Biology and Molecular Genetics imaging core facility for support with confocal microscopy.

The work was supported by the National Institutes of Health AI094773 and AI094195.

Appendices

Appendix A.1

1st strand cDNA synthesis

Priming step.	CL Brener MT	CL Brener TCT emerging from HeLa	CL Brener TCT emerging from LLC-MK2
Gene Specific Primer (MASP 3RT: 2 pmol)	1 µL	1 µL	1 µL
Total RNA (500 ng)	11 µL	2.9 µL	3.5 µL
10 mM dNTP Mix	1 µL	1 µL	1 µL
DEPC-treated water	0.8 µL	8.1 µL	7.5 µL
Total	13 µL	13 µL	13 µL

1st strand synthesis	CL Brener MT	CL Brener TCT emerging from HeLa	CL Brener TCT emerging from LLC-MK2
5X 1st strand buffer	4 µL	4 µL	4 µL
0.1 M DTT	1 µL	1 µL	1 µL
RNase OUT	1 µL	1 µL	1 µL
SS® III RT	1 µL	1 µL	1 µL
Total	20 µL	20 µL	20 µL

Appendix A.2

2nd strand cDNA synthesis

	CL Brener MT	CL Brener TCT emerging from HeLa	CL Brener TCT emerging from LLC-MK2
DEPC-treated	78 µL	78 µL	78 µL

water			
5X 2nd strand reaction buffer	30 µL	30 µL	30 µL
10 mM dNTP mix	3 µL	3 µL	3 µL
T4 DNA ligase (1 U/µL)	10 µL	10 µL	10 µL
DNA Polymerase I (Klenow) (5 U/µL)	8 µL	8 µL	8 µL
RNase H (2 U/µL)	1 µL	1 µL	1 µL
Total	150 µL	150 µL	150 µL

Appendix A.3

TOPO blunt-end cloning:

	CL Brener MT	CL Brener TCT emerging from HeLa	CL Brener TCT emerging from LLC-MK2
Double-stranded cDNA products	4 µL	4 µL	4 µL
Salt solution	1 µL	1 µL	1 µL
pCR™II-Blunt-TOPO® vector	1 µL	1 µL	1 µL
Total	6 µL	6 µL	6 µL

Appendix B.1

The list of primers

Primer name	Sequence (5' – 3')	Note
attb_GPI_MASP_F	***GGGACAAGTTTGTACAAAAAAGCAGGCTCC***ATGGCGATGATGATGACTGG	The full-length MASP1 and MASP4
attb_GPI_MASP1_R	***GGGGACCACTTTGTACAAGAAAGCTGGGT***CGCGGCCACCACCGCAGCA	
attb_GPI_MASP4_R	***GGGGACCACTTTGTACAAGAAAGCTGGGTC***AGCCGCACACGCAAGAAG	
sMASPc1***_attb***_F	***GGGGACAAGTTTGTACAAAAAAGCAGGCTCC***TGGGATTTTGGGAATAATG	Soluble MASP1 and MASP4 fragments
sMASPc1***_attb***_R	***GGGGACCACTTTGTACAAGAAAGCTGGGT***GTCACTGTCGTCAGGCGTC	
sMASPc4***_attb***_F	***GGGGACAAGTTTGTACAAAAAAGCAGGCTCC***TGGTTCTACAAGGAATGTGG	
sMASPc4***_attb***_R	***GGGGACCACTTTGTACAAGAAAGCTGGGT***GTCACTCTCGTCAGGCGTCC	
attb_SNAPIN_F	***GGGGACAAGTTTGTACAAAAAAGCAGGCTCC***ATGGCGGGGGCTGGTTCCGC	The full-length SNAPIN
attb_SNAPIN_R	***GGGGACCACTTTGTACAAGAAAGCTGGGT***TTTGCCTGGGGAGCCAGGGG	
attb_SNAPIN_F	***GGGGACAAGTTTGTACAAAAAAGCAGGCTCC***ATGGCGGGGGCTGGTTCCGC	N-terminal fragment of SNAPIN
attb_NterSNAPIN_R	***GGGGACCACTTTGTACAAGAAAGCTGGGT***GGCGTGTACGTGAGAGTCG	
attb_CterSNAPIN_F	***GGGGACAAGTTTGTACAAAAAAGCAGGCTCC*** GTCAGAGAGAGCCAGGTAG	C-terminal fragment of SNAPIN
attb_SNAPIN_R	***GGGGACCACTTTGTACAAGAAAGCTGGGT***TTTGCCTGGGGAGCCAGGGG	
MASP***BglII***_F	GAGA***AGATCT***GCCATGGCGATGATGATGACTGGC	6xHis-tagged MASP in LEXSY system
MASP***NotI***_R	GAGA***GCGGCCGC***TCACGCGGCCACCACCGCAGC	
HISMASP4	***CATCATCATCATCACCAC***CAAGCAGGTGCCACGAGGACG	
MASP4***HIS***_	***GTGGTGATGATGATGATG***AGCGGCGGCGACTGTTGCTGG	
MASP1SP***XbaI***_F	CGATTT***TCTAGA***ATGGCGATGATGATGGCTGGCCGTGTGCTGCTG	6xHis-tagged MASP in *T. cruzi* expression system
MASP1HIS_R	GTGGTGATGATGATGATGAGCGGAGGTGACTGTTGCTGGT	
MASP1HIS_F	CATCATCATCATCACCACCAAACAAGTGCCACGAGGA	
MASP1GPI***XhoI***_R	CCAGTT***CTCGAG***TCACACAGCCACCACCGCAGCAGCA	
MASP1HIS***XhoI***_F	CCAGTT***CTCGAG***TCAGTGGTGATGATGATGATGACTCTCGTCAGGCGTCCTCGTG	
MASP1***BseRI***_F	CGATTT***GAGGAG***GTCTCCCATGATGGCGATGATGATGGCTGGCCGTGTGCTGCTG	
MASP1***BglII***_R	CCAGTT***AGATCT***TTAGTGGTGATGATGATGATGACTCTCGTCAGGCGTCCTCGTG	

Bibliography

Agusti, R., M. E. Giorgi, et al. (2007). "The trans-sialidase from Trypanosoma cruzi efficiently transfers alpha-(2-->3)-linked N-glycolylneuraminic acid to terminal beta-galactosyl units." Carbohydr Res **342**(16): 2465-2469.

Ahn, D. G., M. J. Kourakis, et al. (2002). "T-box gene tbx5 is essential for formation of the pectoral limb bud." Nature **417**(6890): 754-758.

Almeida, I. C., M. A. Ferguson, et al. (1994). "Lytic anti-alpha-galactosyl antibodies from patients with chronic Chagas' disease recognize novel O-linked oligosaccharides on mucin-like glycosyl-phosphatidylinositol-anchored glycoproteins of Trypanosoma cruzi." The Biochemical journal **304** (Pt 3): 793-802.

Alves, M. J. and W. Colli (2007). "Trypanosoma cruzi: adhesion to the host cell and intracellular survival." IUBMB life **59**(4-5): 274-279.

Ancizu, S., E. Moreno, et al. (2009). "Heterocyclic-2-carboxylic acid (3-cyano-1,4-di-N-oxidequinoxalin-2-yl)amide derivatives as hits for the development of neglected disease drugs." Molecules **14**(6): 2256-2272.

Andrade, L. O. and N. W. Andrews (2004). "Lysosomal fusion is essential for the retention of Trypanosoma cruzi inside host cells." The Journal of experimental medicine **200**(9): 1135-1143.

Andrews, N. W. (1990). "The acid-active hemolysin of Trypanosoma cruzi." Experimental Parasitology **71**(2): 241-244.

Andrews, N. W. (1995). "Lysosome Recruitment during Host-Cell Invasion by Trypanosoma-Cruzi." Trends in Cell Biology **5**(3): 133-137.

Andrews, N. W., C. K. Abrams, et al. (1990). "A T. cruzi-secreted protein immunologically related to the complement component C9: evidence for membrane pore-forming activity at low pH." Cell **61**(7): 1277-1287.

Anez-Rojas, N., P. Garcia-Lugo, et al. (2006). "Isolation, purification and characterization of GPI-anchored membrane proteins from Trypanosoma rangeli and Trypanosoma cruzi." Acta Tropica **97**(2): 140-145.

Angerer, L. M., D. W. Oleksyn, et al. (2001). "Sea urchin goosecoid function links fate specification along the animal-vegetal and oral-aboral embryonic axes." Development **128**(22): 4393-4404.

Atwood, J. A., 3rd, T. Minning, et al. (2006). "Glycoproteomics of Trypanosoma cruzi trypomastigotes using subcellular fractionation, lectin affinity, and stable isotope labeling." Journal of Proteome Research **5**(12): 3376-3384.

Bao, Y., J. A. Lopez, et al. (2008). "Snapin interacts with the exo70 subunit of the exocyst and modulates GLUT4 trafficking." Journal of Biological Chemistry **283**(1): 324-331.

Barry, J. D. and R. McCulloch (2001). "Antigenic variation in trypanosomes: enhanced phenotypic variation in a eukaryotic parasite." Advances in parasitology **49**: 1-70.

Bartholomeu, D. C., G. C. Cerqueira, et al. (2009). "Genomic organization and expression profile of the mucin-associated surface protein (masp) family of the human pathogen Trypanosoma cruzi." Nucleic Acids Research **37**(10): 3407-3417.

Baud, R. H., C. Lovis, et al. (2001). "Conceptual search in electronic patient record." Studies in health technology and informatics **84**(Pt 1): 156-160.

Baud, R. H., C. Lovis, et al. (2001). "A light knowledge model for linguistic applications." Proc AMIA Symp: 37-41.

Beard, C. B., C. Cordon-Rosales, et al. (2002). "Bacterial symbionts of the triatominae and their potential use in control of Chagas disease transmission." Annu Rev Entomol **47**: 123-141.

Bern, C. and S. P. Montgomery (2009). "An estimate of the burden of Chagas disease in the United States." Clinical infectious diseases : an official publication of the Infectious Diseases Society of America **49**(5): e52-54.

Berriman, M., E. Ghedin, et al. (2005). "The genome of the African trypanosome Trypanosoma brucei." Science **309**(5733): 416-422.

Bolhassani, A., T. Taheri, et al. (2011). "Fluorescent Leishmania species: development of stable GFP expression and its application for in vitro and in vivo studies." Experimental Parasitology **127**(3): 637-645.

Branford, W. W. and H. J. Yost (2002). "Lefty-dependent inhibition of Nodal- and Wnt-responsive organizer gene expression is essential for normal gastrulation." Current Biology **12**(24): 2136-2141.

Breitling, R., S. Klingner, et al. (2002). "Non-pathogenic trypanosomatid protozoa as a platform for protein research and production." Protein Expression and Purification **25**(2): 209-218.

Burleigh, B. A. (2005). "Host cell signaling and Trypanosoma cruzi invasion: do all roads lead to lysosomes?" Sci STKE **2005**(293): pe36.

Burleigh, B. A. and N. W. Andrews (1995). "The mechanisms of Trypanosoma cruzi invasion of mammalian cells." Annual review of microbiology **49**: 175-200.

Buscaglia, C. A., V. A. Campo, et al. (2006). "Trypanosoma cruzi surface mucins: host-dependent coat diversity." Nature reviews. Microbiology **4**(3): 229-236.

Buschiazzo, A., M. F. Amaya, et al. (2002). "The crystal structure and mode of action of trans-sialidase, a key enzyme in Trypanosoma cruzi pathogenesis." Molecular Cell **10**(4): 757-768.

Buxton, P., X. M. Zhang, et al. (2003). "Identification and characterization of Snapin as a ubiquitously expressed SNARE-binding protein that interacts with SNAP23 in non-neuronal cells." Biochemical Journal **375**: 433-440.

Cai, Q., L. Lu, et al. (2010). "Snapin-regulated late endosomal transport is critical for efficient autophagy-lysosomal function in neurons." Neuron **68**(1): 73-86.

Caler, E. V., S. Vaena de Avalos, et al. (1998). "Oligopeptidase B-dependent signaling mediates host cell invasion by Trypanosoma cruzi." The EMBO journal **17**(17): 4975-4986.

Campbell, D. A., S. J. Westenberger, et al. (2004). "The determinants of Chagas disease: connecting parasite and host genetics." Current molecular medicine **4**(6): 549-562.

Campo, V. A., C. A. Buscaglia, et al. (2006). "Immunocharacterization of the mucin-type proteins from the intracellular stage of Trypanosoma cruzi." Microbes and infection / Institut Pasteur **8**(2): 401-409.

Carranza, J. C., A. J. Kowaltowski, et al. (2009). "Mitochondrial bioenergetics and redox state are unaltered in Trypanosoma cruzi isolates with compromised

mitochondrial complex I subunit genes." Journal of bioenergetics and biomembranes **41**(3): 299-308.

Carranza, J. C., H. M. Valadares, et al. (2009). "Trypanosoma cruzi maxicircle heterogeneity in Chagas disease patients from Brazil." International journal for parasitology **39**(9): 963-973.

Castro, J. A. and E. G. Diaz de Toranzo (1988). "Toxic effects of nifurtimox and benznidazole, two drugs used against American trypanosomiasis (Chagas' disease)." Biomedical and Environmental Sciences **1**(1): 19-33.

Cazzulo, J. J. and A. C. Frasch (1992). "SAPA/trans-sialidase and cruzipain: two antigens from Trypanosoma cruzi contain immunodominant but enzymatically inactive domains." FASEB journal : official publication of the Federation of American Societies for Experimental Biology **6**(14): 3259-3264.

Cerecetto, H. and M. Gonzalez (2011). "Antiparasitic prodrug nifurtimox: revisiting its activation mechanism." Future microbiology **6**(8): 847-850.

Chen, M., K. G. Lucas, et al. (2005). "A novel role for snapin in dendrite patterning: interaction with cypin." Molecular Biology of the Cell **16**(11): 5103-5114.

Chheda, M. G., S. Mochida, et al. (1999). "PKA phosphorylates snapin, a novel protein implicated in synaptic transmission." Journal of the American Geriatrics Society **47**(9): S13-S13.

Claser, C., M. Curcio, et al. (2008). "Silencing cytokeratin 18 gene inhibits intracellular replication of Trypanosoma cruzi in HeLa cells but not binding and invasion of trypanosomes." BMC cell biology **9**: 68.

Conde, R., R. Cueva, et al. (2004). "A search for hyperglycosylation signals in yeast glycoproteins." The Journal of biological chemistry **279**(42): 43789-43798.

Coura, J. R. (2007). "Chagas disease: what is known and what is needed--a background article." Memorias Do Instituto Oswaldo Cruz **102 Suppl 1**: 113-122.

Coura, J. R. and J. C. Dias (2009). "Epidemiology, control and surveillance of Chagas disease: 100 years after its discovery." Memorias Do Instituto Oswaldo Cruz **104 Suppl 1**: 31-40.

Croft, S. L. (1999). "Pharmacological approaches to antitrypanosomal chemotherapy." Mem Inst Oswaldo Cruz **94**(2): 215-220.

Cunha-Neto, E., M. Duranti, et al. (1995). "Autoimmunity in Chagas disease cardiopathy: biological relevance of a cardiac myosin-specific epitope crossreactive to an immunodominant Trypanosoma cruzi antigen." Proc Natl Acad Sci U S A **92**(8): 3541-3545.

Cunha-Neto, E. and J. Kalil (1995). "Autoimmunity in Chagas' heart disease." Sao Paulo medical journal = Revista paulista de medicina **113**(2): 757-766.

DaRocha, W. D., K. Otsu, et al. (2004). "Tests of cytoplasmic RNA interference (RNAi) and construction of a tetracycline-inducible T7 promoter system in Trypanosoma cruzi." Molecular and Biochemical Parasitology **133**(2): 175-186.

de Carvalho, M. E., R. A. da Silva, et al. (2002). "[The Chagas Disease Control Program of the Sao Paulo State: the contribution of serology to the

epidemiological investigation of triatomine-infested domiciliary units during the 1990s]." Cadernos De Saude Publica **18**(6): 1695-1703.

de Jesus, A. R., R. Cooper, et al. (1993). "Gene deletion suggests a role for Trypanosoma cruzi surface glycoprotein GP72 in the insect and mammalian stages of the life cycle." Journal of Cell Science **106 (Pt 4)**: 1023-1033.

De Pablos, L. M., G. G. Gonzalez, et al. (2011). "Differential expression and characterization of a member of the mucin-associated surface protein family secreted by Trypanosoma cruzi." Infection and Immunity **79**(10): 3993-4001.

De Pablos, L. M. and A. Osuna (2012). "Conserved regions as markers of different patterns of expression and distribution of the mucin-associated surface proteins of Trypanosoma cruzi." Infection and Immunity **80**(1): 169-174.

Di Noia, J. M., C. A. Buscaglia, et al. (2002). "A Trypanosoma cruzi small surface molecule provides the first immunological evidence that Chagas' disease is due to a single parasite lineage." Journal of Experimental Medicine **195**(4): 401-413.

Dumonteil, E. (2007). "DNA Vaccines against Protozoan Parasites: Advances and Challenges." Journal of biomedicine & biotechnology **2007**(6): 90520.

Dvorak, J. A. and T. P. Hyde (1973). "Trypanosoma cruzi: interaction with vertebrate cells in vitro. 1. Individual interactions at the cellular and subcellular levels." Experimental Parasitology **34**(2): 268-283.

El-Sayed, N. M., P. J. Myler, et al. (2005). "The genome sequence of Trypanosoma cruzi, etiologic agent of Chagas disease." Science **309**(5733): 409-415.

El-Sayed, N. M., P. J. Myler, et al. (2005). "Comparative genomics of trypanosomatid parasitic protozoa." Science **309**(5733): 404-409.

Eugenia Giorgi, M. and R. M. de Lederkremer (2011). "Trans-sialidase and mucins of Trypanosoma cruzi: an important interplay for the parasite." Carbohydr Res **346**(12): 1389-1393.

Fernandes, M. C., M. Cortez, et al. (2011). "Trypanosoma cruzi subverts the sphingomyelinase-mediated plasma membrane repair pathway for cell invasion." The Journal of experimental medicine **208**(5): 909-921.

Ferrero-Garcia, M. A., S. E. Trombetta, et al. (1993). "The action of Trypanosoma cruzi trans-sialidase on glycolipids and glycoproteins." European journal of biochemistry / FEBS **213**(2): 765-771.

Franzen, O., S. Ochaya, et al. (2011). "Shotgun sequencing analysis of Trypanosoma cruzi I Sylvio X10/1 and comparison with T. cruzi VI CL Brener." Plos Neglected Tropical Diseases **5**(3): e984.

Frasch, A. C. (2000). "Functional diversity in the trans-sialidase and mucin families in Trypanosoma cruzi." Parasitology Today **16**(7): 282-286.

Garg, N. and V. Bhatia (2005). "Current status and future prospects for a vaccine against American trypanosomiasis." Expert review of vaccines **4**(6): 867-880.

Genovesio, A., M. A. Giardini, et al. (2011). "Visual genome-wide RNAi screening to identify human host factors required for Trypanosoma cruzi infection." Plos One **6**(5): e19733.

Giordano, R., R. Chammas, et al. (1994). "An acidic component of the heterogeneous Tc-85 protein family from the surface of Trypanosoma cruzi is a laminin binding glycoprotein." Molecular and Biochemical Parasitology **65**(1): 85-94.

Gowthaman, R., A. J. Silvester, et al. (2006). "Modeling of the potential coiled-coil structure of snapin protein and its interaction with SNARE complex." Bioinformation **1**(7): 269-275.

Gulbins, E. and R. Kolesnick (2003). "Raft ceramide in molecular medicine." Oncogene **22**(45): 7070-7077.

Gurtler, R. E., U. Kitron, et al. (2007). "Sustainable vector control and management of Chagas disease in the Gran Chaco, Argentina." Proc Natl Acad Sci U S A **104**(41): 16194-16199.

Gutierrez, F. R., P. M. Guedes, et al. (2009). "The role of parasite persistence in pathogenesis of Chagas heart disease." Parasite immunology **31**(11): 673-685.

Haynes, P. A., D. G. Russell, et al. (1996). "Subcellular localization of Trypanosoma cruzi glycoprotein Gp72." Journal of Cell Science **109 (Pt 13)**: 2979-2988.

Heise, N., D. Singh, et al. (2009). "Molecular analysis of a UDP-GlcNAc:polypeptide alpha-N-acetylglucosaminyltransferase implicated in the initiation of mucin-type O-glycosylation in Trypanosoma cruzi." Glycobiology **19**(8): 918-933.

Himle, J. A., S. Rassi, et al. (2001). "Group behavioral therapy of obsessive-compulsive disorder: seven vs. twelve-week outcomes." Depress Anxiety **13**(4): 161-165.

Holetz, F. B., L. R. Alves, et al. (2010). "Protein and mRNA content of TcDHH1-containing mRNPs in Trypanosoma cruzi." The FEBS journal **277**(16): 3415-3426.

Holopainen, J. M., O. P. Medina, et al. (2000). "Sphingomyelinase activity associated with human plasma low density lipoprotein." The Journal of biological chemistry **275**(22): 16484-16489.

Hotez, P. J., M. E. Bottazzi, et al. (2008). "The neglected tropical diseases of Latin America and the Caribbean: a review of disease burden and distribution and a roadmap for control and elimination." Plos Neglected Tropical Diseases **2**(9): e300.

Hunt, R. A., W. Edris, et al. (2003). "Snapin interacts with the N-terminus of regulator of G protein signaling 7." Biochemical and Biophysical Research Communications **303**(2): 594-599.

Idone, V., C. Tam, et al. (2008). "Repair of injured plasma membrane by rapid Ca2+-dependent endocytosis." Journal of Cell Biology **180**(5): 905-914.

Ilardi, J. M., S. Mochida, et al. (1999). "Snapin: a SNARE-associated protein implicated in synaptic transmission." Nature Neuroscience **2**(2): 119-124.

Ivens, A. C., C. S. Peacock, et al. (2005). "The genome of the kinetoplastid parasite, Leishmania major." Science **309**(5733): 436-442.

Kaplan, G. (1977). "Differences in the mode of phagocytosis with Fc and C3 receptors in macrophages." Scandinavian journal of immunology **6**(8): 797-807.

Kawashita, S. Y., C. V. da Silva, et al. (2009). "Homology, paralogy and function of DGF-1, a highly dispersed Trypanosoma cruzi specific gene family and its implications for information entropy of its encoded proteins." Molecular and Biochemical Parasitology **165**(1): 19-31.

Kim, B. C., H. J. Lee, et al. (2004). "Jab1/CSN5, a component of the COP9 signalosome, regulates transforming growth factor beta signaling by binding to Smad7 and promoting its degradation." Molecular and Cellular Biology **24**(6): 2251-2262.

Ko, Y. G. and G. A. Thompson, Jr. (1995). "Purification of glycosylphosphatidylinositol-anchored proteins by modified triton X-114 partitioning and preparative gel electrophoresis." Analytical Biochemistry **224**(1): 166-172.

Kouvaraki, M., V. G. Gorgoulis, et al. (2001). "Alterations of the 16q22.1 and 16q24.3 chromosomal loci in sporadic invasive breast carcinomas: correlation with proliferative activity, ploidy and hormonal status of the tumors." Anticancer Research **21**(2A): 991-999.

Lamesch, P., N. Li, et al. (2007). "hORFeome v3.1: a resource of human open reading frames representing over 10,000 human genes." Genomics **89**(3): 307-315.

Lander, N., C. Bernal, et al. (2010). "Localization and developmental regulation of a dispersed gene family 1 protein in Trypanosoma cruzi." Infection and Immunity **78**(1): 231-240.

Leon, J. S. and D. M. Engman (2001). "Autoimmunity in Chagas heart disease." International journal for parasitology **31**(5-6): 555-561.

Ley, V., N. W. Andrews, et al. (1988). "Amastigotes of Trypanosoma cruzi sustain an infective cycle in mammalian cells." The Journal of experimental medicine **168**(2): 649-659.

Lopez-Molinero, A., A. Villareal, et al. (2002). "Determination of arsenic in homeopathic drugs by bromide volatilization-inductively coupled plasma-atomic emission spectrometry." Journal of AOAC International **85**(1): 31-35.

Lu, L., Q. Cai, et al. (2009). "Snapin associates with late endocytic compartments and interacts with late endosomal SNAREs." Bioscience Reports **29**(4): 261-269.

Macedo, A. M., C. R. Machado, et al. (2004). "Trypanosoma cruzi: genetic structure of populations and relevance of genetic variability to the pathogenesis of chagas disease." Memorias Do Instituto Oswaldo Cruz **99**(1): 1-12.

Macedo, V. (1999). "Indeterminate form of Chagas disease." Memorias Do Instituto Oswaldo Cruz **94 Suppl 1**: 311-316.

Magdesian, M. H., R. Giordano, et al. (2001). "Infection by Trypanosoma cruzi. Identification of a parasite ligand and its host cell receptor." The Journal of biological chemistry **276**(22): 19382-19389.

Manque, P. M., I. Neira, et al. (2003). "Cell adhesion and Ca2+ signaling activity in stably transfected Trypanosoma cruzi epimastigotes expressing the metacyclic stage-specific surface molecule gp82." Infection and Immunity **71**(3): 1561-1565.

Marcello, L. and J. D. Barry (2007). "Analysis of the VSG gene silent archive in Trypanosoma brucei reveals that mosaic gene expression is prominent in antigenic variation and is favored by archive substructure." Genome Research **17**(9): 1344-1352.

Mazzarotto, P., C. Pristipino, et al. (2009). "The use of functional tests and planned coronary angiography after percutaneous coronary revascularization in clinical practice. Results from the AFTER multicenter study." International Journal of Cardiology **137**(2): 151-157.

McNeil, P. L. and R. A. Steinhardt (1997). "Loss, restoration, and maintenance of plasma membrane integrity." The Journal of cell biology **137**(1): 1-4.

Mistry, A. C., R. Mallick, et al. (2007). "The UT-A1 urea transporter interacts with snapin, a SNARE-associated protein." The Journal of biological chemistry **282**(41): 30097-30106.

Moreno, S. N., J. Silva, et al. (1994). "Cytosolic-free calcium elevation in Trypanosoma cruzi is required for cell invasion." The Journal of experimental medicine **180**(4): 1535-1540.

Mortara, R. A., W. K. Andreoli, et al. (2008). "Host cell actin remodeling in response to Trypanosoma cruzi: trypomastigote versus amastigote entry." Sub-cellular biochemistry **47**: 101-109.

Mucci, J., M. G. Risso, et al. (2006). "The trans-sialidase from Trypanosoma cruzi triggers apoptosis by target cell sialylation." Cellular Microbiology **8**(7): 1086-1095.

Nakayasu, E. S., D. V. Yashunsky, et al. (2009). "GPIomics: global analysis of glycosylphosphatidylinositol-anchored molecules of Trypanosoma cruzi." Molecular systems biology **5**: 261.

Nde, P. N., K. J. Simmons, et al. (2006). "Silencing of the laminin gamma-1 gene blocks Trypanosoma cruzi infection." Infection and Immunity **74**(3): 1643-1648.

Page, P. C., G. A. Rassias, et al. (2001). "Functionalized iminium salt systems for catalytic asymmetric epoxidation." Journal of Organic Chemistry **66**(21): 6926-6931.

Pan, P. Y., J. H. Tian, et al. (2009). "Snapin facilitates the synchronization of synaptic vesicle fusion." Neuron **61**(3): 412-424.

Parodi-Talice, A., V. Monteiro-Goes, et al. (2007). "Proteomic analysis of metacyclic trypomastigotes undergoing Trypanosoma cruzi metacyclogenesis." Journal of mass spectrometry : JMS **42**(11): 1422-1432.

Petherick, A. (2010). "Campaigning for Chagas disease." Nature **465**(7301): S21-22.

Prata, A. (2001). "Clinical and epidemiological aspects of Chagas disease." The Lancet infectious diseases **1**(2): 92-100.

Previato, J. O., C. Jones, et al. (1994). "O-glycosidically linked N-acetylglucosamine-bound oligosaccharides from glycoproteins of Trypanosoma cruzi." The Biochemical journal **301 (Pt 1)**: 151-159.

Quaglia, F., L. Ostacolo, et al. (2009). "The intracellular effects of non-ionic amphiphilic cyclodextrin nanoparticles in the delivery of anticancer drugs." Biomaterials **30**(3): 374-382.

Rabinovich, I. M., G. M. Mogilevskii, et al. (1990). "[Immunosuppressive therapy and the reaction of the minor salivary glands in the oral mucosa]." Stomatologiia **69**(6): 20-23.

Rajagopala, S. V., S. Casjens, et al. (2011). "The protein interaction map of bacteriophage lambda." Bmc Microbiology **11**: 213.

Rassi, A., Jr., A. Rassi, et al. (2000). "Chagas' heart disease." Clinical cardiology **23**(12): 883-889.

Rassi, A., Jr., A. Rassi, et al. (2010). "Chagas disease." Lancet **375**(9723): 1388-1402.

Rassi, A., Jr., S. G. Rassi, et al. (2001). "Sudden death in Chagas' disease." Arquivos Brasileiros De Cardiologia **76**(1): 75-96.

Rassiat, E., D. Ragonnet, et al. (2001). "[Acute intermittent porphyria revealed by a paradoxical reaction to a benzodiazepine]." Gastroenterologie clinique et biologique **25**(8-9): 832.

Rassin, E. (2001). "The contribution of thought-action fusion and thought suppression in the development of obsession-like intrusions in normal participants." Behav Res Ther **39**(9): 1023-1032.

Rassin, E., P. Diepstraten, et al. (2001). "Thought-action fusion and thought suppression in obsessive-compulsive disorder." Behav Res Ther **39**(7): 757-764.

Reddy, A., E. V. Caler, et al. (2001). "Plasma membrane repair is mediated by Ca(2+)-regulated exocytosis of lysosomes." Cell **106**(2): 157-169.

Rodriguez, A., I. Martinez, et al. (1999). "cAMP regulates Ca2+-dependent exocytosis of lysosomes and lysosome-mediated cell invasion by trypanosomes." The Journal of biological chemistry **274**(24): 16754-16759.

Rodriguez, A., E. Samoff, et al. (1996). "Host cell invasion by trypanosomes requires lysosomes and microtubule/kinesin-mediated transport." Journal of Cell Biology **134**(2): 349-362.

Rojas, A., P. Garcia-Lugo, et al. (2008). "Isolation, purification, characterization and antigenic evaluation of GPI-anchored membrane proteins from Leishmania (Viannia) braziliensis." Acta Tropica **105**(2): 139-144.

Romano, P. S., M. A. Arboit, et al. (2009). "The autophagic pathway is a key component in the lysosomal dependent entry of Trypanosoma cruzi into the host cell." Autophagy **5**(1): 6-18.

Rual, J. F., K. Venkatesan, et al. (2005). "Towards a proteome-scale map of the human protein-protein interaction network." Nature **437**(7062): 1173-1178.

Ruder, C., T. Reimer, et al. (2005). "EBAG9 adds a new layer of control on large dense-core vesicle exocytosis via interaction with Snapin." Molecular Biology of the Cell **16**(3): 1245-1257.

Ruiz, R. C., S. Favoreto, Jr., et al. (1998). "Infectivity of Trypanosoma cruzi strains is associated with differential expression of surface glycoproteins with differential Ca2+ signalling activity." The Biochemical journal **330 (Pt 1)**: 505-511.

Schenkman, S., M. S. Jiang, et al. (1991). "A novel cell surface trans-sialidase of Trypanosoma cruzi generates a stage-specific epitope required for invasion of mammalian cells." Cell **65**(7): 1117-1125.

Schenkman, S., E. S. Robbins, et al. (1991). "Attachment of Trypanosoma-Cruzi to Mammalian-Cells Requires Parasite Energy, and Invasion Can Be Independent of the Target-Cell Cytoskeleton." Infection and Immunity **59**(2): 645-654.

Schenkman, S., E. S. Robbins, et al. (1991). "Attachment of Trypanosoma cruzi to mammalian cells requires parasite energy, and invasion can be independent of the target cell cytoskeleton." Infection and Immunity **59**(2): 645-654.

Schissel, S. L., X. Jiang, et al. (1998). "Secretory sphingomyelinase, a product of the acid sphingomyelinase gene, can hydrolyze atherogenic lipoproteins at neutral pH. Implications for atherosclerotic lesion development." The Journal of biological chemistry **273**(5): 2738-2746.

Schofield, C. J., J. Jannin, et al. (2006). "The future of Chagas disease control." Trends in Parasitology **22**(12): 583-588.

Shi, H., N. Chamond, et al. (2009). "RNA interference in Trypanosoma brucei: role of the n-terminal RGG domain and the polyribosome association of argonaute." Journal of Biological Chemistry **284**(52): 36511-36520.

Shi, H., C. Tschudi, et al. (2007). "Depletion of newly synthesized Argonaute1 impairs the RNAi response in Trypanosoma brucei." Rna-a Publication of the Rna Society **13**(7): 1132-1139.

Shi, H. F., N. Chamond, et al. (2009). "RNA Interference in Trypanosoma brucei ROLE OF THE N-TERMINAL RGG DOMAIN AND THE POLYRIBOSOME ASSOCIATION OF ARGONAUTE." Journal of Biological Chemistry **284**(52): 36511-36520.

Simmons, K. J., P. N. Nde, et al. (2006). "Stable RNA interference of host thrombospondin-1 blocks Trypanosoma cruzi infection." Febs Letters **580**(9): 2365-2370.

Souto, R. P., O. Fernandes, et al. (1996). "DNA markers define two major phylogenetic lineages of Trypanosoma cruzi." Molecular and Biochemical Parasitology **83**(2): 141-152.

Starcevic, M. and E. C. Dell'Angelica (2004). "Identification of snapin and three novel proteins (BLOS1, BLOS2, and BLOS3/reduced pigmentation) as subunits of biogenesis of lysosome-related organelles complex-1 (BLOC-1)." The Journal of biological chemistry **279**(27): 28393-28401.

Suzuki, F., S. Morishima, et al. (2007). "Snapin, a new regulator of receptor signaling, augments alpha(1A)-adrenoceptor-operated calcium influx through TRPC6." Journal of Biological Chemistry **282**(40): 29563-29573.

Tam, C., V. Idone, et al. (2010). "Exocytosis of acid sphingomyelinase by wounded cells promotes endocytosis and plasma membrane repair." The Journal of cell biology **189**(6): 1027-1038.

Tardieux, I., M. H. Nathanson, et al. (1994). "Role in host cell invasion of Trypanosoma cruzi-induced cytosolic-free Ca2+ transients." The Journal of experimental medicine **179**(3): 1017-1022.

Tardieux, I., P. Webster, et al. (1992). "Lysosome Recruitment and Fusion Are Early Events Required for Trypanosome Invasion of Mammalian-Cells." Cell **71**(7): 1117-1130.

Tarleton, R. L. (2001). "Parasite persistence in the aetiology of Chagas disease." International journal for parasitology **31**(5-6): 550-554.

Tarleton, R. L., R. Reithinger, et al. (2007). "The challenges of Chagas Disease--grim outlook or glimmer of hope." PLoS medicine **4**(12): e332.

Teixeira, A. R., N. Nitz, et al. (2006). "Chagas disease." Postgraduate medical journal **82**(974): 788-798.

Thakur, P., D. R. Stevens, et al. (2004). "Effects of PKA-mediated phosphorylation of Snapin on synaptic transmission in cultured hippocampal neurons." The Journal of neuroscience : the official journal of the Society for Neuroscience **24**(29): 6476-6481.

Tian, J. H., Z. X. Wu, et al. (2005). "The role of snapin in neurosecretion: Snapin knock-out mice exhibit impaired calcium-dependent exocytosis of large dense-core vesicles in chromaffin cells." Journal of Neuroscience **25**(45): 10546-10555.

Tibayrenc, M. (1995). "Population genetics of parasitic protozoa and other microorganisms." Advances in parasitology **36**: 47-115.

Tobler, L. H., P. Contestable, et al. (2007). "Evaluation of a new enzyme-linked immunosorbent assay for detection of Chagas antibody in US blood donors." Transfusion **47**(1): 90-96.

Tomlinson, S., L. Pontes de Carvalho, et al. (1992). "Resialylation of sialidase-treated sheep and human erythrocytes by Trypanosoma cruzi trans-sialidase: restoration of complement resistance of desialylated sheep erythrocytes." Glycobiology **2**(6): 549-551.

Tomoda, K., Y. Kubota, et al. (2002). "The cytoplasmic shuttling and subsequent degradation of p27Kip1 mediated by Jab1/CSN5 and the COP9 signalosome complex." The Journal of biological chemistry **277**(3): 2302-2310.

Tonelli, R. R., R. J. Giordano, et al. (2010). "Role of the gp85/trans-sialidases in Trypanosoma cruzi tissue tropism: preferential binding of a conserved peptide motif to the vasculature in vivo." Plos Neglected Tropical Diseases **4**(11): e864.

Tostes, S., Jr., D. Bertulucci Rocha-Rodrigues, et al. (2005). "Myocardiocyte apoptosis in heart failure in chronic Chagas' disease." International Journal of Cardiology **99**(2): 233-237.

Turner, C. M. (1997). "The rate of antigenic variation in fly-transmitted and syringe-passaged infections of Trypanosoma brucei." Fems Microbiology Letters **153**(1): 227-231.

Tyler, K. M. and D. M. Engman (2001). "The life cycle of Trypanosoma cruzi revisited." International journal for parasitology **31**(5-6): 472-481.

Tyler, K. M., G. W. Luxton, et al. (2005). "Responsive microtubule dynamics promote cell invasion by Trypanosoma cruzi." Cellular Microbiology **7**(11): 1579-1591.

Urbina, J. A. (1999). "Parasitological cure of Chagas disease: is it possible? Is it relevant?" Memorias Do Instituto Oswaldo Cruz **94 Suppl 1**: 349-355.

Vago, A. R., L. O. Andrade, et al. (2000). "Genetic characterization of Trypanosoma cruzi directly from tissues of patients with chronic Chagas disease: differential distribution of genetic types into diverse organs." The American journal of pathology **156**(5): 1805-1809.

Vazquez-Prokopec, G. M., C. Spillmann, et al. (2009). "Cost-effectiveness of chagas disease vector control strategies in Northwestern Argentina." PLoS Negl Trop Dis **3**(1): e363.

Villar, A., V. Jimenez-Yuste, et al. (2002). "The use of haemostatic drugs in haemophilia: desmopressin and antifibrinolytic agents." Haemophilia : the official journal of the World Federation of Hemophilia **8**(3): 189-193.

Villar, J. C., J. A. Marin-Neto, et al. (2002). "Trypanocidal drugs for chronic asymptomatic Trypanosoma cruzi infection." Cochrane Database Syst Rev(1): CD003463.

Wall, W. and Z. El Rassi (2001). "Electrically driven microseparation methods for pesticides and metabolites: V. Micellar electrokinetic capillary chromatography of aniline pesticidic metabolites derivatized with fluorescein isothiocyanate and their detection in real water at low levels by laser-induced fluorescence." Electrophoresis **22**(11): 2312-2319.

Wang, S. C., J. T. Lin, et al. (2009). "Novel regulation of adenylyl cyclases by direct protein-protein interactions: insights from snapin and ric8a." Neuro-Signals **17**(3): 169-180.

Wei, S., Y. Xu, et al. (2010). "EHD1 is a synaptic protein that modulates exocytosis through binding to snapin." Molecular and cellular neurosciences **45**(4): 418-429.

WHO (2002). "Control of Chagas disease." World Health Organ Tech Rep Ser **905**: i-vi, 1-109, back cover.

WHO (2010). "First WHO report on neglected tropical diseases 2010: working to overcome the global impact of neglected tropical diseases.".

Wilkinson, S. R. and J. M. Kelly (2009). "Trypanocidal drugs: mechanisms, resistance and new targets." Expert Rev Mol Med **11**: e31.

Wilkinson, S. R., M. C. Taylor, et al. (2008). "A mechanism for cross-resistance to nifurtimox and benznidazole in trypanosomes." Proceedings of the National Academy of Sciences of the United States of America **105**(13): 5022-5027.

Woolsey, A. M., L. Sunwoo, et al. (2003). "Novel PI 3-kinase-dependent mechanisms of trypanosome invasion and vacuole maturation." Journal of Cell Science **116**(17): 3611-3622.

Yakubu, M. A., S. Majumder, et al. (1994). "Changes in Trypanosoma cruzi infectivity by treatments that affect calcium ion levels." Molecular and Biochemical Parasitology **66**(1): 119-125.

Yoshida, A., N. Yoneda-Kato, et al. (2010). "CSN5/Jab1 controls multiple events in the mammalian cell cycle." Febs Letters **584**(22): 4545-4552.

Yoshida, N. and M. Cortez (2008). "Trypanosoma cruzi: parasite and host cell signaling during the invasion process." Sub-cellular biochemistry **47**: 82-91.

Young, C., P. Losikoff, et al. (2007). "Transfusion-acquired Trypanosoma cruzi infection." Transfusion **47**(3): 540-544.

Yu, H., L. Tardivo, et al. (2011). "Next-generation sequencing to generate interactome datasets." Nature Methods **8**(6): 478-480.

Zhang, L. and R. L. Tarleton (1999). "Parasite persistence correlates with disease severity and localization in chronic Chagas' disease." Journal of Infectious Diseases **180**(2): 480-486.

Zingales, B., S. G. Andrade, et al. (2009). "A new consensus for Trypanosoma cruzi intraspecific nomenclature: second revision meeting recommends TcI to TcVI." Mem Inst Oswaldo Cruz **104**(7): 1051-1054.

Zissimopoulos, S., D. J. West, et al. (2006). "Ryanodine receptor interaction with the SNARE-associated protein snapin." Journal of Cell Science **119**(11): 2386-2397.